Measurement of the airborne sound insulation of traffic noise barriers using impulse response techniques

by

John Bull

A thesis submitted in partial fulfilment
of the requirements for the degree of
Masters of Engineering

in the

Department of Mechanical Engineering,
University of Canterbury,
Christchurch, New Zealand

January 2014

Abstract

This research thesis involves the measurement of the airborne sound insulation of road traffic noise barriers, with the goal of gaining a more in depth understanding of the factors that influence noise barrier performance. A measurement system is developed, based on EN 1793-6:2012, to quantify the airborne sound insulation of a noise barrier in situ. Validation testing is performed to ensure that the system meets the requirements of EN 1793-6:2012. MATLAB code is developed, incorporating all of the signal processing tasks into a single graphical user interface. The measurement system is then used to measure the airborne sound insulation of eight existing traffic noise barriers located around Auckland, New Zealand.

The results from the Auckland field tests show that consistent single number ratings of airborne sound insulation can be achieved on different samples of the same noise barrier. The presence of air gaps and hidden defects will degrade the acoustic performance of a noise barrier, most significantly at the high frequencies. The comparison of single number ratings calculated with differing measurement frequency ranges is discussed, and some comments are made on the measurement standard itself.

Acknowledgements

I would like to thank my supervisor Dr John Pearse and mentor Dr Greg Watts. Greg for his extensive knowledge on noise barrier performance and his efforts to make himself available to me despite being on the other side of the world. John has been a fantastic organiser and has always been able to point me in the direction of valuable advice.

Dr Stephen Chiles has been an excellent source of information from an industrial perspective, I am truly grateful for his practical viewpoint and the considerable amount of time he has spent advising and motivating me.

I would like to thank Rob Hannaby from the NZTA for sponsoring the Auckland testing work, and the AMA for assisting with test site access.

Thanks to the members of the Acoustics Research Group for always being willing to help out with the project, and for providing a light-hearted and thoroughly enjoyable working environment.

Finally I would like to thank my family. My parents for their continued support, and for making the courageous move from South Africa to New Zealand that has given me so many opportunities for a prosperous career and life. My brother for always being there in trying times. And my Grandparents for their financial support and love.

Contents

1. Introduction and Literature Review

1.1. Introduction

Road traffic noise is a significant source of environmental noise. Along with general annoyance [1], traffic noise has been linked to cardiovascular disease [2] and disruption to learning [3]. The main sources of noise on vehicles are the power unit (engine, exhaust, transmission and fan), wind turbulence and tyre/road noise [4]. At low speeds noise from the power unit will dominate the total noise. As the vehicle speed increases the tyre/road noise will become dominant, the speed at which this occurs is known as the crossover speed (between 16 and 40 km/h for cars). At high speeds noise from wind turbulence becomes the most significant noise source [5].

Noise levels can be reduced by treating the noise source, the transmission path, or the receiver [6]. In the case of road vehicles, treatment of the noise source is done through the use of quieter engines, improved silencers and reduction of air turbulence from the vehicle body. The interaction between the vehicle tyre and road surface is the most significant contributor to the total noise at highway speeds [5]. In addition to playing a part in the generation of noise, the road surface makes up part of the transmission path and a quiet road surface can provide improved sound absorption as sound propagates across it [5]. Much work has been conducted in an effort to design quieter road surfaces [7].

Blocking the direct sound path is achieved through the use of traffic noise barriers. A high performance traffic noise barrier will attenuate most of the noise passing through it; however, a diffraction path over the barrier is then introduced, which often becomes the most significant sound path between the source and receiver (Figure 1.1). Treatment of the receiver generally involves improving the sound transmission loss of the walls, windows and roof of a dwelling. In

some situations it is necessary to install a ventilation system so that the windows can remain closed.

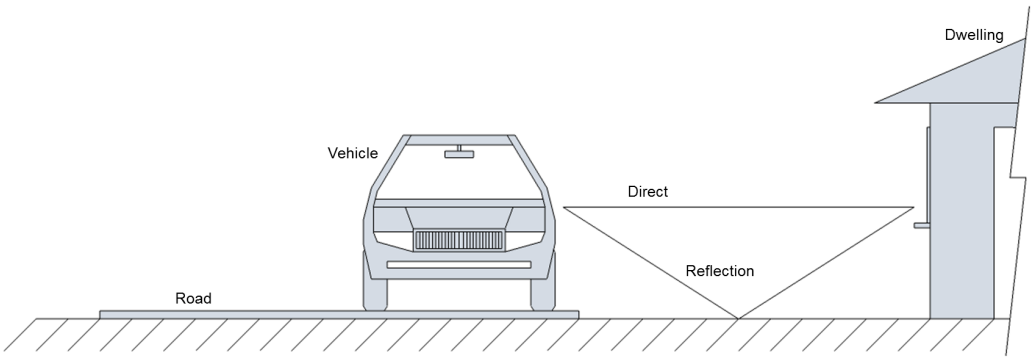

(a) Sound paths without a noise barrier installed

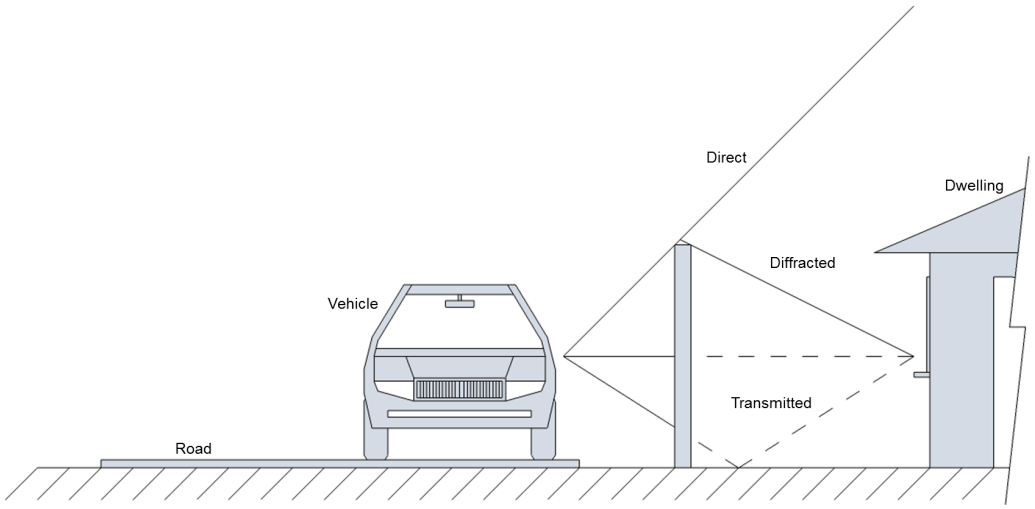

(b) Sound paths with a noise barrier installed

Figure 1.1.: Possible sound paths between a vehicle and dwelling

Traffic noise barriers are used throughout the developed world to reduce public exposure to the high noise levels associated with highways. In New Zealand the NZ Transport Agency's (NZTA) environmental plan [8] gives some objectives regarding noise from the NZ state highway network:

N1 Reduce exposure to high traffic noise levels from existing state highway network

N2 Determine reasonable noise requirements when seeking new or altering existing designations including when designating existing local roads by using Resource Management Act procedures

Funding may be available if the noise level at an affected residence ($L_{Aeq,24hrs}$) is above 65 dBA, however, other criteria are also considered as funding is limited [8].

The performance of traffic noise barriers at reducing the transmitted sound path is the focus of this work. A European standard has recently been published that defines a method to measure the airborne sound insulation of a traffic noise barrier in situ, EN 1793-6:2012, *Road traffic noise reducing devices - Test method for determining the acoustic performance - Part 6: Intrinsic characteristics - In situ values of airborne sound insulation under direct sound field conditions* [9]. The standard makes use of an impulse response measurement technique using deterministic excitation signals, allowing measurements to be conducted in the presence of background noise.

Due to the presence of the diffracted sound path it is not always necessary to use a noise barrier that maximises the airborne sound insulation. Once the noise level due to the diffracted sound becomes the dominant component there is no need to further increase the airborne sound insulation of the noise barrier. Therefore, lower cost noise barriers consisting of timber planks or plywood can provide similar overall acoustic performance as more expensive concrete, metallic and acrylic noise barriers.

Timber noise barriers tend to be more susceptible to weathering than concrete, metallic and acrylic noise barriers. Weathering can lead to the development of air gaps between the timber panels, the resulting sound leakage may degrade the acoustic performance of the noise barrier [10]. The panel joint and mounting details are therefore important if the noise barrier is to perform consistently throughout its design life.

In addition to reducing the noise level at a dwelling, consideration must also be made of the appearance, location, maintenance requirements, safety, cost and sustainability of a noise barrier [11].

The motivation for this work was to improve the airborne sound insulation of cost effective traffic noise barriers such that they may become a more acceptable noise control solution on new and existing highways.

1.1.1. Objectives

Traffic noise barriers around New Zealand are typically constructed from timber products, these tend to degrade more rapidly and are more prone to construction defects than other barrier types (concrete, acrylic and metallic). Reduced screening performance has been attributed to leakage caused by shrinking, warping and splitting of panels, and weathering of acoustic seals [10]. The objective of this work was to gain a better understanding of the factors influencing the airborne sound insulation of traffic noise barriers by:

- developing a measurement system that complies with EN 1793-6:2012
- investigating the factors that influence the measured values of airborne sound insulation
- investigating the influence of construction/design defects and degradation on the airborne sound insulation index of traffic noise barriers

1.2. Airborne Sound Insulation Measurements

Measurement of airborne sound insulation has been a subject of research in Europe over the past two decades, initially being investigated by a European Commission funded research project called "Adrienne" between 1995 and 1997. The research focused on designing a method for measuring the sound absorption and airborne sound insulation of noise reducing devices [12].

Verification of the airborne sound insulation measurement method developed during the Adrienne project has been conducted [13–16] and a measurement standard initially released by the European Committee for Standardization (CEN) as CEN/TS 1793-5:2003 [17]. This standard was concerned with measuring both the sound reflection and airborne sound insulation; the measurement of the airborne sound insulation component was later released individually in an improved version as EN 1793-6.

1.2.1. Measurement standard (EN 1793-6:2012)

EN 1793-6:2012 describes a method for measuring the airborne sound insulation of traffic noise reducing devices in situ, making use of an impulse response method. It is intended to be used to:

- determine the airborne sound insulation of noise reducing devices in actual use
- compare the actual performance of the noise reducing device with the design specifications following construction
- verify the long term performance of noise reducing devices
- assist in the design of new noise reducing devices

Two impulse response measurements are needed, a free-field measurement and a barrier measurement (Figures 1.2 and 1.3, respectively), with microphone signals being recorded at nine positions on a measurement grid for each of the two impulse response measurements. The measurement grid consists of nine microphone positions on a three by three grid (400 mm spacing). The measurement grid is placed on the resident-side, 250 mm away from the most protruding part of the barrier structure (this includes any structural elements). A loudspeaker is placed on the road-side, 1 metre away from the most protruding part of the barrier structure. The centre microphone position and the loudspeaker lie on the same axis.

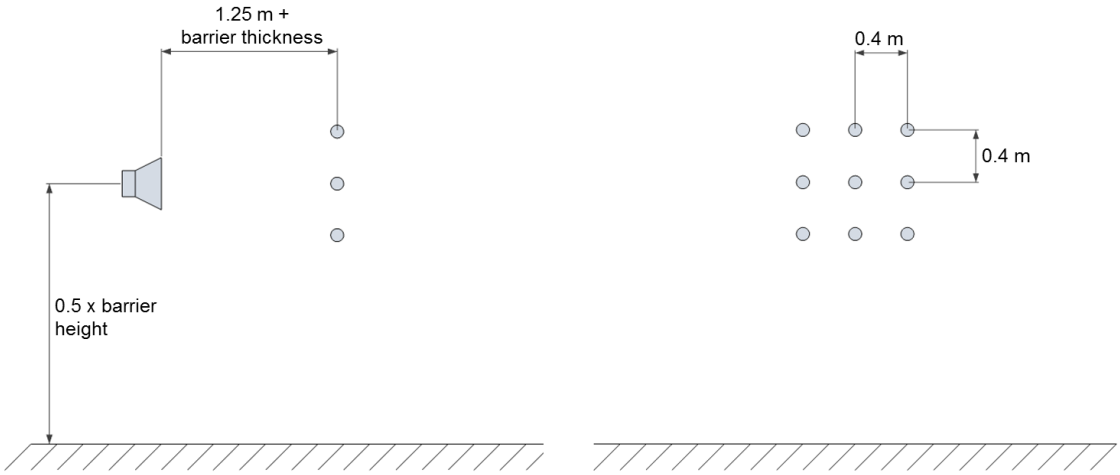

Figure 1.2.: Free-field measurement setup

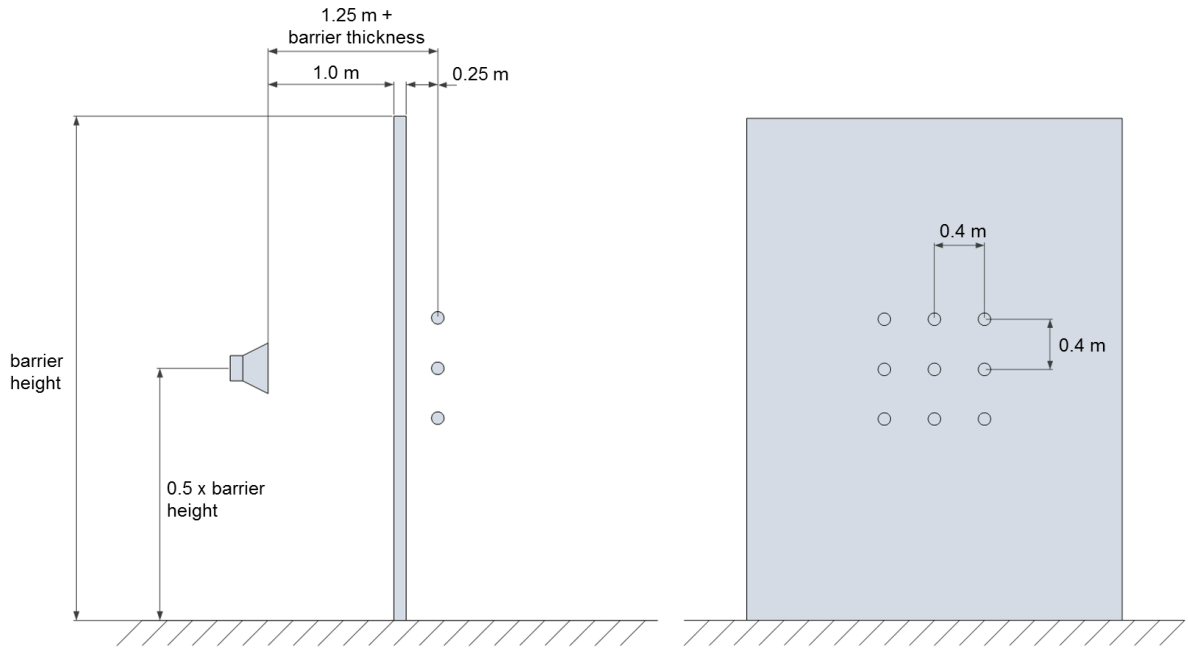

Figure 1.3.: Barrier measurement setup

A time window, known as the Adrienne temporal window, is used to remove the diffracted component and any parasitic reflections from the measured impulse responses. The shape of the time window is specified in EN 1793-6:2012 and consists of a 0.5 millisecond half Blackman-Harris rise, a 5.18 millisecond rectangular section and a 2.24 millisecond half Blackman-Harris tail (Figure 1.4).

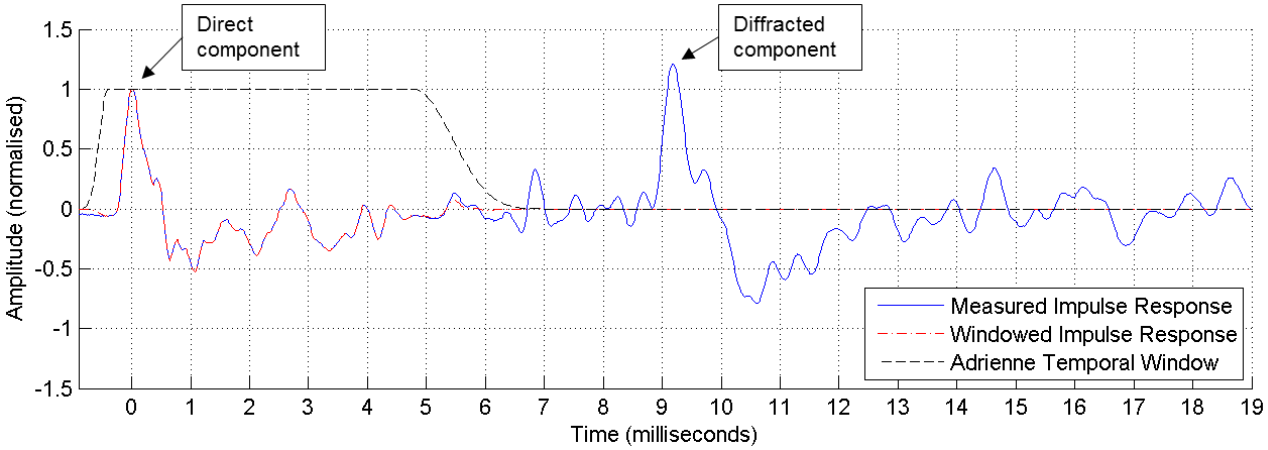

Figure 1.4.: Impulse response showing the removal of the diffracted sound with the Adrienne temporal window

The sound insulation index is calculated in each one-third octave band between 100 Hz and 5 kHz using the impulse responses from both the free-field and barrier measurements (Equation 1.1).

$$SI_j = -10 \log_{10} \left\{ \frac{1}{n} \sum_{k=1}^{n} \frac{\int\limits_{\Delta f_j} |F[h_{tk}(t) w_{tk}(t)]|^2 \, \mathrm{d}f}{\int\limits_{\Delta f_j} |F[h_{ik}(t) w_{ik}(t)]|^2 \, \mathrm{d}f} \right\} \tag{1.1}$$

where

$h_{ik}(t)$ is the free-field impulse response at the kth microphone position

$h_{tk}(t)$ is the barrier impulse response at the kth microphone position

$w_{ik}(t)$ is the Adrienne temporal window for the free-field impulse response at the kth microphone position

$w_{tk}(t)$ is the Adrienne temporal window for the barrier impulse response at the kth microphone position

F is the symbol for the Fourier transform

j is the index of the jth one-third octave band between 100 Hz and 5 kHz

Δf_j is the bandwidth of the jth one-third octave band

n is the number of microphone positions, $n = 9$

Barrier measurements are conducted at element (A) and post (B) positions as defined in Figure 1.5. The dashed circles represent the tested area.

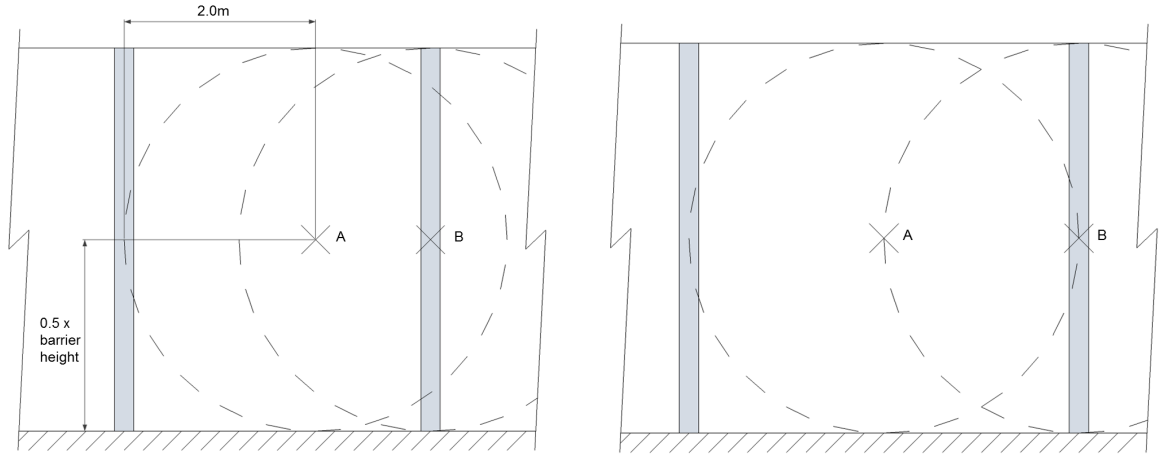

(a) Post spacing < 4.0m

(b) Post spacing ≥ 4.0m

Figure 1.5.: Element (a) and post (b) measurement positions, as viewed from the front of the barrier

Single number ratings for the sound insulation index are defined in EN 1793-6:2012 to provide a means of quickly comparing the performance of different noise barriers. It is based on weighting the one-third octave band sound insulation values with a reference traffic spectrum.

Single number ratings for the sound insulation index (DL_{SI}) are calculated for the elements and posts using Equation 1.2.

$$DL_{SI} = -10 \log_{10} \left\{ \frac{\sum_{i=m}^{18} \left[10^{0.1L_i} \times 10^{-0.1SI_i} \right]}{\sum_{i=m}^{18} 10^{0.1L_i}} \right\} \tag{1.2}$$

where

SI_i is the sound insulation index in the ith one-third octave band

m is the lowest reliable one-third octave band, based on the length of the Adrienne temporal window

L_i is the relative A-weighted sound pressure level of the normalised traffic noise spectrum in the ith one-third octave band, as specified in EN 1793-3:1997 [18] (Figure 1.6)

A global single number rating for the sample ($DL_{SI,G}$) is calculated using Equation 1.3.

$$DL_{SI,G} = -10 \log_{10} \left\{ \frac{10^{-0.1DL_{SI,E}} + 10^{-0.1DL_{SI,P}}}{2} \right\} \tag{1.3}$$

where

$DL_{SI,E}$ is the single number rating of the element, calculated using Equation 1.2

$DL_{SI,P}$ is the single number rating of the post, calculated using Equation 1.2

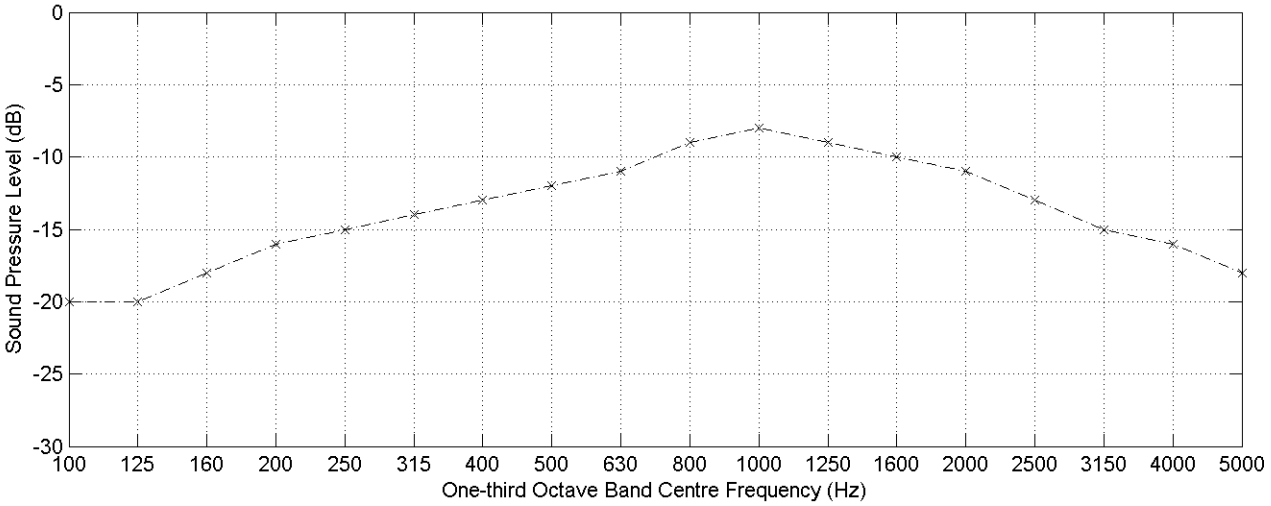

Figure 1.6.: Normalised traffic noise spectrum

1.2.2. Existing noise barrier measurements

Garai and Guidorzi [13] performed a detailed verification of the Adrienne test method on 17 noise barriers available on the European market at the time. The noise barriers were tested using the Adrienne method as well as in the laboratory according to EN 1793-2:1997 *Road traffic noise reducing devices - Test method for determining the acoustic performance - Part 2: Intrinsic characteristics of airborne sound insulation* [19]. Garai and Guidorzi highlighted the importance of an in situ test method, as the presence of sound leakage due to poor workmanship and design cannot be detected using the laboratory method.

Comparisons between the laboratory and in situ results found that the laboratory results were generally lower than the in situ results. This was attributed to the difference in sound fields used for each method (diffuse sound field in the laboratory, free-field outdoors), with a clear coincidence dip present in some of the laboratory results. The difference in boundary conditions was also considered an influencing factor, with four sides clamped in the laboratory. Outdoors three sides are usually clamped, with the top edge free.

Generally the in situ sound insulation index values from post measurements were lower than the element measurements, especially at high frequencies. This supported the idea that sound leakage from poor workmanship and design can lower the performance of a noise barrier. When the low values of airborne sound insulation at the posts were due to poor design rather than poor workmanship the laboratory results were closer to the in situ post results.

Garai and Guidorzi found that the new Adrienne test method was easy to use and reliable for a range of noise barrier types, being sensitive to defects that result in reduced airborne sound insulation. A relationship was found between the laboratory and in situ results that allows prediction of the outdoor airborne sound insulation of both elements and posts from laboratory test results (Equation 1.4 and 1.5). These relationships should only be considered valid for noise barriers with similar values of airborne sound insulation to those involved in the researchers' work (ie. $DL_R \geq 23$ dB).

$$DL_{SI,E} = 1.18DL_R - 0.94 \tag{1.4}$$

$$DL_{SI,P} = 1.18DL_R - 3.16 \tag{1.5}$$

where

DL_R is the laboratory single number rating for airborne sound insulation

A relationship between the weighted sound reduction index (R_w) and laboratory single number rating for airborne sound insulation (DL_R) was also determined, Equation 1.6.

$$DL_R = 0.98R_w - 3.05 \tag{1.6}$$

Watts and Morgan [14] performed a verification of the MLS based methods for characterising the sound absorption and sound transmission of a range of noise barriers and road surfaces. They highlight the high noise immunity and absence of calibration that make the method attractive for in situ testing. It is also shown that a leak will behave as a small sound source on the resident-side of a barrier, with a spreading factor dependent on the size and shape of the leak. Therefore, the measurement results can vary depending on the distance between a microphone and air gap.

Garai and Guidorzi [20, 21] successfully used the Adrienne method in the first large scale noise barrier testing program in Europe. The in situ measurement results were compared to in situ and laboratory results from four to six years earlier. The researchers found that the uncertainty in the measurement method led to a maximum variation in the single number ratings of 2 dB between

samples of the same noise barrier. Any variations larger than 2 dB were attributed to sound leakage due to poor workmanship and design. In one case a poorly designed and constructed panel-post joint led to large differences between the laboratory and in situ measurement results. The laboratory results gave a single number rating of 45 dB, which dropped to 37 dB and 20 dB for the in situ element and post measurements, respectively. These variations show the usefulness of the in situ test method in detecting defects, including poor construction practices.

Watts and Morgan [16] performed laboratory and in situ measurements on six timber noise barriers. The work was focused on verifying the in situ method for noise barriers with low airborne sound insulation values, which had not previously been done, and finding a relationship between laboratory and in situ results for such noise barriers. Equation 1.7 represents the relationship between a laboratory measurement (including both an element and a post in the test sample) and an in situ element measurement over the full measurement frequency range. The relationship is valid for the range of noise barriers tested, $17 < DL_R < 27$ dB(A).

$$DL_{SI,E} = 1.207 DL_R + 2.824 \tag{1.7}$$

1.2.3. Measurement uncertainty

EN 1793-6:2012 calls for the determination of the measurement uncertainty in any airborne sound insulation measurement results, preferably in compliance with ISO/IEC Guide 98 [22]. The recommended procedure is based on an uncertainty budget where all sources of uncertainty are identified and quantified.

Due to the young and complex nature of the measurement technique, some researchers have decided to undertake inter-laboratory tests over an uncertainty budget approach [23]. In this work eight European laboratories measured the airborne sound insulation of eight element samples and five post samples, constructed at two different test sites.

Since the true values of airborne sound insulation are unknown only the repeatability and reproducibility could be determined. The repeatability (r) is defined as the random variation under constant measurement conditions and the reproducibility (R) is defined as the random variation under changed conditions. The repeatability is then expressed as $2 \times s_r$, where s_r is

the standard deviation of consecutive measurements on the same sample within a short time interval. Similarly, the reproducibility is expressed as $2 \times s_R$, where s_R is the standard deviation of measurements on the same sample under changed conditions. The researchers state that there is an inter-laboratory variation between measurement results, and that reproducibility should be chosen as the quantity to define the 95% confidence interval (i.e. $\pm R$ dB).

The maximum and minimum values of reproducibility of DL_{SI} are included in Table 1.1 for both elements and posts. The conservative 95% confidence interval can be determined by applying the maximum values of reproducibility to the unrounded single number ratings and then rounding to the nearest integer. For the purposes of this work measurement uncertainties will not be included; comparisons between results from different samples tested in this work are considered appropriate as all measurements were conducted using the same system.

Table 1.1.: Maximum and minimum values of reproducibility of DL_{SI} for both elements and posts [23]

Measurement	Reproducibility (dB)	
	Min	Max
Element	1.62	2.61
Post	1.03	1.83

1.3. System Impulse Response Measurement

The impulse response of a system is simply the system response when subjected to an impulse excitation. In the field of acoustics it is often necessary to determine the frequency dependent behaviour of a system, which for a linear time-invariant (LTI) system is achieved through measurement of the impulse response. Impulse responses and transfer functions are frequently used to characterise the response of a room, transducer, or barrier.

In practice it is difficult to generate an impulsive excitation that has the required frequency distribution and gives a good signal to noise ratio (SNR) [24], as it is necessary for the excitation signal's energy to be distributed evenly over all frequencies and to contain sufficient energy to overcome any background noise. To remedy these issues an impulse excitation is often replaced with signals of longer duration, permitting more energy to be applied to the system and allowing

better control of the spectral distribution of the signal energy. The system output is then the convolution of the input signal and the system's impulse response; the impulse response may be determined by deconvolution. Some of the excitation signals commonly used in acoustics are sine sweeps, pseudorandom noise in the form of maximum length sequences (MLS), and random noise. The excitation signal requirements are listed below [25]:

- The excitation signal should be perfectly repeatable or deterministic
- The excitation signal and deconvolution process should maximise the effective SNR of the measured impulse response

Having a perfectly repeatable excitation signal allows multiple measurements of the system response to be averaged, the noise is then reduced as any incoherent noise will eventually sum to zero. The signal-to-noise ratio can be increased by 3 dB for each doubling of the excitation signal length or doubling of the number of periods used [26]. Maximum length sequences and sine sweeps are the most commonly chosen deterministic excitation signals due to the above two criteria; both meet the requirements of EN 1793-6:2012.

1.3.1. Maximum length sequences

A maximum length sequence (MLS), also referred to as an m-sequence, is a pseudorandom signal that can be generated by an m-stage shift register and has a period of length $2^m - 1$, where m is known as the sequence order. They have the important property that their auto-correlation is the Dirac delta function except for a small dc error, meaning that they have a flat magnitude spectrum everywhere except at dc [24]. The binary sequence is mapped to ± 1 to form the system excitation signal that is symmetric around zero [25].

The discrete Fourier transform and auto-correlation of an m-sequence of order $m = 8$ (length $N = 255$) are shown in Figure 1.7. The discrete Fourier transform is flat everywhere apart from at dc and the auto-correlation is approximately an impulse.

Since the cross-correlation of an input $n(k)$ and output $y(k)$ is the convolution of the input's auto-correlation (Φ_{nn}) and the impulse response of the system under test $h(k)$, the cross-correlation of the output $y(k)$ with the m-sequence $n(k)$ will give the system impulse response [24].

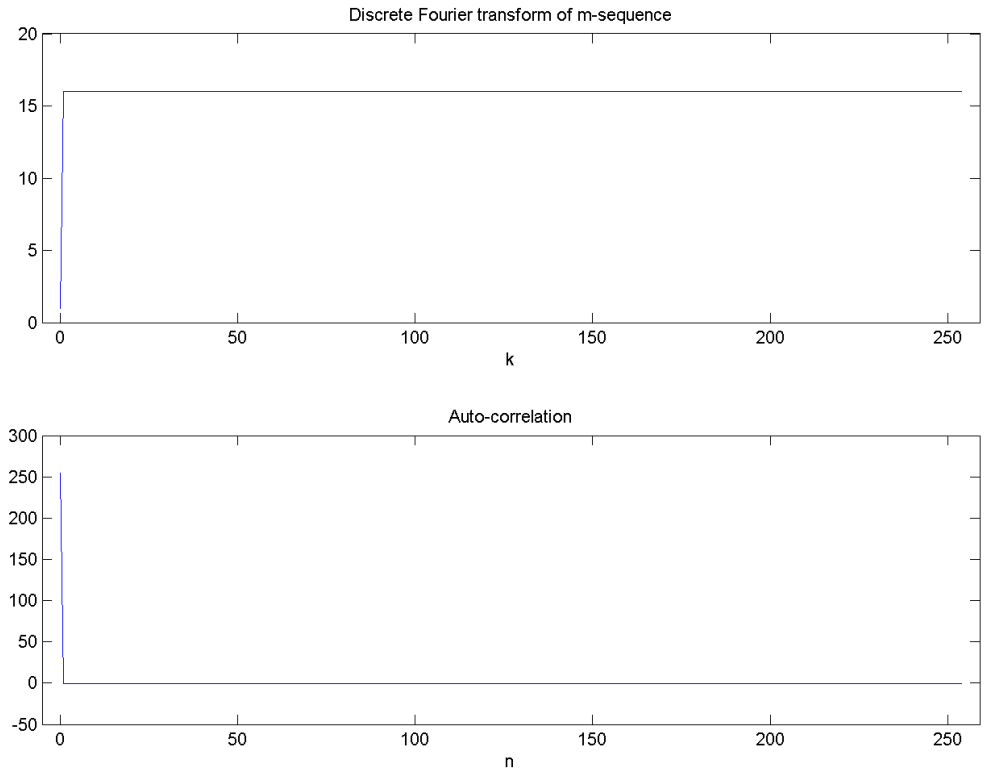

Figure 1.7.: Discrete Fourier transform and auto-correlation of an m-sequence of order 8

$$\phi_{ny}(k) = \phi_{nn}(k) \otimes h(k) \tag{1.8}$$

$$\phi_{nn}(k) = \delta(k) \tag{1.9}$$

$$\therefore \phi_{ny}(k) = h(k) \tag{1.10}$$

where $\otimes$ is the symbol for the linear convolution.

Since the impulsive auto-correlation characteristic of a maximum length sequence requires periodic auto-correlation, the sequence indices used in the correlation operation must be modulo N (where N is the length of the m-sequence) [24]. The cross-correlation of the m-sequence $n(k)$ and the output $y(k)$ is then:

$$\phi_{ny}(k) = \frac{1}{N} \sum_{j=0}^{N-1} n\big((j-k)\big) y(j) \tag{1.11}$$

where $n\big((j-k)\big)$ refers to $n(j-k)$ modulo N.

This can also be implemented as a matrix multiplication:

$$\Phi_{ny}(k) = \frac{1}{N}\boldsymbol{M}_N Y \tag{1.12}$$

where

Φ_{ny} is a vector containing the cross-correlation values

Y is a vector containing the measured output signal

$\boldsymbol{M}_N$ is referred to as the noise matrix containing shifted versions of the m-sequence with length N. That is, each row of $\boldsymbol{M}_N$ is equal to the previous row circularly shifted one element to the right.

There are potential computational advantages resulting from the fact that each element of $\boldsymbol{M}_N$ is either $+1$ or -1, so only additions and subtractions are needed to perform the cross-correlation. Furthermore if a Fast Hadamard Transform (FHT) algorithm is used then the number of operations reduces from N^2 to approximately $2.5N \log_2 N$ [24].

Fast Hadamard transform

To take full advantage of the fact that only additions and subtractions are needed and reduce the number of operations required, it is necessary to use the Fast Hadamard Transform (FHT) algorithm. This will also eliminate the risk of running out of memory when storing the N_n matrix, which may become extremely large when long impulse responses need to be measured. In room acoustics the impulse response length is often on the order of 2 seconds. Considering a sampling frequency of 48,000Hz, the m-sequence needed must be at least order 17 and the $\boldsymbol{N}_n$ matrix will contain 2^{18} elements. The FHT method is described in [24] and [27]. The increase in computational power of low cost computers over the past two decades has also allowed the FFT technique to be used for many deconvolution calculations [28].

1.3.2. Swept sine

Alternatively, an exponential sine sweep (ESS) can be used as the excitation signal; the excitation signal is defined in Equation 1.13.

$$x(t) = \sin\left[\frac{\omega_1 T}{\ln\left(\frac{\omega_1}{\omega_2}\right)}\left(\exp\left(\frac{t}{T}\ln\left(\frac{\omega_2}{\omega_1}\right)\right) - 1\right)\right] \tag{1.13}$$

The exponential sine sweep starts at angular frequency ω_1, ends at angular frequency ω_2 and has a length of T seconds.

The swept sine method has the ability to separate the harmonic distortion, introduced by the loudspeaker and amplifier, from the linear impulse response giving an improved signal-to-noise ratio. This is achieved by performing either a linear convolution of the measured microphone signal with a signal known as the inverse filter [29,30], or by zero-padding the microphone and excitation signals to double their length and performing the deconvolution in the frequency domain [31]. The inverse filter is generated by reversing the excitation signal along the time axis and modulating the amplitude to compensate for the varying energy through the sweep.

By performing the deconvolution using one of the above two techniques the non-linear components of the system response are placed in the first half of the resulting impulse response signal. The linear impulse response can then be separated from the harmonic distortion products using an appropriate time window.

1.3.3. Considerations when using MLS and ESS

Distortion immunity

Impulse response measurements made using the ESS technique allow the distortion products to be removed from the linear impulse response of the system under test, the measurement will then only be limited by the background noise. Measurements made using the MLS technique cause the distortion products to be distributed throughout the resulting impulse response as spurious peaks, and the maximum achievable signal-to-noise ratio will be limited by the distortion products.

Synchronous averaging will not remove the distortion products from impulse responses measured using the MLS techniques as they are completely correlated with the excitation signal [31].

Time varying systems

Both techniques suffer problems when the system under test is even slightly time-variant [28, 32, 33]. This is the case when performing measurements outdoors where air movement and temperature drifts occur. The ESS is more immune to these effects than the MLS technique. The impulse responses resulting from measurements using the MLS technique tends to spread the energy throughout the time domain; measurements using the ESS technique give impulse responses that are more consistent with measurements made under time-invariant conditions [30].

Furthermore, problems with synchronous averaging result when the system under test is time varying. In this case a single period of a longer duration excitation signal will provide improved results compared to multiple periods of a shorter excitation signal [29, 30, 33]. The use of longer excitation signals will require more computational power than several periods of a shorter duration signal. This has become less of a concern with modern high performance personal computers, and the use of the fast Fourier transform (FFT) and other fast convolution algorithms [34].

Impulsive noise

MLS and ESS techniques both have good immunity to background noise due to the relatively large amount of energy used to excite the system, as well as synchronous averaging when appropriate. Impulsive noises (e.g. truck-trailer rattle) are treated effectively by the MLS technique, where the energy is distributed evenly throughout the time domain [35]. Measurements made using the ESS technique can be influenced by impulsive noise, however, when only a short segment of the impulse response is of interest the negative effects are limited [33]. Farina [30] and Ciric *et al.* [36] give methods to reduce the effects of impulsive noise on the resulting impulse response. These are generally aimed at applications in room acoustics where longer duration impulse responses are involved.

1.4. Signal-to-Noise Ratio

EN 1793-6:2012 states that the effective signal-to-noise ratio, taking into account sample averaging, must be made greater than 10 dB over the entire measurement frequency range; however, no information is given regarding the manner in which this "effective signal-to-noise ratio" should be calculated. Clearly the calculated value will vary depending on the method chosen.

Recently a method for calculating the signal-to-noise ratio has been proposed that makes use of two 3.5 millisecond segments of an impulse response, one representing the background noise and the other representing the transmitted signal [37]. The background noise segment is taken from the part of the impulse response that precedes the arrival of the transmitted sound, hence limiting the segment length to 3.5 milliseconds (Figure 1.8) and giving the calculation a low frequency limit of 400 Hz. The researchers propose an equation for the calculation of the signal-to-noise ratio at a particular microphone that uses the energy in these two segments of the impulse response (Equation 1.14). The signal-to-noise ratio in each one-third octave band may be calculated by removing the frequency band summation.

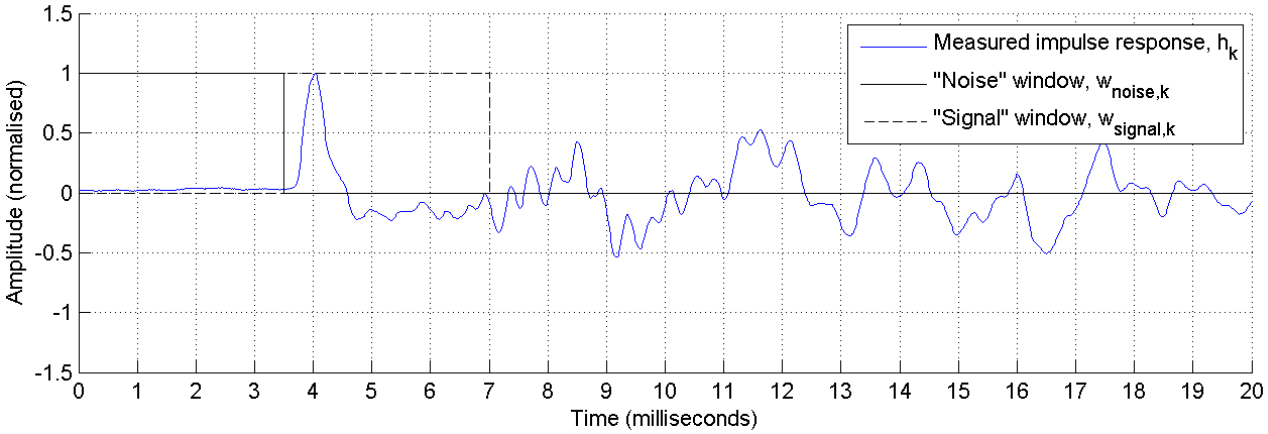

Figure 1.8.: Signal-to-noise ratio calculation method defined in [37], valid above 400 Hz

$$\mathrm{SNR}_{SI,k} = 10\log_{10}\left\{\frac{\sum_{j=26}^{37}\int\limits_{\Delta f_j}\left|F[h_k(t)w_{signal,k}(t)]\right|^2\,\mathrm{d}f}{\sum_{j=26}^{37}\int\limits_{\Delta f_j}\left|F[h_k(t)w_{noise,k}(t)]\right|^2\,\mathrm{d}f}\right\} \tag{1.14}$$

where

$h_k(t)$ is the measured impulse response at the kth microphone position

$w_{signal,k}(t)$ is the time window for the signal evaluation of the impulse response, equal to 1 from 3.5 ms to 7 ms and zero elsewhere

$w_{noise,k}(t)$ is the time window for the background noise evaluation of the impulse response, equal to 1 from 0 ms to 3.5 ms and zero elsewhere

j is the index of the one-third octave frequency bands between 400 Hz and 5 kHz

F is the symbol of the Fourier transform

Δf_j is the bandwidth of the jth one-third octave band

2. Measurement System

2.1. System Hardware

The requirements of the measurement system's electro-acoustical hardware are outlined in EN 1793-6:2012. The measurement system consists of:

- an electrical signal generator
- a power amplifier and loudspeaker
- microphones and microphone amplifiers
- a signal analyser capable of preforming transformations between the time and frequency domains

The components of the electro-acoustical system are shown in Figure 2.1.

Measurement of sound in the 100 Hz to 5 kHz one-third octave bands is required (88 Hz to 5650 Hz). The complete measurement system must meet the requirements of an IEC 61672 type 1 instrument [38], except for the microphone which may meet the requirements of a type 2 instrument having a maximum diaphragm diameter of $^1/_2$ inch.

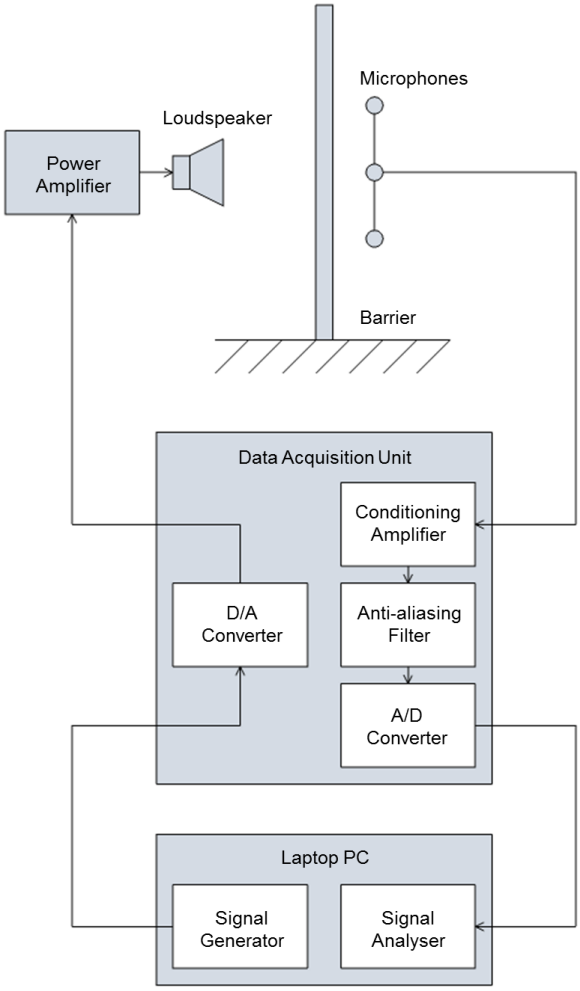

Figure 2.1.: Schematic diagram of the electro-acoustical system

2.1.1. Data acquisition unit

A Brüel & Kjær PULSE C-frame was chosen for the data acquisition unit. The unit is field portable and contains a number of the electro-acoustical components required in a single unit (Figure 2.2). Its specifications are included in Table 2.1.

Figure 2.2.: Brüel & Kjær PULSE C-frame

Table 2.1.: Brüel & Kjær PULSE C-frame specifications

PULSE modules:	B&K type 7539
	B&K type 3038
Number of input channels:	17
Number of output channels:	1
Frequency range:	0 Hz - 25.6 kHz
Input connectors:	17× LEMO
Output connectors:	1× BNC
Sampling rate:	65,536 Hz
Anti-aliasing filter:	3^{rd} order Butterworth

2.1.2. Loudspeaker and amplifier

The loudspeaker must consist of a single driver, contained in a sealed enclosure. Electrically active or passive components may not be used in the loudspeaker as they can affect the frequency response of the whole system [9]. Furthermore, the loudspeaker must have a smooth magnitude frequency response throughout the measurement range, resulting in a free-field impulse response with a maximum length of 3 milliseconds.

A 12 inch diameter JBL 2262H driver was acquired, having a maximum power capacity of 600 Watts. The enclosure was constructed from 12 mm thick MDF with overall dimensions of 400mm × 400mm × 450mm and filled with fibreglass wool (Figure 2.3).

Figure 2.3.: Loudspeaker

Impulse response measurements were conducted to verify that the loudspeaker met the requirements of EN 1793-6:2012. These results are presented in Chapter 3.

2.1.3. Microphones

The test method requires that measurements be conducted at nine points on the measurement grid, either simultaneously or by using a single microphone and performing measurements at each position individually. In order to reduce the measurement time during field measurements, possibly in hazardous environments near live traffic lanes, it was decided that nine microphones should be used.

According to EN 1793-6:2012 the microphones to be used in the measurement system are to be a minimum of type 2 with a maximum diaphragm diameter of 1/2 inch. Brüel & Kjær type 4189 microphones with type 2669-C preamplifiers were chosen over the lower cost 1/4 inch array microphones as they have superior sensitivity and noise-floor specifications. The microphone specifications are listed in Table 2.2.

Table 2.2.: Microphone specifications

Sensitivity:	50 mV/Pa
Frequency range:	6.3 Hz - 20 kHz
Dynamic range:	15.2 - 146 dB
Optimised:	Free-field
Polarisation:	Pre-polarised

2.1.4. Microphone array

A microphone array structure was designed and manufactured. The array was required to securely hold the nine microphones, be easy to assemble and have no effect on the measured impulse response (reflections from the array structure must be sufficiently weak). The microphone array is shown in Figure 2.4. The array is easily disassembled and packed into a transport case.

Results of the microphone array reflection measurements are presented in Chapter 3 along with other system validation test results.

A microphone clip was designed as part of the microphone array to securely hold the microphones (Figure 2.5). It consists of an aluminium cylinder with two internal groves that locate o-rings. The o-rings provide an interference fit with the 1/2 inch microphones.

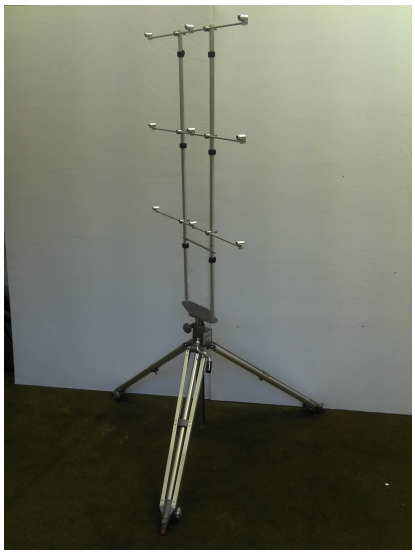

Figure 2.4.: Microphone array

Figure 2.5.: Microphone clip, internal o-rings ensure that the microphone is held securely

2.2. Signal Processing

Data analysis was conducted in MATLAB. In addition to the signal processing tasks, MATLAB has the capability of communicating with the Brüel & Kjær PULSE C-frame through its LabShop software using Microsoft Windows Object Linking and Embedding (OLE). An overview of the signal processing structure is show in Figure 2.6.

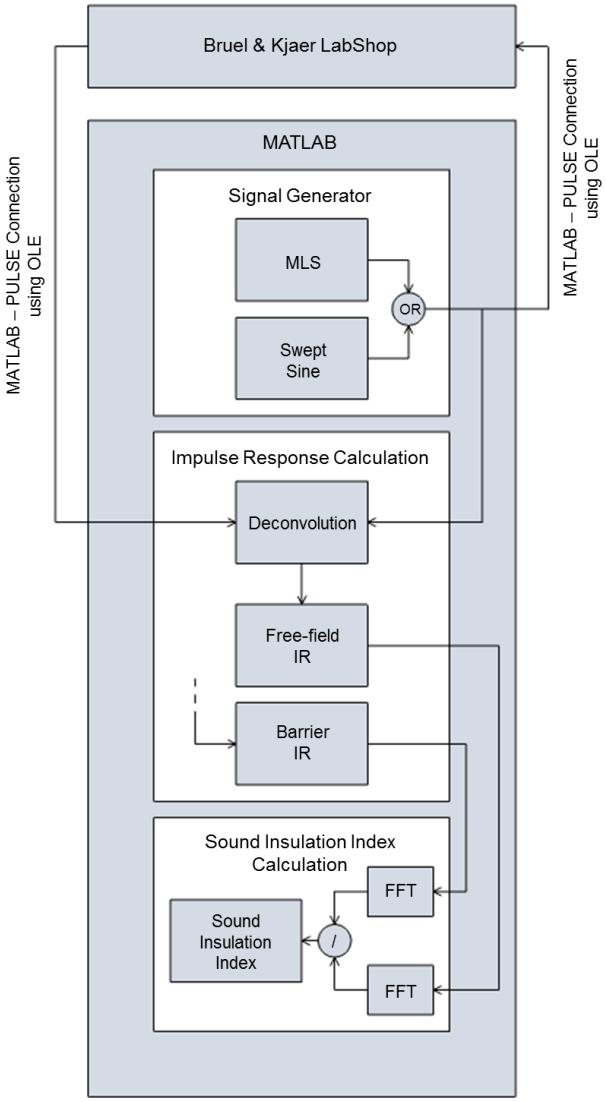

Figure 2.6.: Signal processing overview

2.2.1. Signal generator

The generation of the excitation signals is performed by a MATLAB code that allows the generation of various length MLS or ESS signals. There is a limit of 30.5 seconds on the length of the excitation signal that can be stored on the Brüel & Kjær PULSE C-frame, and should be considered when choosing the period length and number of periods.

Maximum length sequences

The MLS excitation code permits the generation of signals of order 3 through order 16 (length 7 through 65,535), with a specified number of periods. An additional period of MLS is added to the beginning of the excitation signal in order to stabilise the system [35]; this first period is discarded during the calculation of the impulse response.

In addition to the excitation signal itself, the permutation matrices must be determined. The process is described in [24, 27]; from this a MATLAB code was developed to determine the permutation matrices for a given MLS excitation signal.

Exponential swept sine

The ESS excitation code permits the generation of signals of any length, with a specified number of periods. The deconvolution is performed in the frequency domain so an inverse filter does not need to be calculated.

2.2.2. Impulse response calculation

Two methods were used to calculate the impulse responses from the microphone signal, this depended on the choice of excitation. The MLS impulse response measurement method makes use of the fast Hadamard transform (FHT) algorithm to perform the required cross-correlation between the measured and excitation signals. The ESS impulse response measurement method makes use of the fast Fourier transform (FFT) algorithm and inverse FFT to perform the deconvolution in the frequency domain. Generally, several periods of the excitation signal are

used to increase the signal-to-noise ratio, therefore the recorded microphone signals are first split by period and averaged before calculating a single impulse response for each of the nine microphone positions.

2.2.3. Sound insulation index

The sound insulation index is calculated for a specific pair of free-field and barrier impulse responses at each of the nine microphone positions. The results are then logarithmically averaged to give the mean sound insulation index as a function of frequency. The single number rating of airborne sound insulation is calculated from the frequency dependent sound insulation index.

2.2.4. File management and user interface

A set of graphical user interfaces (GUI) were developed in MATLAB to simplify the amount of data handling required by the operator while in the field. These integrate all of the signal processing tasks, allowing:

- generation of the excitation signal (Figures 2.7 and 2.8)
- documentation of global measurement details, eg. name, location, measurement data folder, panel dimensions
- documentation of individual impulse response measurement details, eg. microphone height, environmental conditions
- initialisation of the impulse response measurement, sending the excitation signal to PULSE and saving the microphone signals as a 9 channel wave file in the measurement data folder
- calculation of the impulse responses from the recorded microphone signals
- positioning of the Adrienne temporal window for each impulse response
- calculation of the sound insulation index and single number rating
- generation of a test report

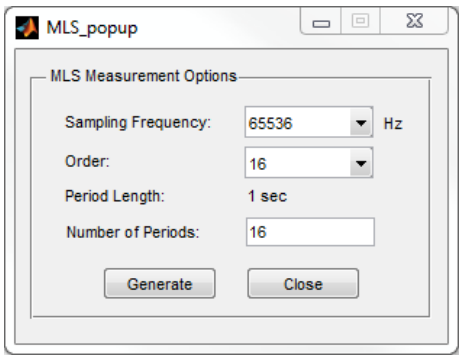

Figure 2.7.: MLS excitation signal generator

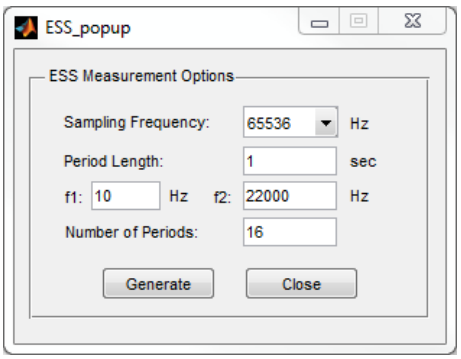

Figure 2.8.: ESS excitation signal generator

A screen shot of the main GUI is shown in Figure 2.9. Instructions on how to use the GUI are included in Appendix B.

The data files for each measurement session are stored in a single folder, the *measurement data folder*. The folder contains:

- excitation signal (wave file) with associated files required for the deconvolution process
- recorded microphone signals (9 channel wave files)
- measurement data file (*data_file.mat*) containing the calculated impulse responses, airborne sound insulation data and measurement details
- test report (latex files), if they have been generated

A full list of the data files contained in the *measurement data folder* is included in Table B.1, Appendix B.

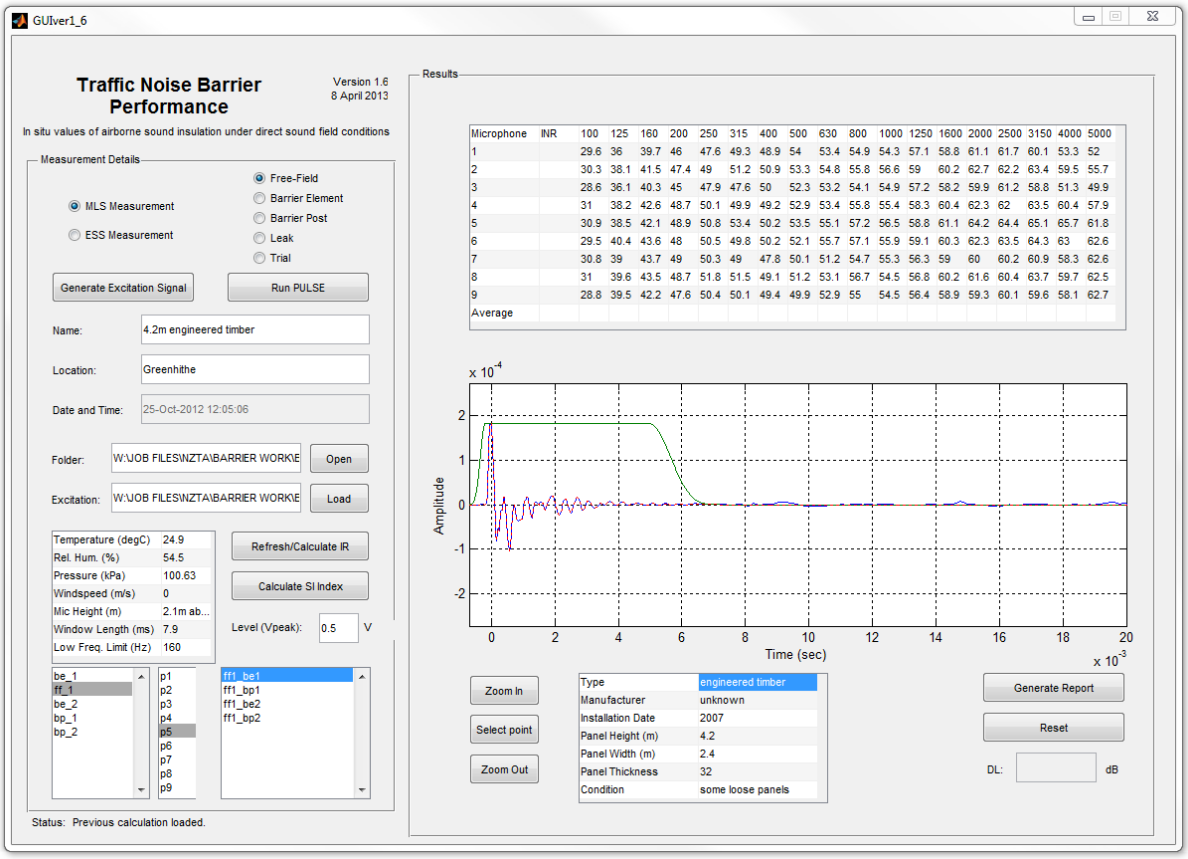

Figure 2.9.: Main graphical user interface

3. System Validation

Impulse response measurements were performed on various parts of the system to verify that the requirements of EN 1793-6:2012 were being met and that the influence of any reflections from the hardware would have a negligible effect on the airborne sound insulation measurements. The impulse response measurements were performed inside an anechoic chamber, using Brüel & Kjær Dirac 4.1 on a laptop PC. A Brüel & Kjær type 2260 sound level meter was used as an interface between the laptop PC and a Brüel & Kjær type 4189 microphone. The loudspeaker drivers were powered by a QSC GX3 amplifier. Unless otherwise stated, impulse response measurements were performed using a maximum length sequence (MLS) excitation signal of length 5.46 seconds, with 3 pre-averages to increase the signal-to-noise ratio. The microphone was located 1.25 m in front of the loudspeaker driver (on axis), as shown in Figure 3.1.

3.1. Loudspeaker Impulse Response

The impulse responses of three loudspeakers were measured to verify that the specifications of EN 1793-6:2012 were being met. The microphone was positioned 1.25 m in-front of the loudspeaker (on-axis) and held in a microphone clip attached to a standard microphone stand (Figure 3.1). The requirements are listed in Section 4.2.2 of EN 1793-6:2012; the loudspeaker must:

- consist of a single driver contained in a sealed enclosure
- be constructed without any electrically active or passive components that can affect the frequency response of the whole system
- have a smooth magnitude frequency response throughout the measurement range, resulting in a free-field impulse response with a maximum length of 3 milliseconds

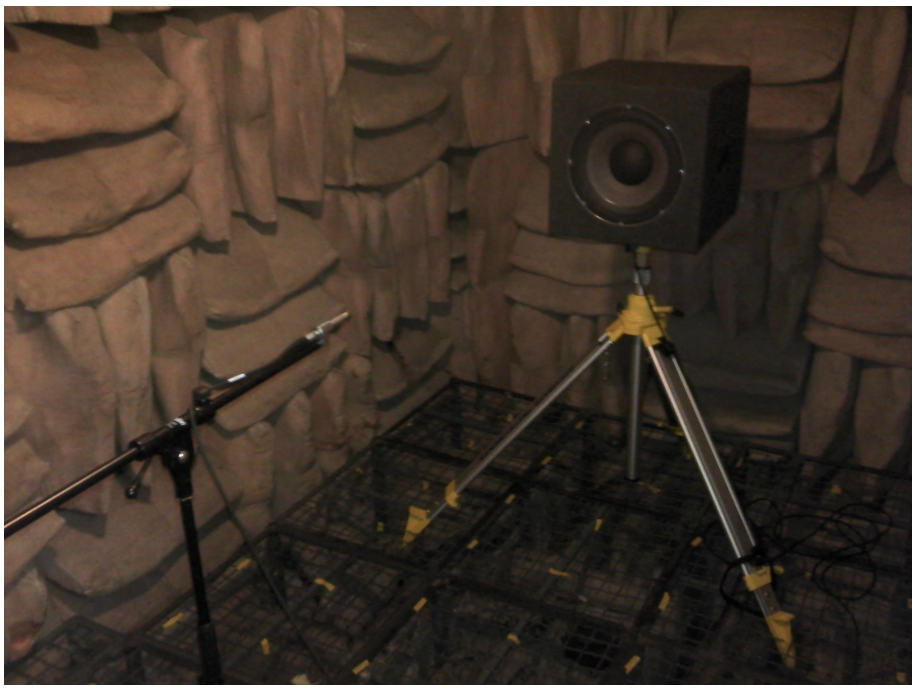

Figure 3.1.: Loudspeaker impulse response measurement setup in the anechoic chamber

3.1.1. Presentation of results

In the graphs below, the measured impulse responses are presented as follows:

- the Adrienne temporal window has been applied to eliminate any late room reflections and background noise, giving a smoother frequency response. This is applied in the same manner as it is to the free-field impulse responses measured according to EN 1793-6:2012, the window is shown in Figure 3.2
- the impulse responses are also presented as pressure squared to make the peaks more recognisable

The frequency response measurements are presented as follows:

- presented in each one-third octave band as $20\log_{10}(p_{rms})$, and shifted vertically such that the level at 1 kHz corresponds to 0 dB

3.1.2. 600 Watt loudspeaker

The loudspeaker consists of a $455 \times 400 \times 400$ mm MDF enclosure completely filled with fibreglass wool. A 12 inch diameter JBL type 2262HPL driver is mounted in the centre of the 400×400 mm face. The impulse response of the loudspeaker is shown in Figures 3.2.

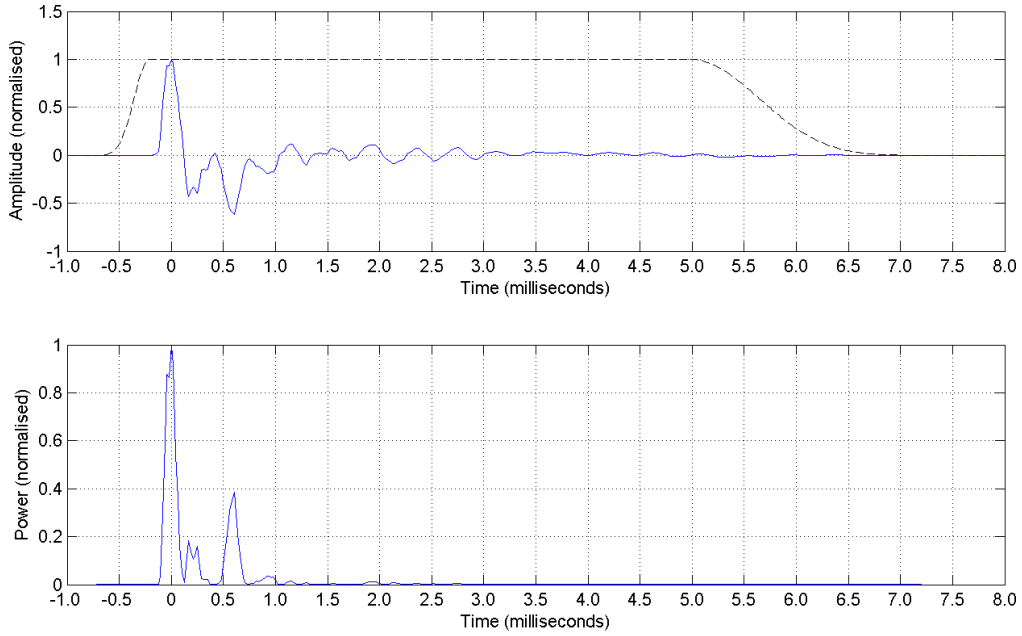

Figure 3.2.: Impulse response of the 600 Watt loudspeaker, the Adrienne temporal window is overlaid for reference

The secondary peaks in the impulse response are an effect of the loudspeaker driver. Tests were performed using different source-receiver distances, excitation signals, amplifiers and enclosure packing with no significant changes to the resulting impulse response. The impulse response amplitude drops by 29 dB 3 milliseconds after the direct peak. The frequency response is shown in Figure 3.5 and has a magnitude variation of ± 15 dB measured in the one-third octave bands between 100 Hz and 5 kHz. The loudspeaker characteristics are considered adequate for the purposes of EN 1793-6:2012.

3.1.3. 90 Watt loudspeaker

The loudspeaker consists of a $250 \times 250 \times 250$ mm MDF enclosure completely filled with fibreglass wool. An 8 inch diameter CW2189 driver is mounted in the centre of one face. The impulse response of the loudspeaker is shown in Figures 3.3.

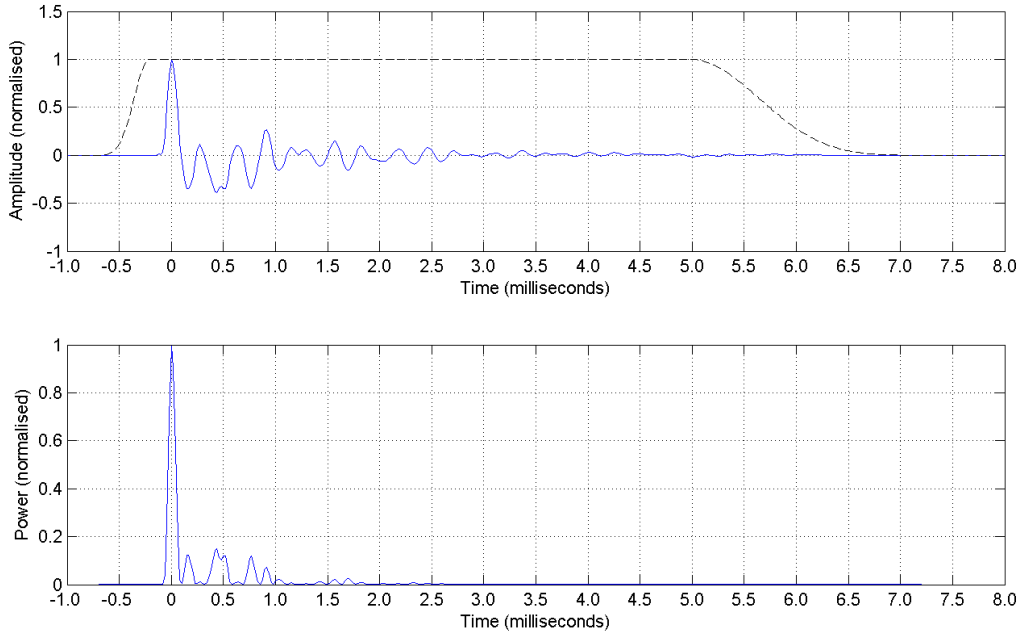

Figure 3.3.: Impulse response of the 90 Watt loudspeaker

The impulse response amplitude drops by 27 dB 3 milliseconds after the direct peak. The frequency response is shown in Figure 3.5 and has a magnitude variation of ± 15 dB measured in the one-third octave bands between 100 Hz and 5 kHz. The loudspeaker characteristics are considered adequate for the purposes of EN 1793-6:2012, however, the low power capacity may limit the maximum measurable sound insulation index due to signal-to-noise requirements.

3.1.4. 80 Watt loudspeaker

The loudspeaker consists of a $250 \times 250 \times 250$ mm MDF enclosure completely filled with fibreglass wool. A 6 inch diameter Beta Three 06LB050-U driver is mounted in the centre of one face. The impulse response of the loudspeaker is shown in Figures 3.4.

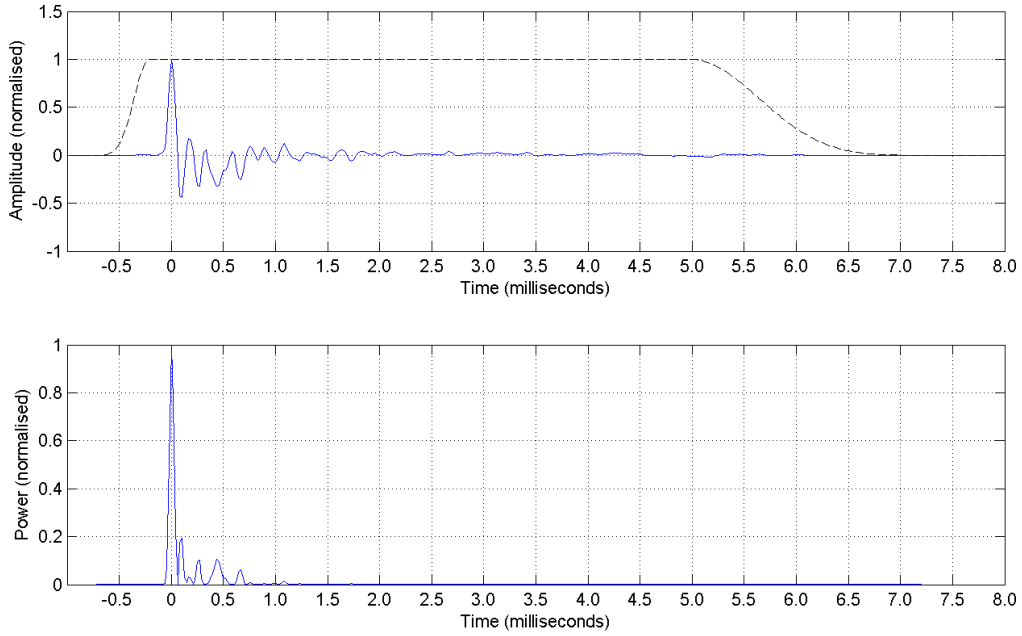

Figure 3.4.: Impulse response of the 80 Watt loudspeaker

The impulse response amplitude drops by 31 dB 3 milliseconds after the direct peak. The frequency response is shown in Figure 3.5 and has a magnitude variation of ±17 dB measured in the one-third octave bands between 100 Hz and 5 kHz. The loudspeaker characteristics are considered adequate for the purposes of EN 1793-6:2012, again the low power capacity may limit the maximum measurable sound insulation index.

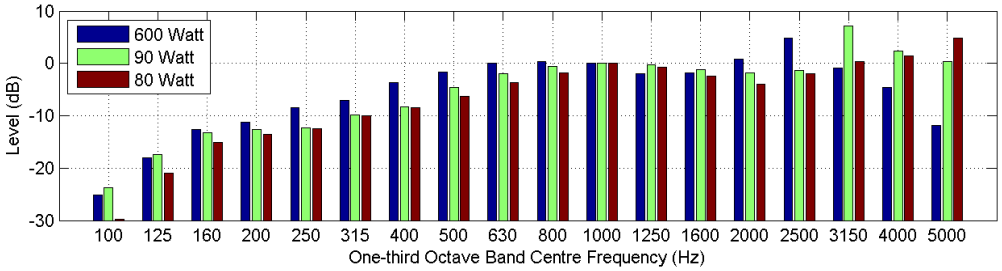

Figure 3.5.: Frequency response of the three loudspeakers in one-third octave bands

The 600 Watt loudspeaker is the preferred choice due to its higher power capacity and consequent enhanced ability to meet the signal-to-noise ratio requirements.

3.2. Microphone Clip Reflections

Impulse response measurements were performed to ensure that no large reflections were introduced with the addition of the microphone clip (Figure 2.5). A Brüel & Kjær type 4189 microphone was held in a microphone clip attached to a standard microphone stand (Figure 3.1) and the impulse response of the 600 Watt loudspeaker measured. A second impulse response measurement was performed using a Brüel & Kjær type 2260 handheld analyser attached to a tripod. The Brüel & Kjær type 2260 measurement was used as a reference, as the hardware is designed to have minimal effect on the surrounding sound field [39].

The results are included in Figure 3.6 and show that the microphone clip has a negligible effect on the frequency response compared to measurements made using the Brüel & Kjær type 2260. The largest variation is 1.5 dB in the 5 kHz one-third octave band.

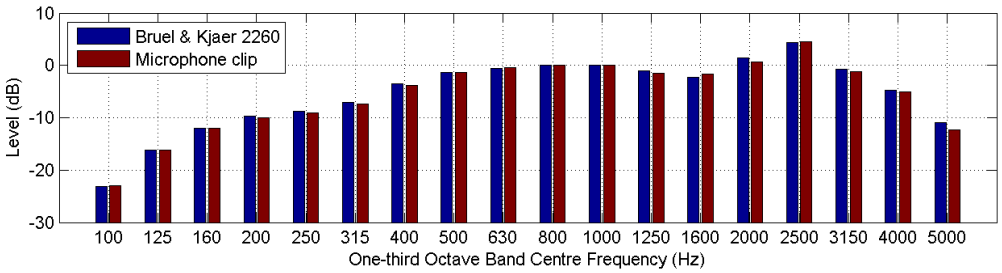

Figure 3.6.: Frequency response of the microphone clip in one-third octave bands

3.3. Microphone Array Reflections

Impulse response measurements were performed for several variations of the microphone array setup to check for the introduction of any large reflections. The reference case was that of the 600 Watt loudspeaker (Figure 3.2) with the microphone held in a microphone clip attached to a standard microphone stand (Figure 3.1).

Impulse responses were measured for the following cases; a) microphone in centre bottom position, b) microphone in centre bottom position with vertical struts covered with fibreglass, c) microphone in centre bottom position with base plate covered with fibreglass, d) microphone in centre bottom position with vertical struts and base plate covered with fibreglass. The four arrangements are shown in Figure 3.7.

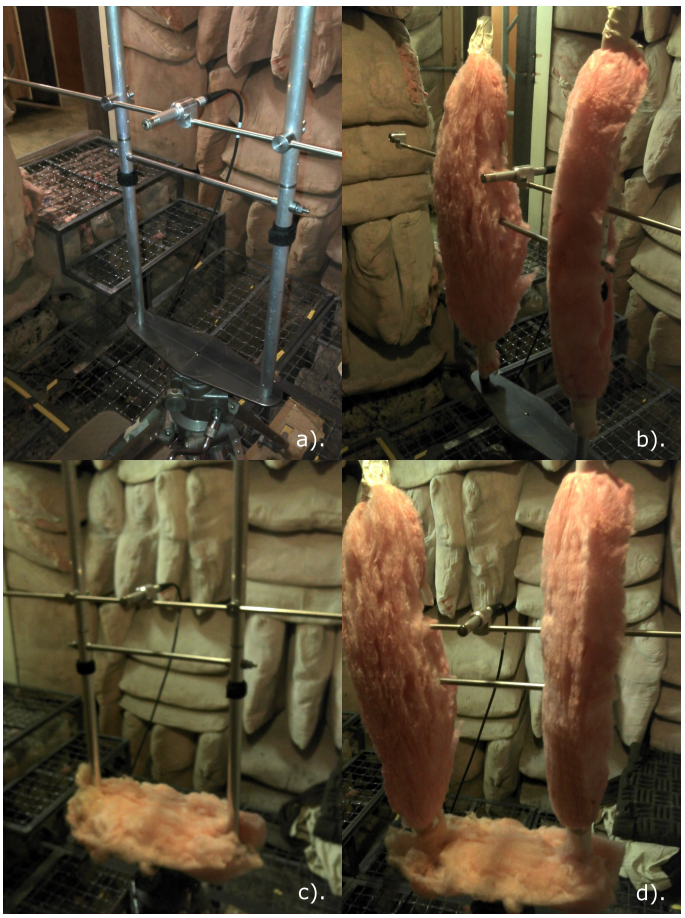

Figure 3.7.: Microphone array setups for impulse response measurements

The frequency response for setup a) is shown in Figure 3.8 along with the reference case. The largest variation is 1.2 dB in the 3.15 kHz one-third octave band. Similar results were obtained for setups b), c) and d); from the results it is concluded that any reflections off the microphone array will have an insignificant effect on the measured sound insulation index.

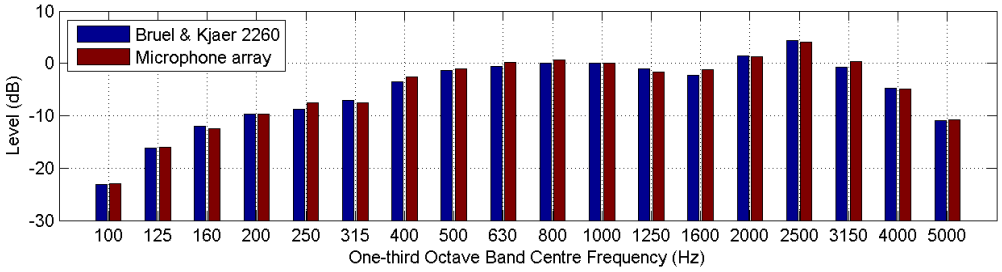

Figure 3.8.: Frequency response of the microphone array, setup a).

3.4. Effect of the Microphone Windshield

Windshields will be used during field measurements to reduce the effect of wind noise as air moves over the microphones. The impulse response of the 600 Watt loudspeaker was measured using a Brüel & Kjær type 4189 microphone with and without a windshield. The windshield can be seen to have an insignificant effect on the measured frequency response (Figure 3.9).

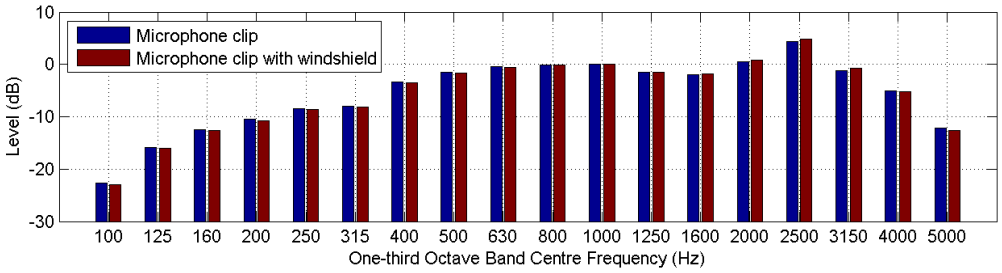

Figure 3.9.: Impulse response of the microphone with and without a windshield

3.5. Conclusions

Impulse response measurements were performed on three different loudspeakers to verify that they meet the requirements of EN 1793-6:2012. All of the loudspeakers had impulse response lengths of 3 milliseconds or less and relatively smooth frequency responses (maximum variation of ±17 dB in the measurement frequency range). The 600 Watt loudspeaker is the preferred choice due to its higher power capacity and consequent enhanced ability to meet the signal-to-noise ratio requirements.

The influence of the microphone clip was investigated by comparing impulse response measurements of the 600 Watt loudspeaker made using a Brüel & Kjær type 4189 microphone held in the microphone clip with measurements made using a Brüel & Kjær type 2260 handheld analyser. No significant variations were observed in the measured impulse responses and the frequency response showed a maximum variation of 1.5 dB in the 5 kHz one-third octave band. The microphone clip will therefore have a negligible influence on the measured impulse responses, with no significant reflections being introduced.

Impulse response measurements were performed for four different microphone array setups to check for any additional reflections. Fibreglass wool was attached to various parts of the

microphone array to reduce the amplitude of any undesirable sound reflections. A measurement using the Brüel & Kjær 2260 handheld analyser was used as the reference case. Only slight variations were observed in the measured impulse responses, with the frequency response of the untreated array having a maximum variation of 1.2 dB in the 3.15 kHz one-third octave band when compared to the reference case. Any reflections from the microphone array structure were therefore considered weak enough to have a negligible influence on the measured impulse responses.

A Brüel & Kjær type 4189 microphone with a 90 mm windshield was used to measure the impulse response of the 600 Watt loudspeaker. A maximum variation of 0.5 dB was observed in the 5 kHz one-third octave band when compared to the case of the Brüel & Kjær type 4189 microphone without a windshield. The windshield was considered to have a negligible influence on the measured impulse responses.

4. Field Measurements

4.1. Introduction

Airborne sound insulation measurements were performed on existing traffic noise barriers located along New Zealand State highways in the Auckland area. The work has provided details of the acoustic performance of a range of barrier types (concrete, engineered timber, plywood, slatted timber and acrylic), as well as experience with the practical aspects of performing field measurements using EN 1793-6:2012. Measurements were performed at eight sites. Table 4.1 contains a list of the measurements with the site classification; a map of the test locations is shown in Figure 4.1.

4.2. Practical Aspects

Being an in situ test method, the location of the traffic noise barrier dictates the safety, access and time requirements associated with each test. The NZ Transport Agency (NZTA) provided health and safety training, and access to the test sites.

4.2.1. Measurement equipment

The measurement equipment was packed into two Pelican travel cases, and the loudspeaker and tripods were packaged in cardboard boxes for transport between Christchurch and Auckland. Figure 4.2 shows the measurement equipment laid out on the ground at a test site.

Table 4.1.: Auckland test sites

Site Name	Material	Measurements	Site Classification
St Marys Bay	acrylic	2× panels 1× post	semi-static closure
Greenhithe	engineered timber	2× panels 2× posts	road inspection
Maioro Street	engineered timber	2× panels 2× posts	residential
Maioro Street	concrete	1× panel 1× post	residential
Hobsonville	plywood	2× panels	road inspection
Green Lane	concrete	1× panel 1× post	semi-static closure
Kingsland Cycleway	timber	2× panels	residential
Northern Busway	plywood	1× panel	road inspection

4.2.2. Test site classification

Sites where the operators were able to access both sides of the noise barrier on foot from local roads were classified as residential sites. An example of a residential site is shown in Figure 4.3.

Sites where the operators were able to park and work more than 5 metres away from the live traffic lane, with good protection being provided by crash barriers or road layout, were classified as road inspection test sites. All of these sites involved Level 3 roads (high volume, high speed multi-lane roads and motorways) and the operators were only permitted to work outside of peak traffic flows (9am to 3pm and 7pm to 6am). The Auckland Motorway Alliance (AMA) traffic management plan (TMP) for generic inspections was used (TMP-18261), with the Joint Transport Operations Centre (JTOC) being notified at the beginning and end of each testing session. An example of a road inspection site is shown in Figure 4.4.

Figure 4.1.: Map of the Auckland traffic noise barrier test sites. Map from Auckland Council GIS Viewer

Figure 4.2.: Measurement equipment

Figure 4.3.: Residential site layout, Kingsland Cycleway

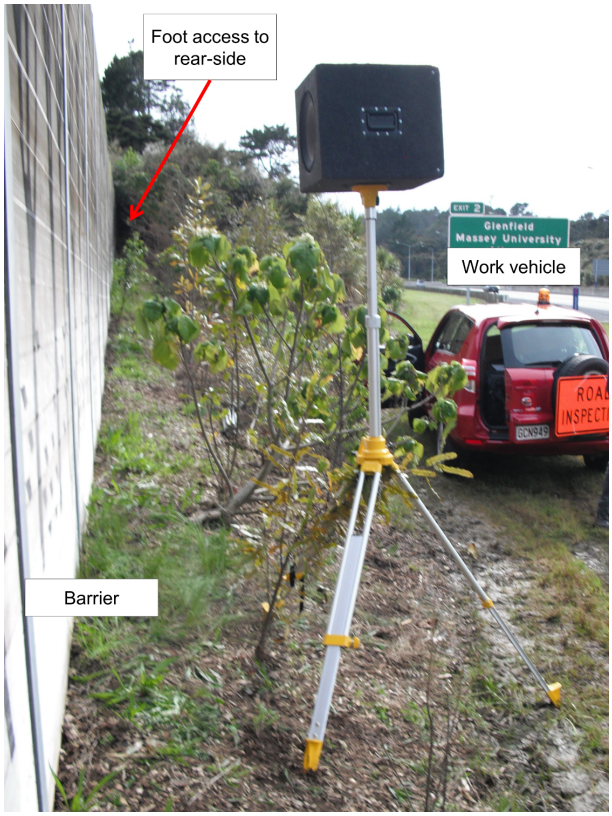

Figure 4.4.: Road inspection site layout, Greenhithe

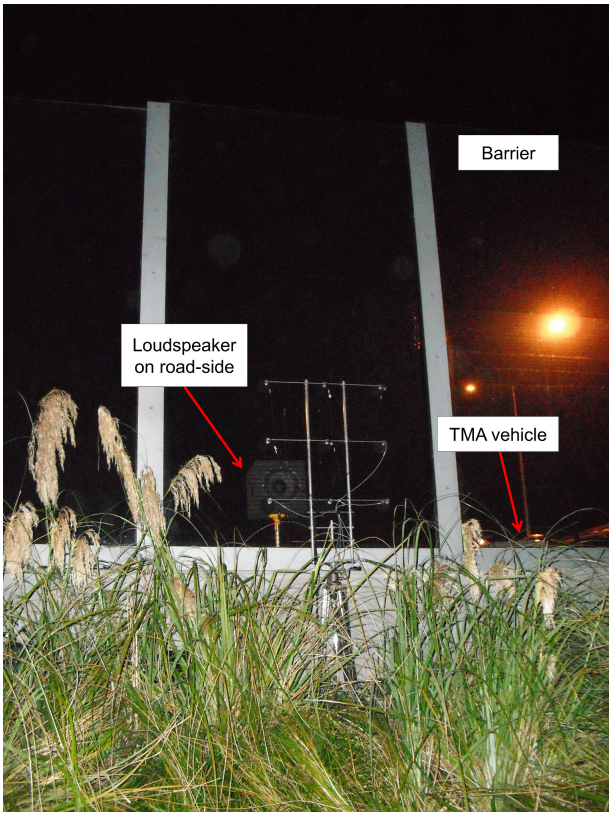

Figure 4.5.: Semi-static closure site layout, St Marys Bay

Sites where the operators had to work within 5 metres of the live lane and/or were not adequately protected by crash barriers or road layout were classified as semi-static closure sites. These sites required the use of mobile crash barriers, known as truck mounted attenuators (TMA), to protect the operators. The TMAs were only permitted to stop for 30 minutes at a time. Measurements at these sites had to be conducted during a night-time testing session (between 9pm and 5am) due to heavy traffic flows. An example of a semi-static closure site is shown in Figure 4.5.

4.2.3. Communication with residents

There was a possibility that the traffic noise barrier testing work would be noticed by nearby residents, both visibly and audibly. The NZTA Communications Team developed a communications plan for the project. The operators visited the test sites prior to performing the testing work to advise residents of the project and allow them to raise any concerns.

4.2.4. Time requirements

The time required to conduct the measurements depended on the ease of access to the specific site, Table 4.2 gives the approximate duration of each measurement activity.

Table 4.2.: Approximate time required to conduct a measurement

Activity	Time Required
setup	60 minutes
free-field/panel/post measurement	15 minutes each
pack up	30 minutes

4.3. Results

The sound insulation index and minimum signal-to-noise ratios are presented for each measurement position. A discussion of the results will be reserved for the next section.

4.3.1. 3.6 m acrylic barrier at St Marys Bay

The barrier is a single-leaf, reflective acrylic traffic noise barrier. The barrier height varies from 2 m to 5 m along its length. The element under test was 2 m wide by 3.6 m high, supported by T-section posts. The section of barrier is situated on the western side of SH1. Figure 4.6 shows the traffic noise barrier viewed from the road-side; the crosses mark the approximate positions of the loudspeaker/centre microphone axis.

Three measurements were performed at the St Marys Bay site. Element measurements were conducted with the measurement grid located horizontally in the middle of an element at a height of 1.25 m (element measurement, position 1) and at a height of 0.8 m (element measurement, position 3) above the concrete crash barrier. A post measurement was conducted with the measurement grid located in line with a post (post measurement, position 2) at a height of 0.8 m above the concrete crash barrier. The barrier element thickness is 15 mm.

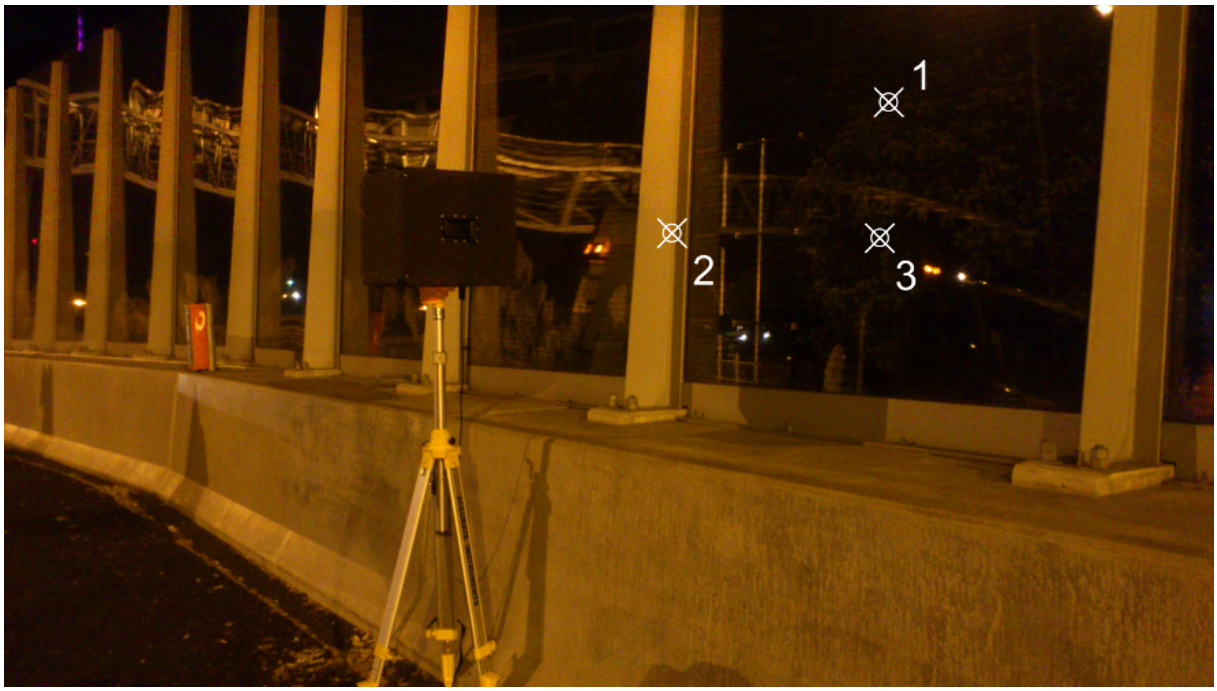

Figure 4.6.: Road-side view of the acrylic barrier at St Marys Bay, the crosses mark the measurement positions

The length of the Adrienne temporal window (T_w) used was adjusted to include or exclude the leakage components due to an air gap between the elements and the concrete crash barrier. The sound insulation index and minimum signal-to-noise ratios with the leakage excluded are presented in Figures 4.7 and 4.8, respectively.

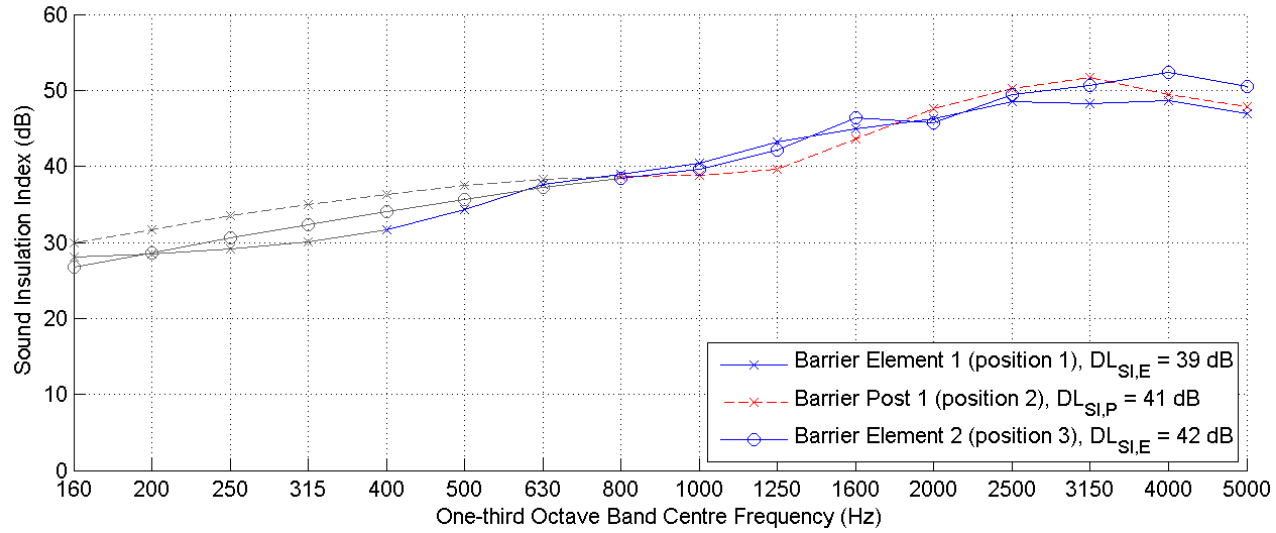

Figure 4.7.: Sound insulation index and single number rating at each measurement position on the St Marys Bay barrier, excluding the sound leakage component. The grey lines represent values below the low frequency limit of the measurement

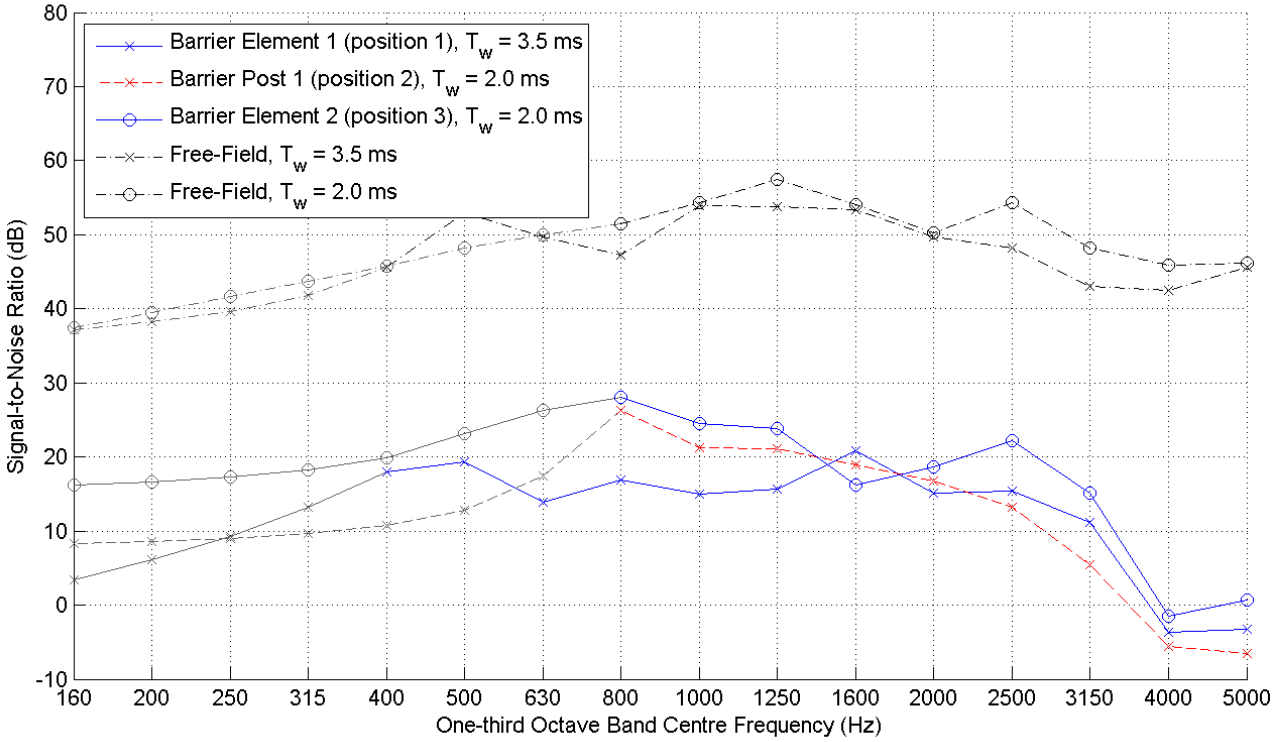

Figure 4.8.: Minimum signal-to-noise ratio at each measurement position on the St Marys Bay barrier, excluding the sound leakage component. The grey lines represent values below the low frequency limit of the measurement

The sound insulation index and minimum signal-to-noise ratios with the leakage included are presented in Figures 4.9 and 4.10, respectively.

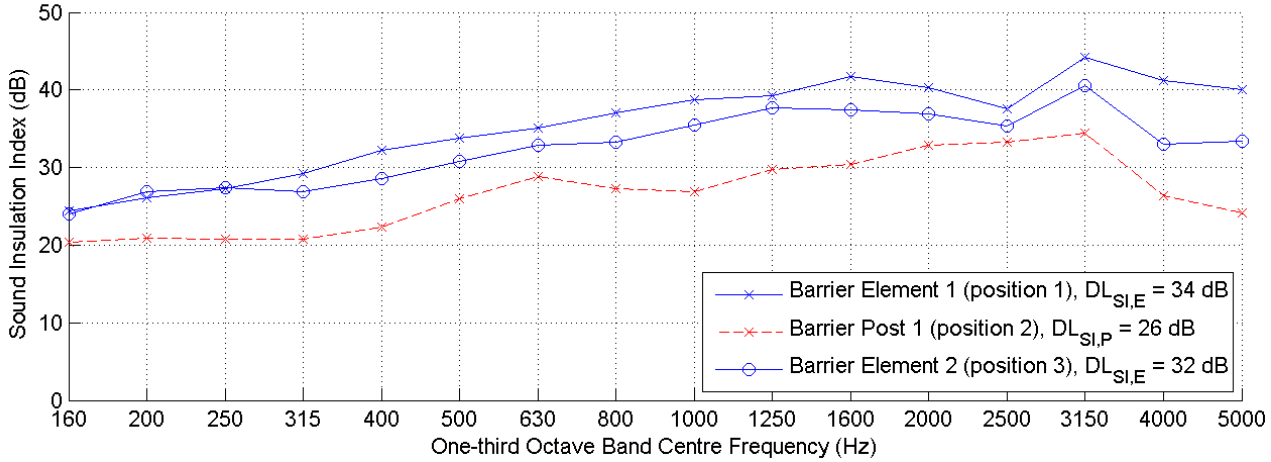

Figure 4.9.: Sound insulation index and single number rating at each measurement position on the St Marys Bay barrier, including the sound leakage component

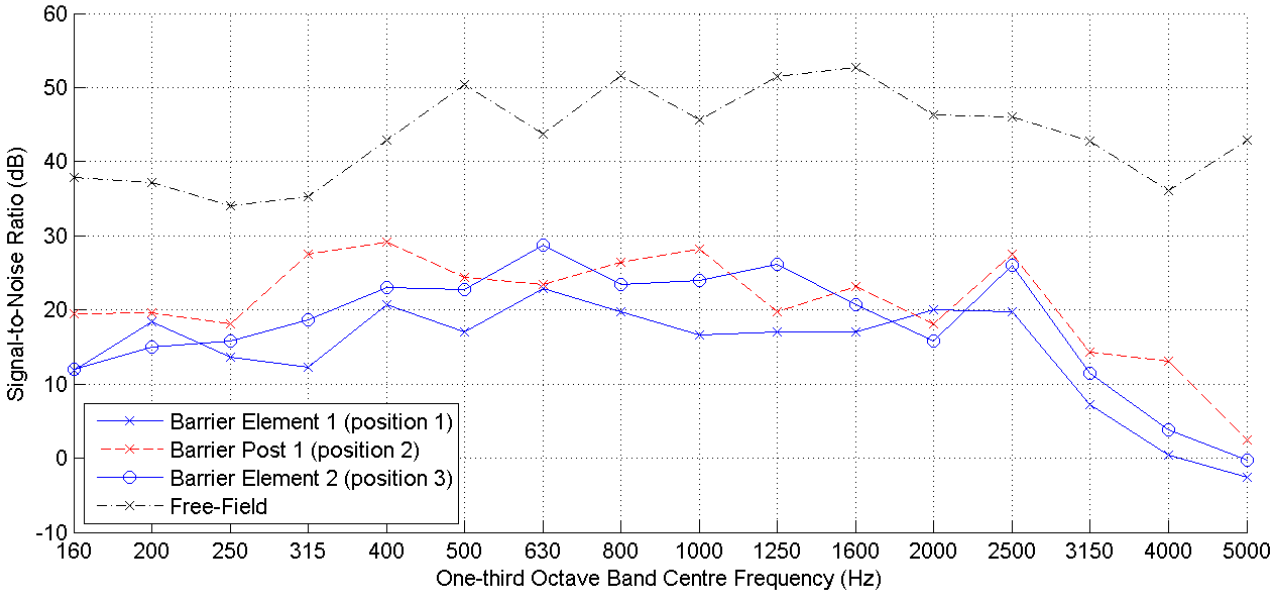

Figure 4.10.: Minimum signal-to-noise ratio at each measurement position on the St Marys Bay barrier, including the sound leakage component

4.3.2. 4.2 m engineered timber barrier at Greenhithe

The barrier is a single-leaf, reflective engineered timber traffic noise barrier. The element under test was 2.4 m wide by 4.2 m high, supported by I-section posts. The section of barrier is situated on the northern side of SH18. Figure 4.11 shows the traffic noise barrier viewed from the road-side; the crosses mark the approximate positions of the loudspeaker/centre microphone axis.

Four measurements were performed at the Greenhithe site. All measurements were conducted with a loudspeaker/centre microphone height of 2.1 m below the barrier top. Element measurements were conducted with the measurement grid located horizontally in the middle of an element (positions 1 and 3); post measurements were conducted with the measurement grid located in line with a post (positions 2 and 4). The barrier element thickness is 32 mm.

Figure 4.11.: Road-side view of the engineered timber barrier at Greenhithe, the crosses mark the measurement positions. Image from Google Maps

An Adrienne temporal window length of 7.9 milliseconds was used, giving a low frequency limit of 160 Hz. The sound insulation index and minimum signal-to-noise ratios are presented in Figures 4.12 and 4.13, respectively.

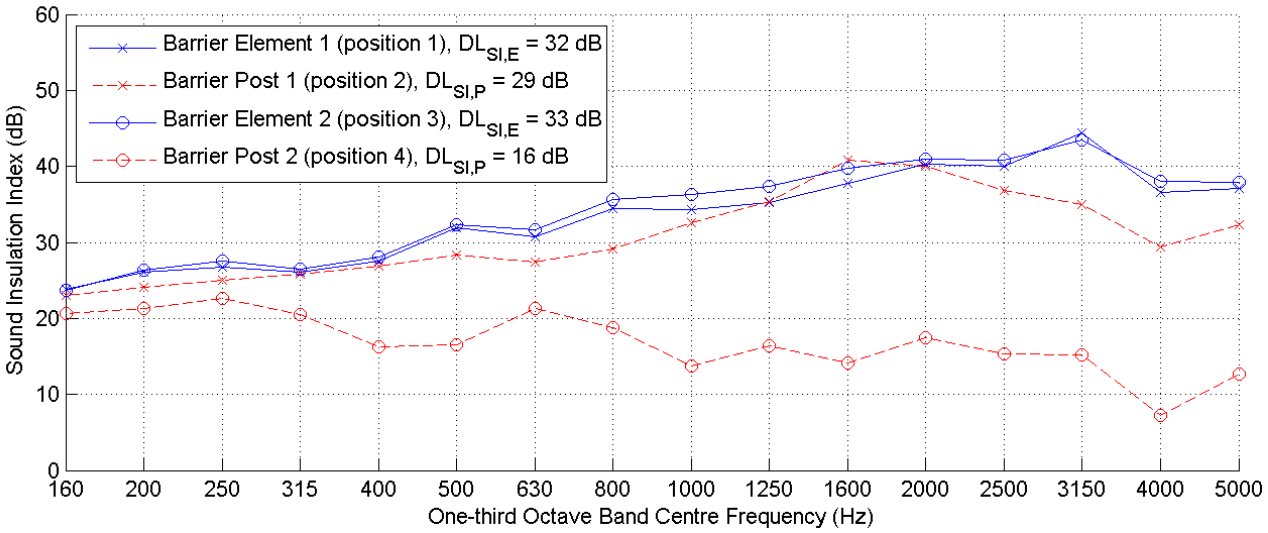

Figure 4.12.: Sound insulation index and single number rating at each measurement position on the Greenhithe barrier

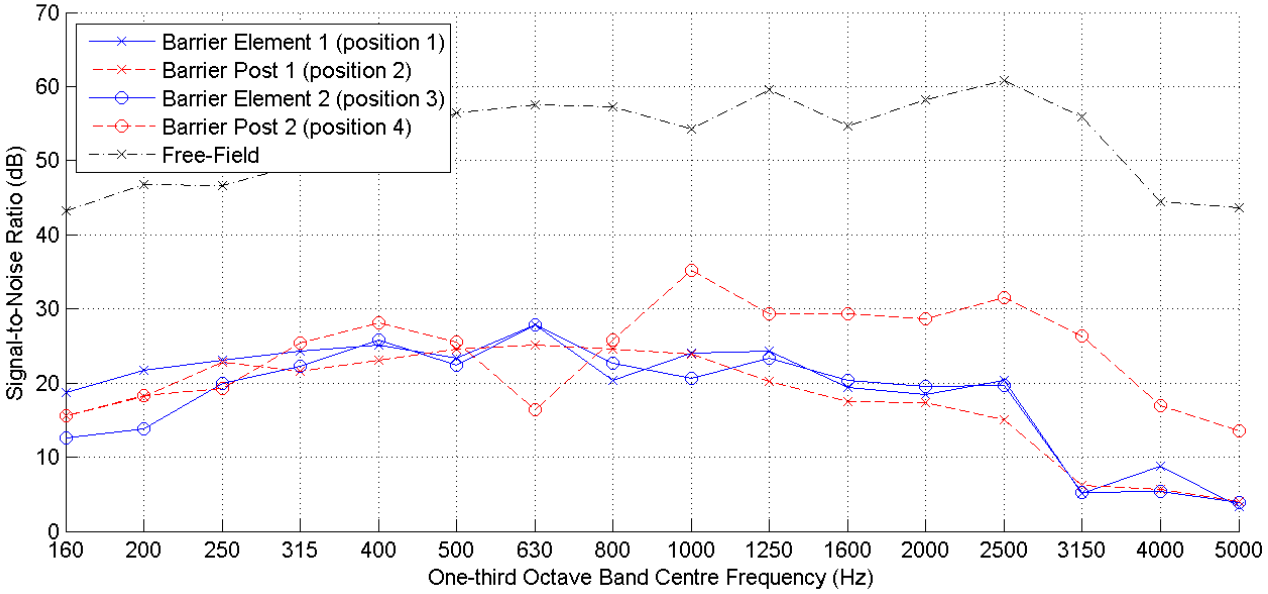

Figure 4.13.: Minimum signal-to-noise ratio at each measurement position on the Greenhithe barrier

4.3.3. 2.9 m engineered timber barrier at Maioro Street

The barrier is a single-leaf, reflective engineered timber traffic noise barrier. The element under test was 2.6 m wide by 2.9 m high, supported by I-section posts. The section of barrier is situated at the eastern end of Ernie Pinches Street. Figure 4.14 shows the traffic noise barrier viewed from the road-side; the crosses mark the approximate positions of the loudspeaker/centre microphone axis.

Four measurements were performed at the Maioro Street engineered timber site. All measurements were conducted with a loudspeaker/centre microphone height of 1.25 m below the barrier top. Element measurements were conducted with the measurement grid located horizontally in the middle of an element (positions 1 and 3); post measurements were conducted with the measurement grid located in line with a post (positions 2 and 4). The barrier element thickness is 32 mm.

Figure 4.14.: Road-side view of the engineered timber barrier at Maioro Street, the crosses mark the measurement positions

An Adrienne temporal window length of 4.0 milliseconds was used, giving a low frequency limit of 400 Hz. The sound insulation index and minimum signal-to-noise ratios are presented in Figures 4.15 and 4.16, respectively.

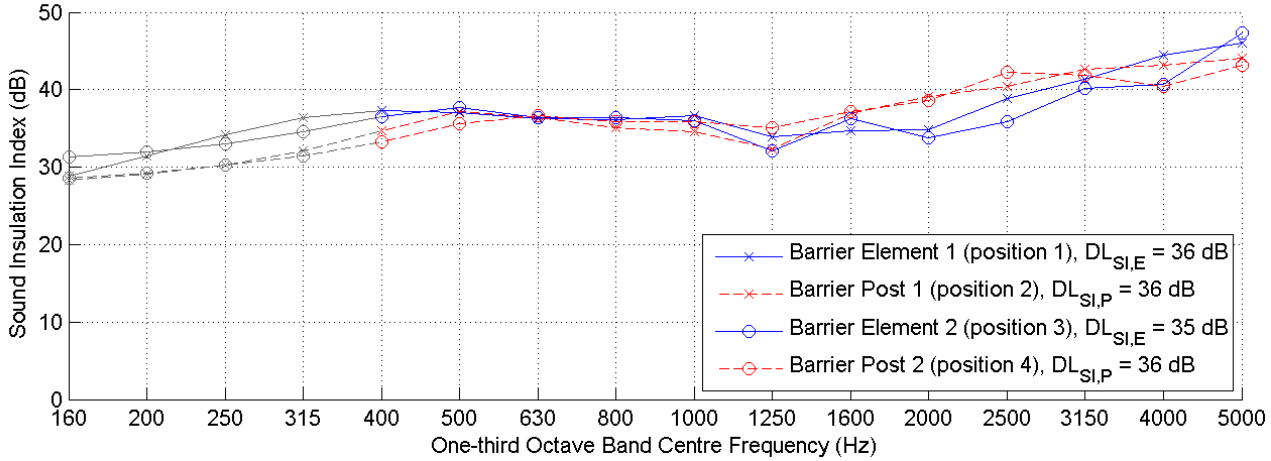

Figure 4.15.: Sound insulation index and single number rating at each measurement position on the Maioro Street engineered timber barrier. The grey lines represent values below the low frequency limit of the measurement

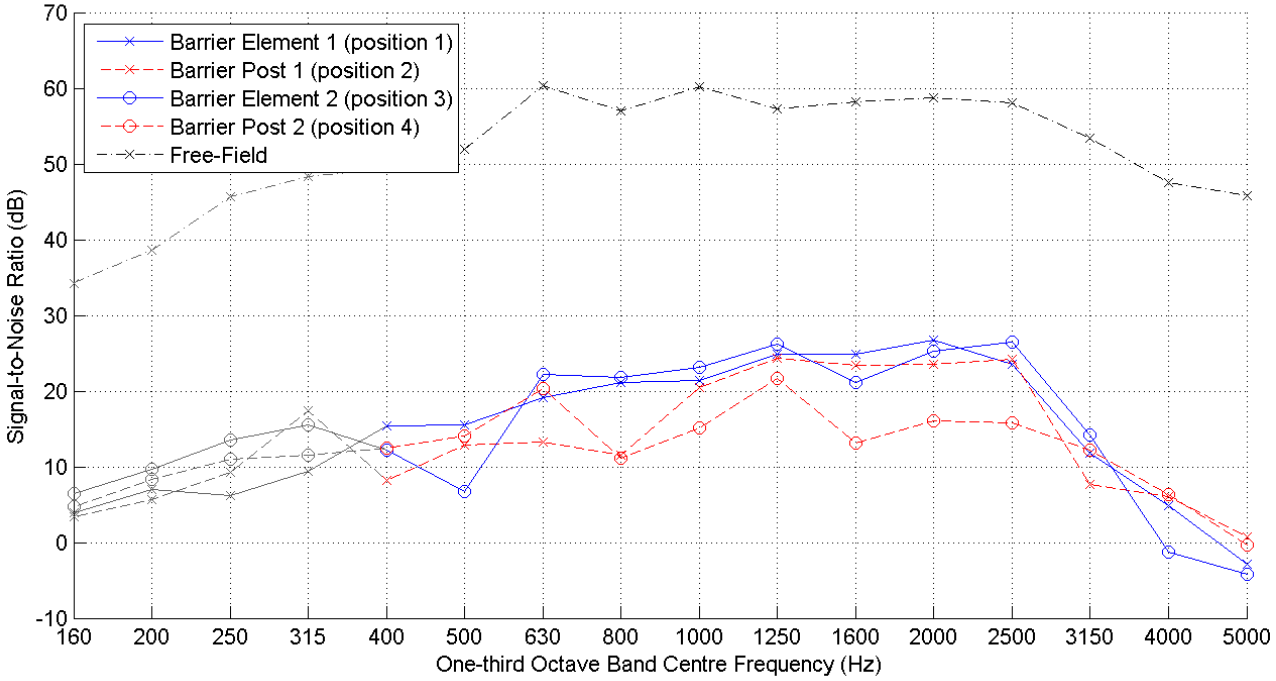

Figure 4.16.: Minimum signal-to-noise ratio at each measurement position on the Maioro Street engineered timber barrier. The grey lines represent values below the low frequency limit of the measurement

4.3.4. 3.2 m concrete barrier at Maioro Street

The barrier is a single-leaf, reflective concrete traffic noise barrier. Each element under test was 2.5 m wide by 3.2 m high, supported by I-section posts. The section of barrier is situated on the Maioro Street boundary of Christ the King School. Figure 4.17 shows the traffic noise barrier viewed from the road-side; the crosses mark the approximate positions of the loudspeaker/centre microphone axis.

Two measurements were performed at the Maioro Street concrete site. All measurements were conducted with a loudspeaker/centre microphone height of 1.55 m below the barrier top. The element measurement was conducted with the measurement grid located horizontally in the middle of an element (position 1); the post measurement was conducted with the measurement grid located in line with a post (position 2). The barrier element thickness is 150 mm.

Figure 4.17.: Road-side view of the concrete barrier at Maioro Street, the crosses mark the measurement positions

An Adrienne temporal window length of 5.5 milliseconds was used, giving a low frequency limit of 250 Hz. The sound insulation index and minimum signal-to-noise ratios are presented in Figures 4.18 and 4.19, respectively.

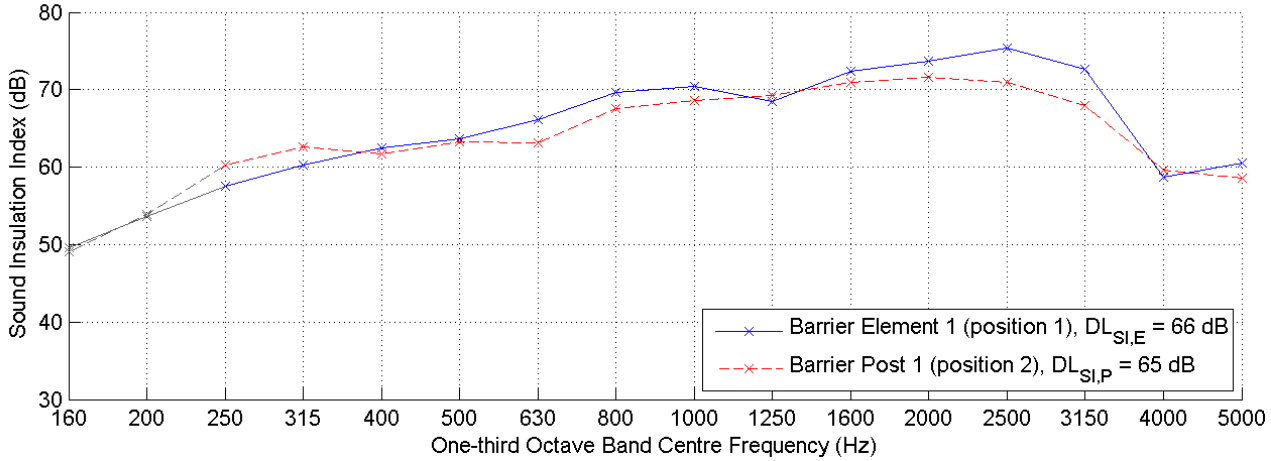

Figure 4.18.: Sound insulation index and single number rating at each measurement position on the Maioro Street concrete barrier. The grey lines represent values below the low frequency limit of the measurement

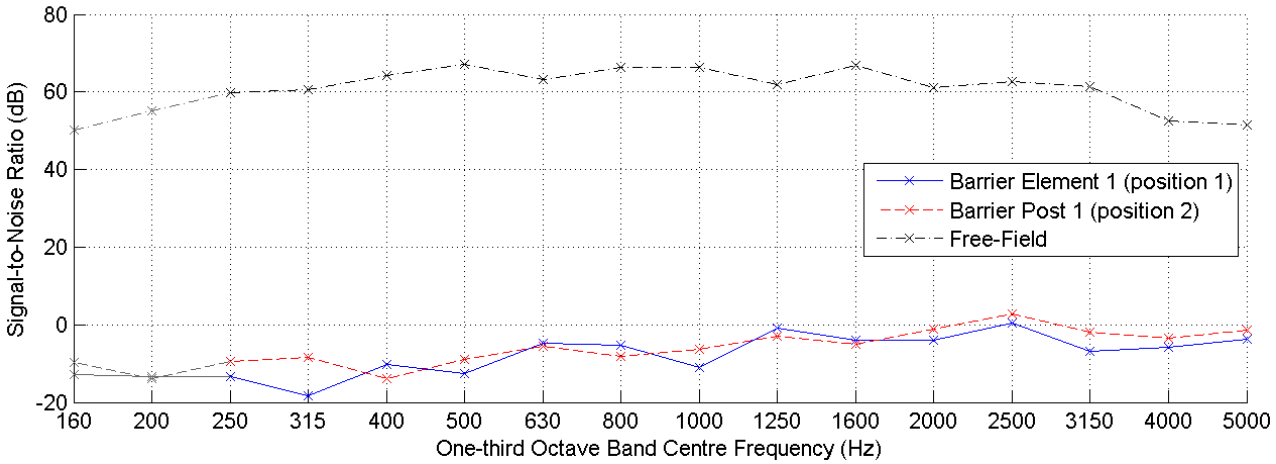

Figure 4.19.: Minimum signal-to-noise ratio at each measurement position on the Maioro Street concrete barrier. The grey lines represent values below the low frequency limit of the measurement

4.3.5. 3.9 m plywood barrier at Hobsonville

The barrier is a single-leaf, reflective plywood traffic noise barrier. The element under test was 2.4 m wide by 3.9 m high, constructed from three and a half 1.2 m by 2.4 m plywood sheets with lengths of 2×4 timber across the joints. The elements were attached to round timber posts at 2.4 m centres. The section of barrier is situated on the northern side of SH18. Figure 4.20 shows the traffic noise barrier viewed from the road-side; the crosses mark the approximate positions of the loudspeaker/centre microphone axis.

Two measurements were performed at the Hobsonville site. All measurements were conducted with a loudspeaker/centre microphone height of 1.9 m above the ground. Element measurements were conducted with the measurement grid located horizontally in the middle of a plywood sheet; no post measurements were conducted as they were not considered part of the acoustic design. The barrier element thickness is 21 mm.

Figure 4.20.: Road-side view of the plywood barrier at Hobsonville, the crosses mark the measurement positions

An Adrienne temporal window length of 7.0 milliseconds was used, giving a low frequency limit of 200 Hz. The sound insulation index and minimum signal-to-noise ratios are presented in Figures 4.21 and 4.22, respectively.

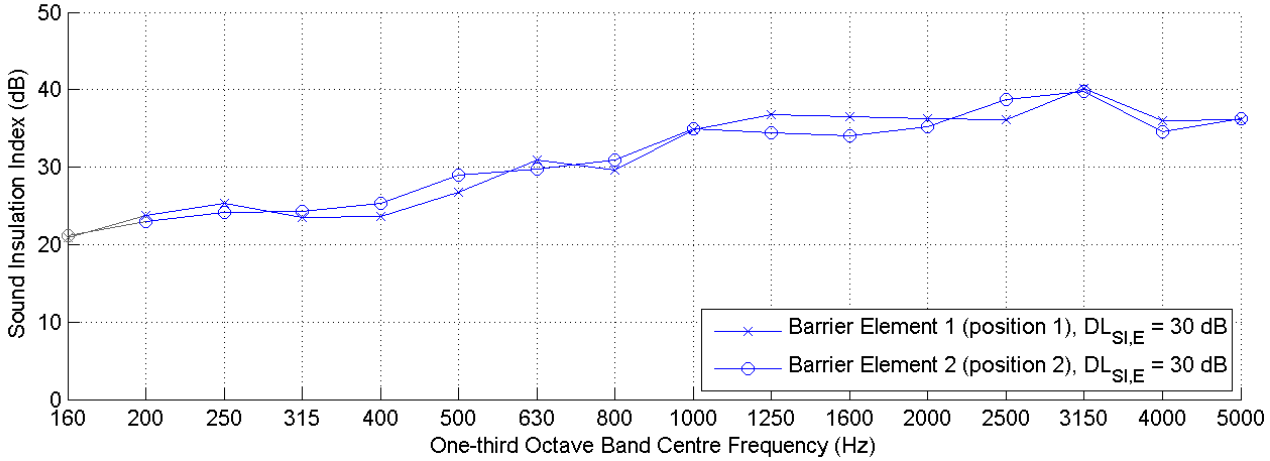

Figure 4.21.: Sound insulation index and single number rating at each measurement position on the Hobsonville barrier. The grey lines represent values below the low frequency limit of the measurement

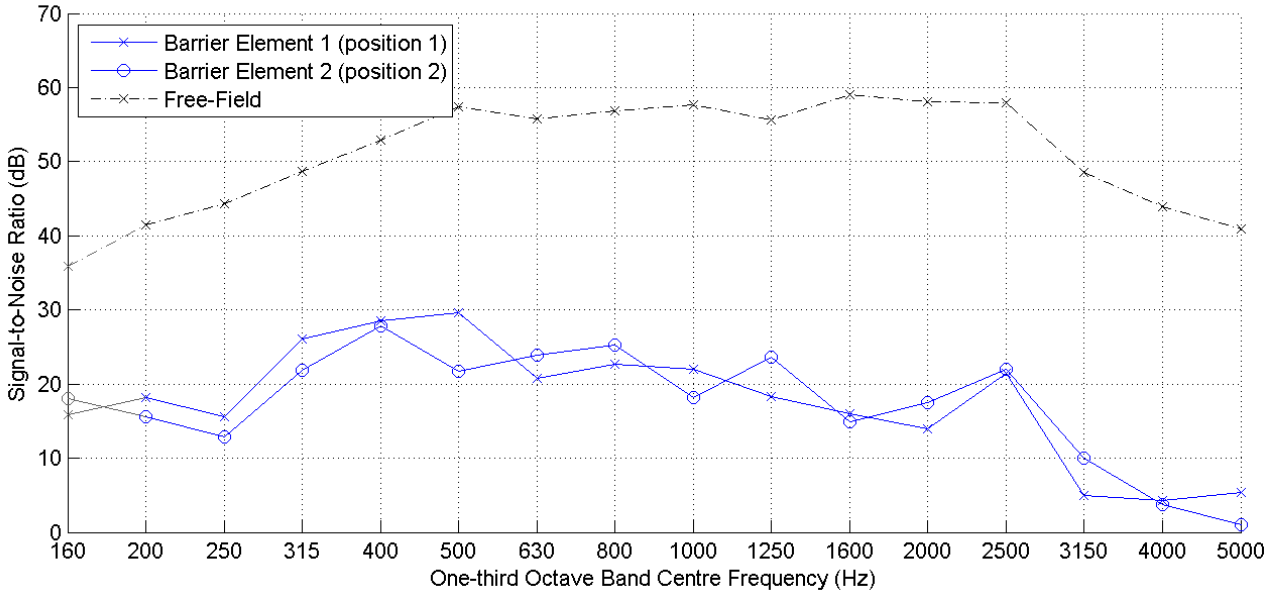

Figure 4.22.: Minimum signal-to-noise ratio at each measurement position on the Hobsonville barrier. The grey lines represent values below the low frequency limit of the measurement

4.3.6. 3.3 m concrete barrier at Green Lane

The barrier is a single-leaf, reflective concrete traffic noise barrier. Each element under test was 2.5 m wide by 3.3 m high and self supported with gaps between each element sealed using a sealing compound. The section of barrier is situated on the eastern side of SH1. Figure 4.23 shows the traffic noise barrier viewed from the resident-side; the crosses mark the approximate positions of the loudspeaker/centre microphone axis.

Two measurements were performed at the Green Lane site. All measurements were conducted with a loudspeaker/centre microphone height of 1.7 m below the barrier top. The element measurement was conducted with the measurement grid located horizontally in the middle of an element (position 1); the post measurement was conducted with the measurement grid located in line with an element-element joint (position 2). The barrier element thickness is 150 mm.

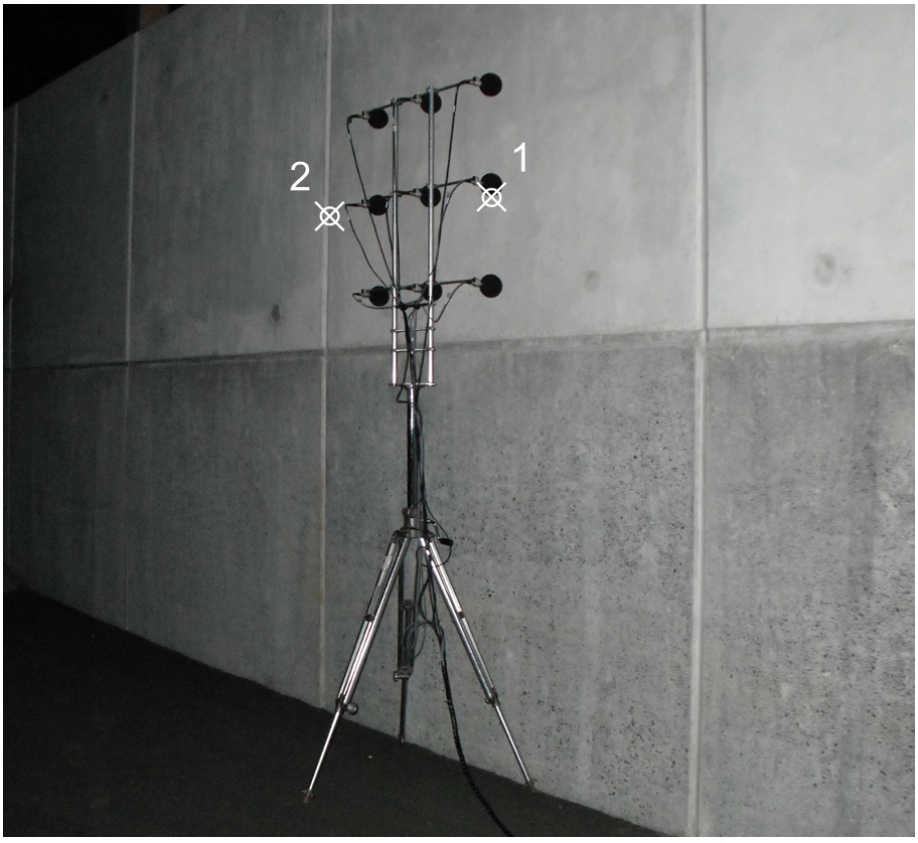

Figure 4.23.: Resident-side view of the concrete barrier at Green Lane, the crosses mark the measurement positions

An Adrienne temporal window length of 6.5 milliseconds was used, giving a low frequency limit of 250 Hz. The sound insulation index and minimum signal-to-noise ratios are presented in Figures 4.24 and 4.25, respectively.

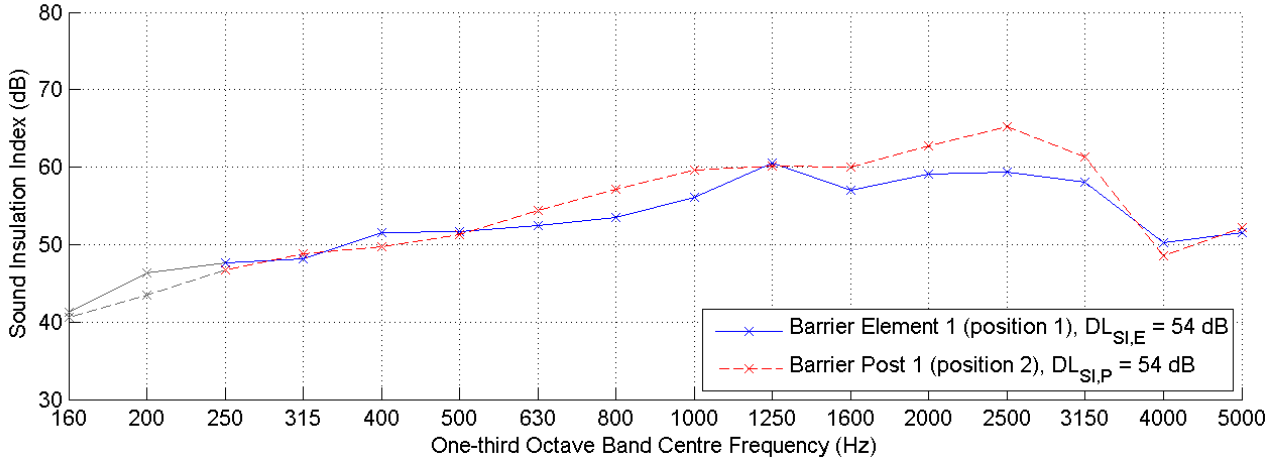

Figure 4.24.: Sound insulation index and single number rating at each measurement position on the Green Lane barrier. The grey lines represent values below the low frequency limit of the measurement

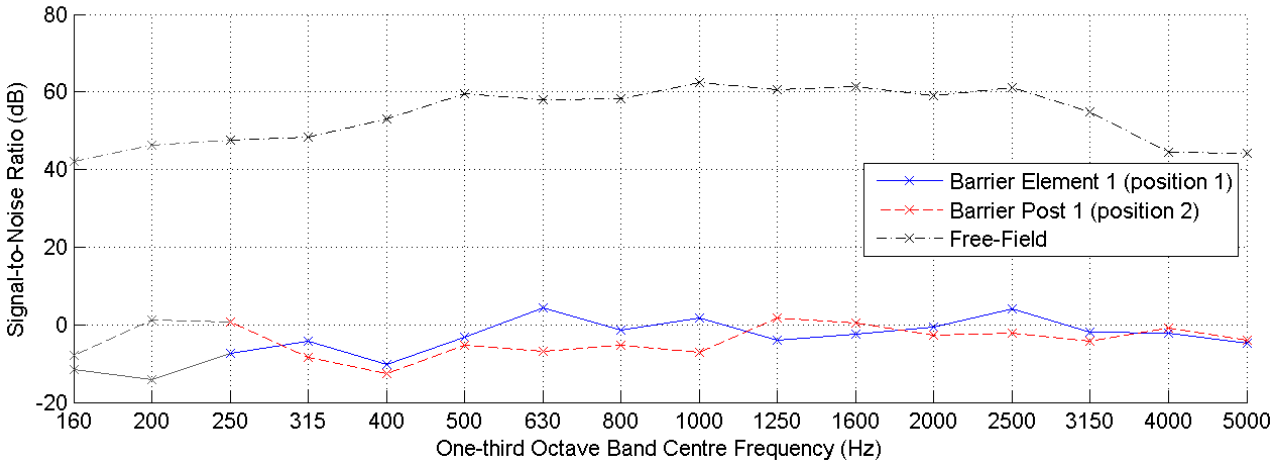

Figure 4.25.: Minimum signal-to-noise ratio at each measurement position on the Green Lane barrier. The grey lines represent values below the low frequency limit of the measurement

4.3.7. 3.9 m timber barrier at Kingsland Cycleway

The barrier is a single-leaf, reflective slatted timber traffic noise barrier. The element under test was 2 m wide by 3.9 m high, constructed from narrow lengths of timber held in place by lengths of 2×4 timber on the resident-side of the barrier. The elements were attached to round timber posts at 2 m centres. The section of barrier is situated on the southern side of SH16. Figure 4.26 shows the traffic noise barrier viewed from the road-side; the crosses mark the approximate positions of the loudspeaker/centre microphone axis.

Two measurements were performed at the Kingsland Cycleway site. All measurements were conducted with a loudspeaker/centre microphone height of 2.1 m above the ground. Element measurements were conducted with the measurement grid located horizontally in the middle of two posts; no post measurements were conducted as they were not considered part of the acoustic design. The barrier element thickness is 20 mm.

Figure 4.26.: Road-side view of the timber barrier at the Kingsland Cycleway, the crosses mark the measurement positions

An Adrienne temporal window length of 6.5 milliseconds was used, giving a low frequency limit of 250 Hz. The sound insulation index and minimum signal-to-noise ratios are presented in Figures 4.27 and 4.28, respectively.

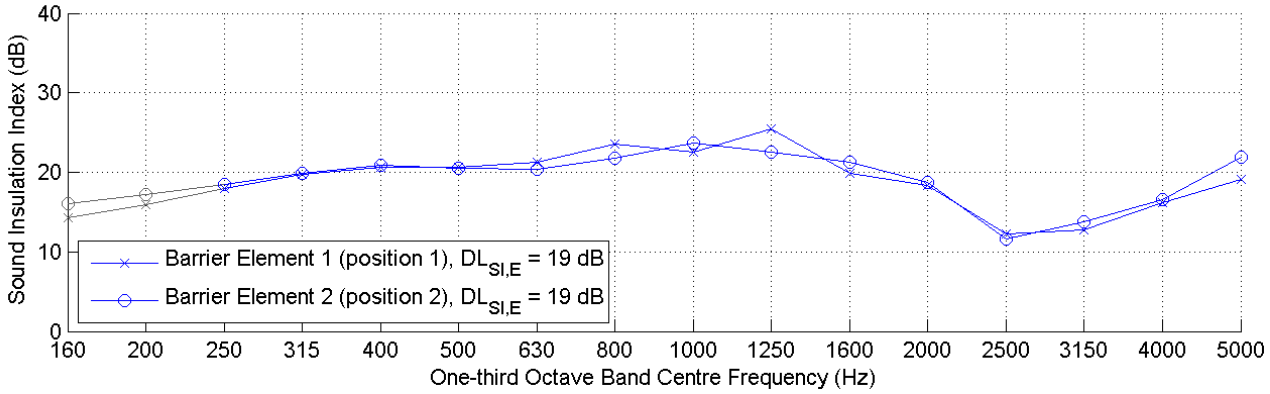

Figure 4.27.: Sound insulation index and single number rating at each measurement position on the Kingsland Cycleway barrier. The grey lines represent values below the low frequency limit of the measurement

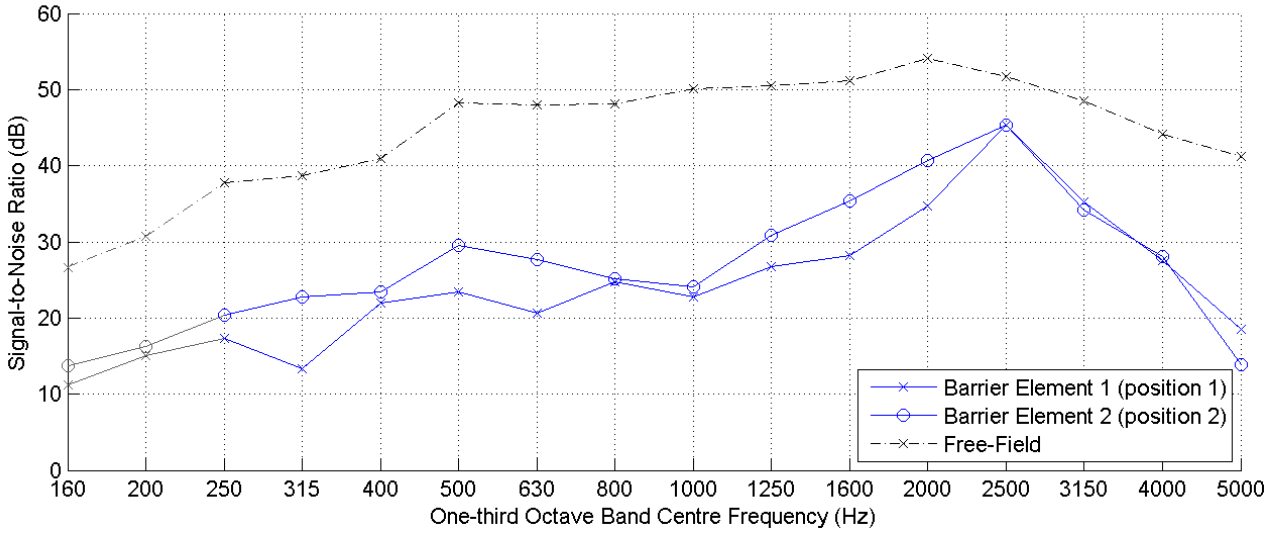

Figure 4.28.: Minimum signal-to-noise ratio at each measurement position on the Kingsland Cycleway barrier. The grey lines represent values below the low frequency limit of the measurement

4.3.8. 2.1 m plywood barrier at Northern Busway

The barrier is a single-leaf, reflective plywood traffic noise barrier. The element under test was 1.2 m wide by 2.1 m high, supported by timber posts at 1.2 m centres. The section of barrier is situated at the eastern side of SH1. Figure 4.29 shows the traffic noise barrier viewed from the resident-side; the cross marks the approximate position of the loudspeaker/centre microphone axis.

One measurement was performed at the Northern Busway site. The measurement was conducted with a loudspeaker/centre microphone height of 1.2 m above the ground and the measurement grid located horizontally in the middle of an element. The barrier element thickness is 21 mm.

Figure 4.29.: Resident-side view of the plywood barrier at the Northern Busway, the cross marks the measurement position

An Adrienne temporal window length of 3.5 milliseconds was used, giving a low frequency limit of 400 Hz. The sound insulation index and minimum signal-to-noise ratios are presented in Figures 4.30 and 4.31, respectively.

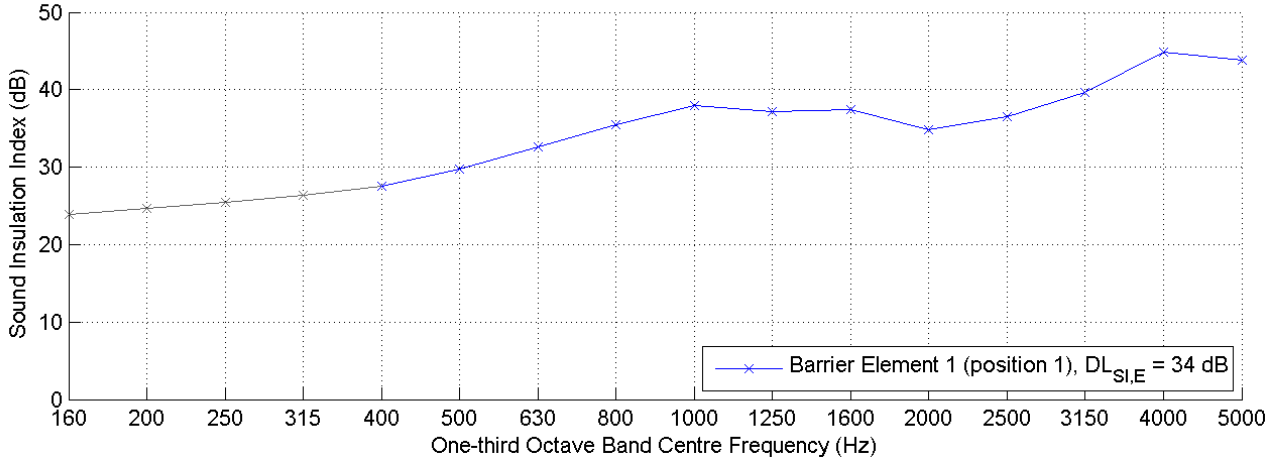

Figure 4.30.: Sound insulation index and single number rating for the element measurement on the Northern Busway barrier. The grey lines represent values below the low frequency limit of the measurement

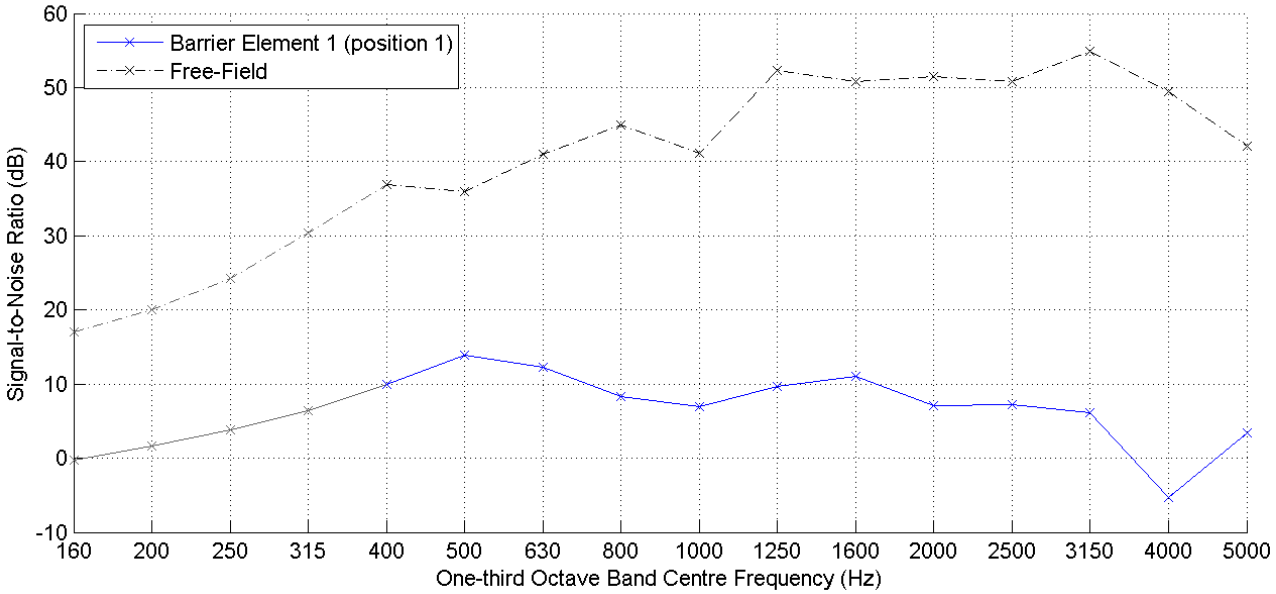

Figure 4.31.: Minimum signal-to-noise ratio at each measurement position on the Northern Busway barrier. The grey lines represent values below the low frequency limit of the measurement

4.4. Discussion

The results from the field measurements are used to investigate a range of topics that are important for reliable measurements of the airborne sound insulation. A variation of 2 dB in the single number rating has previously been found between samples of the same barrier [20,21]; similar variations were observed in the Auckland testing work. The method used to calculate the signal-to-noise ratios from the measured impulse responses is described.

Short barriers require a shorter Adrienne temporal window to exclude the diffracted sound path, which gives reduced accuracy at the low frequencies. The effect of the modified low frequency limit on the single number rating and the reduced sample area is discussed.

Sound leakage degrades the performance of a barrier and the test method is sensitive to these defects, classified as either air gaps (visible during an inspection of the barrier) or hidden defects (whose presence are not known prior to measurements).

During an impulse response measurement on noise barriers with high values of airborne sound insulation, the amount of sound transmitted through the barrier is reduced to levels comparable to the background noise level. There is a risk that the performance of the barrier will be under-predicted by the test method in such cases. Comments are made on the accuracy of the measured sound insulation index and signal-to-noise ratios of the two concrete barriers.

Unless otherwise stated, the 600 Watt loudspeaker was used with a maximum length sequence (MLS) excitation signal of order 16, repeated 16 times. A sampling frequency of 65,536 Hz provided a total excitation signal length of 16 seconds. Photographs of the measurement positions at each test site are included in the results section above.

4.4.1. Signal-to-noise ratio

The low frequency limit on the signal-to-noise ratio calculations could be extended if the full Adrienne temporal window could be used, rather than the previously specified 3.5 ms rectangular window [37]. To this end the signal-to-noise ratio in the current work is calculated using a background noise segment from the tail of the measured impulse response, and the Adrienne temporal window applied to this segment (Figure 4.32). The windowed impulse response used in the sound insulation index calculations is taken as the signal segment. The signal-to-noise ratio may now be calculated over the full measurement frequency range. Equation 4.1 is only specified for calculation of the signal-to-noise ratio in one-third octave bands as this is the most important quantity required when assessing the validity of a measurement.

$$\mathrm{SNR}_{SI,k,j} = 10\log_{10}\left\{\frac{\int\limits_{\Delta f_j} \left|F[h_k(t)w_{signal,k}(t)]\right|^2 \,\mathrm{d}f}{\int\limits_{\Delta f_j} \left|F[h_k(t)w_{noise,k}(t)]\right|^2 \,\mathrm{d}f}\right\} \tag{4.1}$$

where

$h_k(t)$ is the measured impulse response at the kth microphone position

$w_{signal,k}(t)$ is the Adrienne temporal window for the signal evaluation of the impulse response, identical to that used during airborne sound insulation calculations

$w_{noise,k}(t)$ is the Adrienne temporal window for the background noise evaluation of the impulse response, placed at the end of the measured impulse response

j is the index of the one-third octave frequency bands between 160 Hz and 5 kHz

F is the symbol of the Fourier transform

Δf_j is the bandwidth of the jth one-third octave band

The results section includes the minimum signal-to-noise ratio values in each one-third octave band. These are determined from the microphone position having the lowest signal-to-noise ratio in a particular frequency band. The signal-to-noise ratios of measurements that fail to meet the 10 dB requirement in a limited number of bands are included in Appendix C.

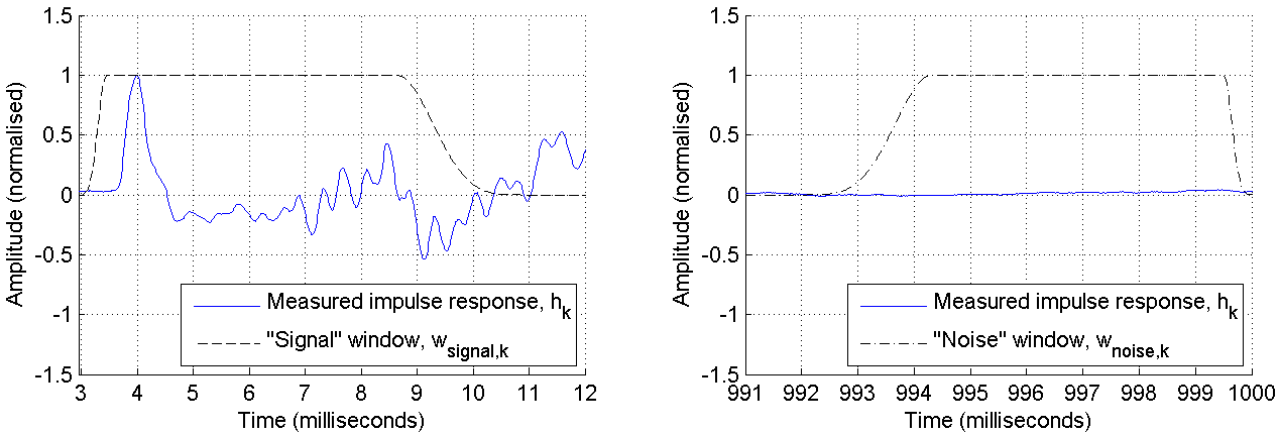

Figure 4.32.: Modified signal-to-noise ratio calculation method, valid over the full measurement frequency range of a particular measurement

Measurement validity

According to EN 1793-6:2012 the effective signal-to-noise ratio, taking into account sample averaging, must be made greater than 10 dB over the entire measurement frequency range. Clearly this was not achieved during a number of impulse response measurements, particularly in the 3150 Hz to 5 kHz one-third octave bands. The lack of a recognised signal-to-noise ratio calculation method at the time of testing meant that these deficiencies in the measurements went undetected.

In the case of the concrete traffic noise barriers and the Northern Busway barrier, the signal-to-noise ratios are below 10 dB across the entire measurement frequency range and the results represent the lower limit on the airborne sound insulation. The difference in airborne sound insulation between the two concrete barriers (Figures 4.18 and 4.24) is therefore due to the variation in the background noise level between the sites.

The signal-to-noise ratios for the St Marys Bay (including and excluding leakage), Greenhithe, Maioro Street engineered timber, and Hobsonville barriers are included in Appendix C. Failure to meet the 10 dB requirement at only one microphone position in any given one-third octave band is treated as a valid measurement in that band; the calculated sound insulation index values are not expected to be noticeably affected in these cases. Failure to meet the 10 dB requirement at more than one microphone position in a given one-third octave band is treated as an invalid measurement in that band; the calculated results will represent a lower limit on the

sound insulation index. Table 4.3 lists the affected measurements.

Table 4.3.: Invalid measurements; the calculated results in the affected one-third octave bands will represent a lower limit on the sound insulation index

Measurement	Position	Invalid measurement
St Marys Bay (excluding leakage)	1	4 kHz, 5 kHz
	2	3.15 kHz, 4 kHz, 5 kHz
	3	4 kHz, 5 kHz
St Marys Bay (including leakage)	1	4 kHz, 5 kHz
	3	4 kHz, 5 kHz
Greenhithe	1	4 kHz, 5 kHz
	2	4 kHz, 5 kHz
	3	4 kHz, 5 kHz
Maioro Street (engineered timber)	1	4 kHz, 5 kHz
	2	4 kHz, 5 kHz
	3	4 kHz, 5 kHz
	4	4 kHz, 5 kHz
Hobsonville	1	5 kHz
	2	5 kHz

The signal-to-noise ratios may be improved in future measurements by increasing the test signal length and using a loudspeaker with improved radiation characteristics at the high frequencies. The new signal-to-noise ratio calculation procedure should be incorporated into the measurement system to allow calculation immediately after a measurement.

4.4.2. Airborne sound insulation of short barriers

Existing traffic noise barriers used in New Zealand generally have heights of less than 4 m. A shortened Adrienne temporal window must be used to remove the diffraction sound component from the measured impulse responses. This reduced window length results in reduced spectral resolution after the window is applied to the measured impulse response; consequently, the single number rating must be calculated over a limited frequency range. The low frequency limit is taken as corresponding with the end of the main lobe in the frequency response of the Adrienne temporal window [13], shown in Figure 4.33 for a 7.9 millisecond time window. Figure 4.34 shows the relationship between the Adrienne temporal window length and the low frequency limit of the measurement.

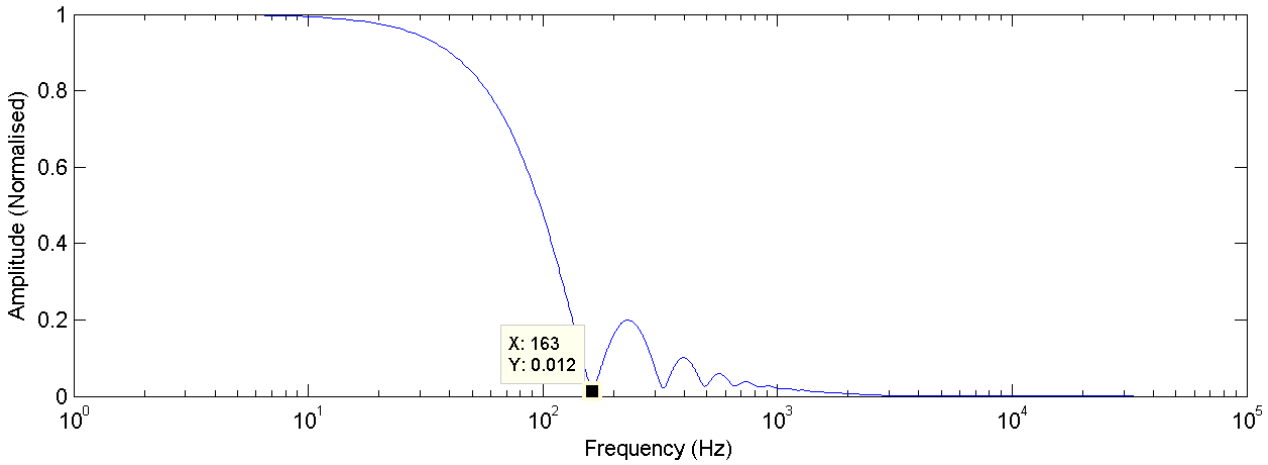

Figure 4.33.: Frequency response of a 7.9 millisecond Adrienne temporal window, the low frequency limit is indicated and corresponds to the end of the main lobe, 163 Hz in this case

In addition, a shorter time window results in a reduced test area. The 7.9 millisecond Adrienne temporal window provides a tested area with a radius of 2 m and any sound leakage from defects within the tested area will influence the measured airborne sound insulation. The relationship between the Adrienne temporal window length and the test area radius is also shown in Figure 4.34 for a noise barrier of negligible thickness.

The single number rating for airborne sound insulation must be calculated over the valid measurement frequency range according to EN 1793-6:2012. The effect of the shortened Adrienne temporal window and the modified measurement frequency range on the airborne sound insulation is investigated using the results from an element measurement (position 1) at Greenhithe.

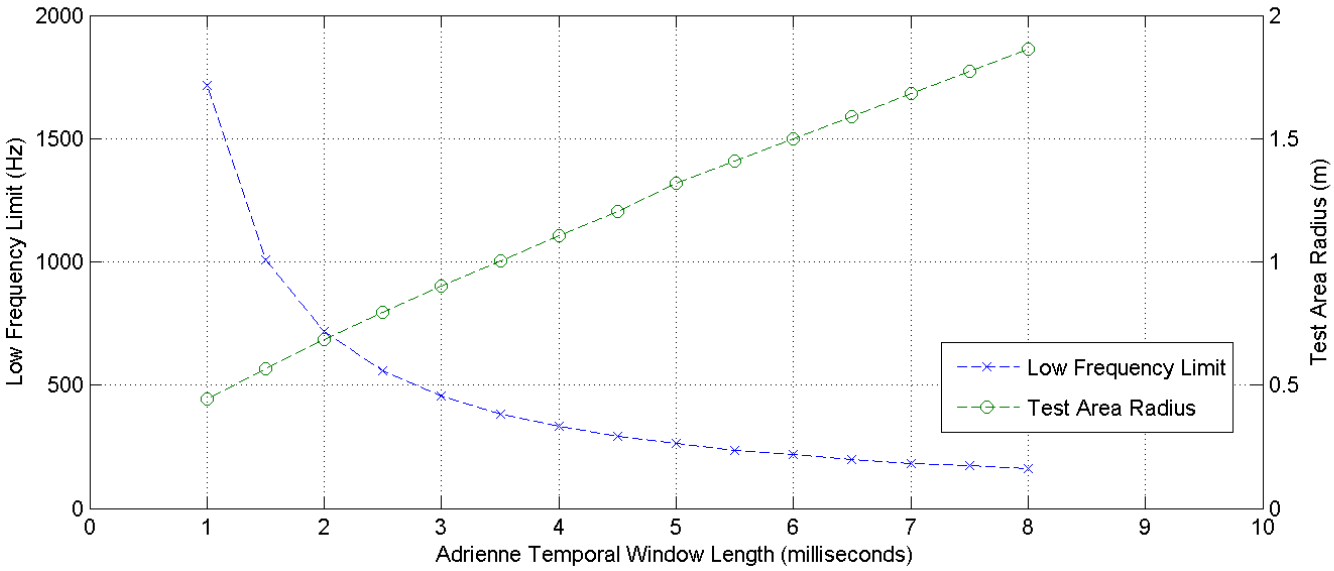

Figure 4.34.: Relationship between the Adrienne temporal window length, the low frequency limit of the measurement and the radius of the tested area

The single number rating of airborne sound insulation will vary depending on the measurement frequency range given a constant Adrienne temporal window length. Considering the element measurement (position 1) at Greenhithe with a 7.9 millisecond Adrienne temporal window, Table 4.4 shows the effect of the measurement frequency range on the single number rating. Calculating the single number rating over a reduced measurement frequency range will give higher values.

Table 4.4.: Single number ratings of airborne sound insulation at Greenhithe, showing the variation due to different measurement frequency ranges. Based on the sound insulation index with an Adrienne temporal window length of 7.9 milliseconds

Low Frequency Limit	Single Number Rating of Airborne Sound Insulation
160 Hz	32 dB
200 Hz	32 dB
315 Hz	33 dB
500 Hz	35 dB

A reduction in the length of the Adrienne temporal window (in order to remove diffraction components) will also affect the calculated airborne sound insulation as the reduced test area will result in fewer sound leakage components being included in the barrier impulse response. Figure 4.35 shows the combined effect of the reduced influence of sound leakage, due to a smaller

test area, and the reduced measurement frequency range, due to insufficient information at the low frequencies.

It is important to consider the low frequency limit of a measurement when comparing the performance of different noise barriers. Shorter noise barriers will require a reduced Adrienne temporal window length to remove the diffraction component, which may be the main contributor to any differences in airborne sound insulation. The effect could be reduced by using a common low frequency limit, regardless of the noise barrier height. While this is not strictly correct, the sound insulation index at low frequencies is generally a good representation of the noise barrier performance even for short Adrienne temporal windows, as is seen in Figure 4.35. Table 4.5 shows the single number ratings when a common low frequency limit of 160 Hz is used.

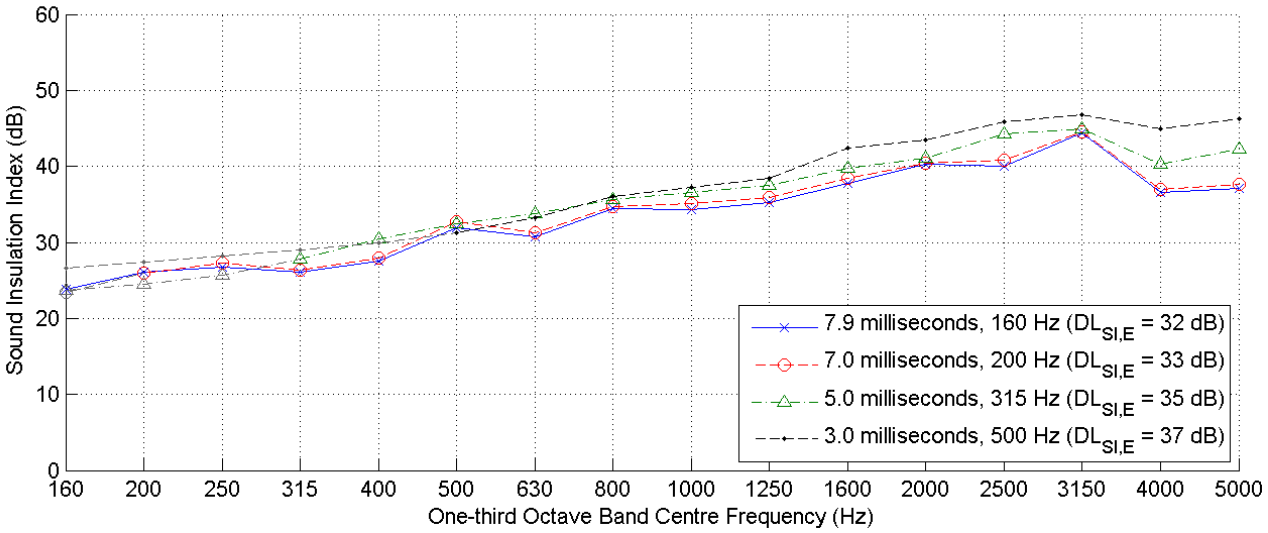

Figure 4.35.: Influence of the Adrienne temporal window length on the airborne sound insulation at Greenhithe, the single number ratings and low frequency limits are included. The grey lines represent values below the low frequency limit of the measurement

Table 4.5.: Single number ratings of airborne sound insulation at Greenhithe using a common low frequency limit of 160 Hz

Adrienne Temporal Window Length	Single Number Rating of Airborne Sound Insulation
7.9 milliseconds	32 dB
7.0 milliseconds	32 dB
5.0 milliseconds	33 dB
3.0 milliseconds	34 dB

4.4.3. Expected variation in the measured airborne sound insulation

In situ tests performed on a number of samples of the same noise barrier have shown that a variation of 2 dB in the single number ratings can be expected [20,21]. Larger variations would be expected if a sound leakage component were present in a particular sample of the barrier. Results from measurements at Greenhithe, Maioro Street (engineered timber) and Hobsonville support the findings from the previous study. The single number ratings are included in Table 4.6, varying by up to 1 dB between barrier samples at a particular test site.

There is also good agreement between the frequency dependent sound insulation index for the measurements (Figures 4.36 to 4.38).

Table 4.6.: Single number ratings of airborne sound insulation for element measurements at three test sites, the low frequency limits of the calculation are also included

Test Site	Single Number Rating, DL	
	Measurement 1	Measurement 2
Greenhithe (elements)	32 dB (160 Hz)	33 dB (160 Hz)
Maioro Street (elements)	36 dB (400 Hz)	35 dB (400 Hz)
Hobsonville (elements)	30 dB (200 Hz)	30 dB (200 Hz)

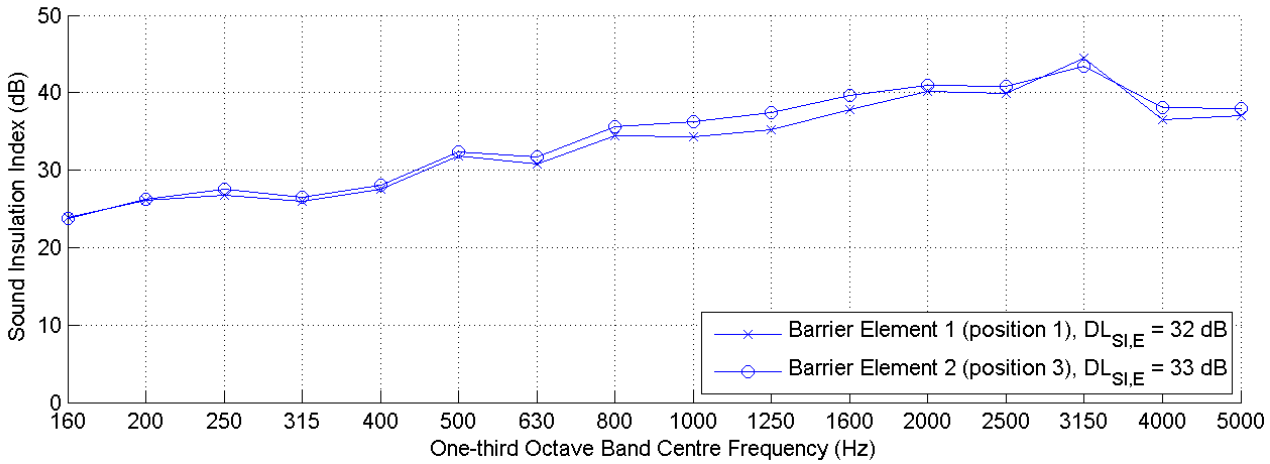

Figure 4.36.: Sound insulation index values for the engineered timber elements at Greenhithe with an Adrienne temporal window length of 7.9 milliseconds

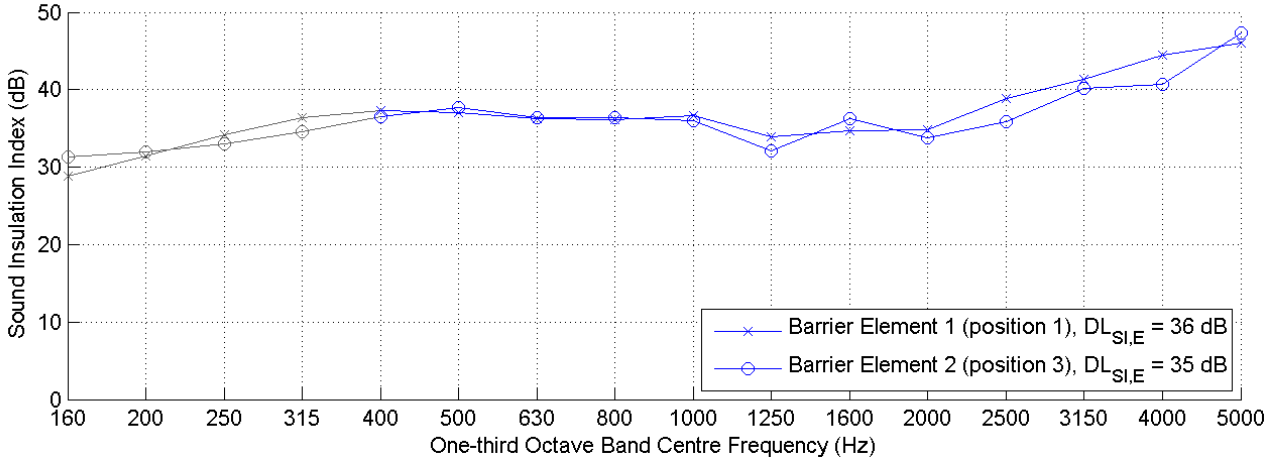

Figure 4.37.: Sound insulation index values for the engineered timber elements at Maioro Street with an Adrienne temporal window length of 4 milliseconds. The grey lines represent values below the low frequency limit of the measurement

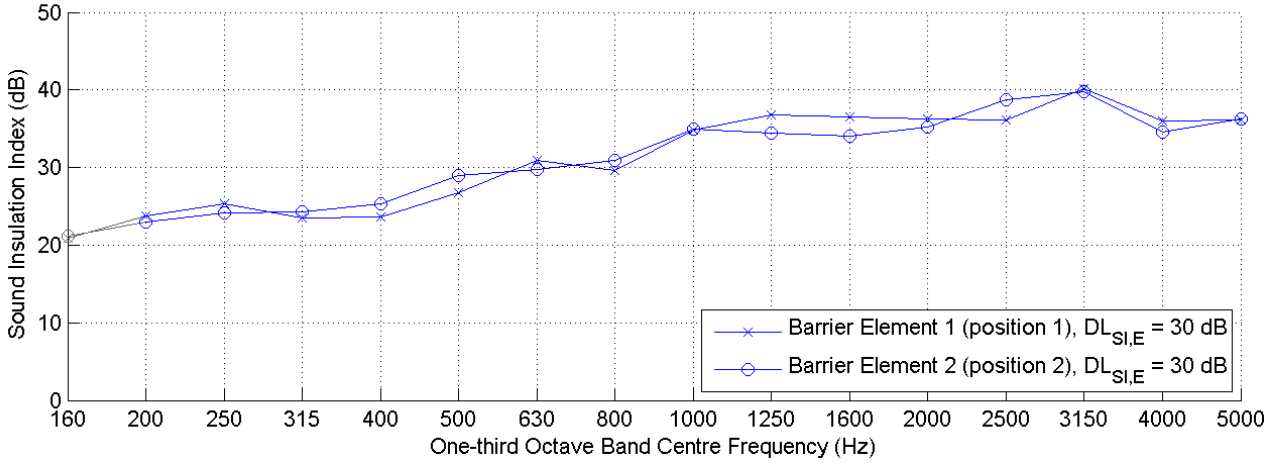

Figure 4.38.: Sound insulation index values for the plywood elements at Hobsonville with an Adrienne temporal window length of 7 milliseconds. The grey lines represent values below the low frequency limit of the measurement

4.4.4. Influence of sound leakage

Sound leakage degrades the airborne sound insulation by providing an additional path for sound to pass through the noise barrier. Two types of sound leakage can be defined; that caused by air gaps (noticeable during a visual inspection of the noise barrier) and that caused by hidden defects.

Air gaps at St Marys Bay

At the St Marys Bay site sound leakage components were identified between the acrylic elements and the concrete crash barrier (Figure 4.39).

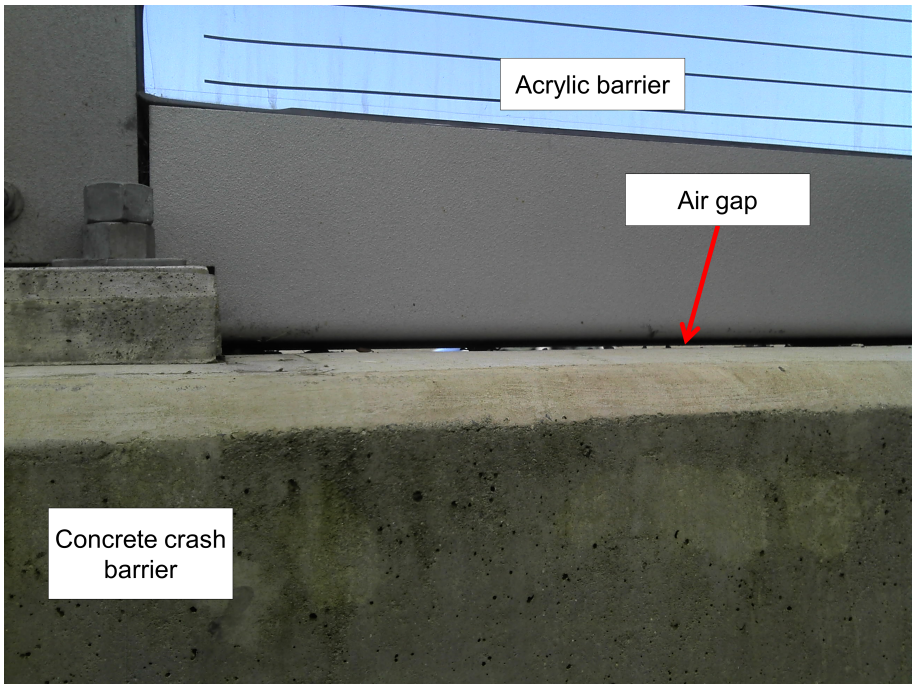

Figure 4.39.: Air gap between the concrete crash barrier and acrylic panel at St Marys Bay

An impulse response for the element measurement at position 1 (Figure 4.6) is shown in Figure 4.40 for the centre bottom microphone. The leakage and diffraction peaks occur at approximately 3.5 milliseconds and 12 milliseconds, respectively. The figure includes the standard Adrienne temporal window and a shortened time window, which would be required to remove the sound leakage component.

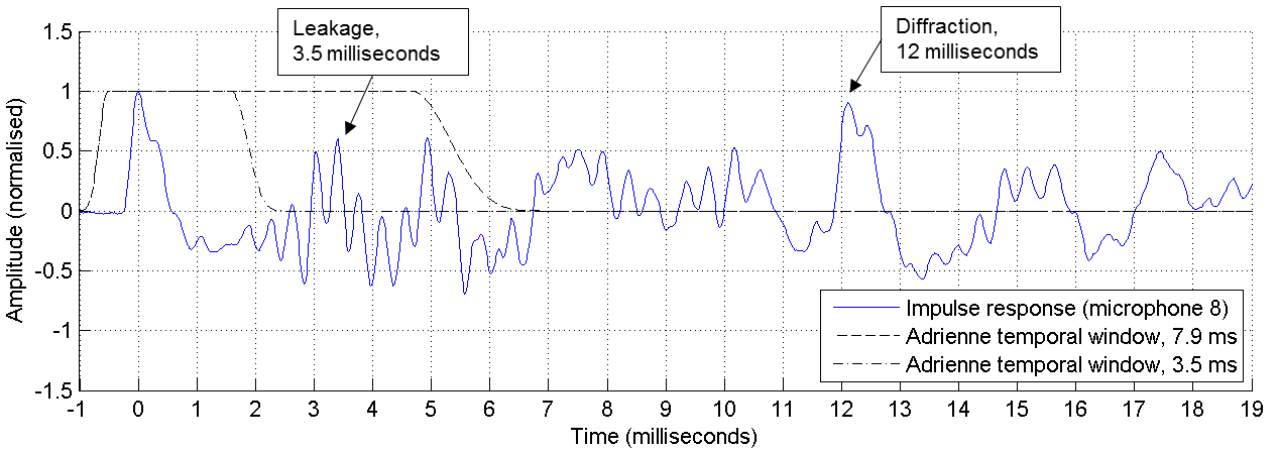

Figure 4.40.: Impulse response for the element measurement at position 1 with two different Adrienne temporal window lengths, centre bottom microphone

The impulse response for the element measurement at position 3 (Figure 4.6) is shown in Figure 4.41 for the centre bottom microphone. In this case the first leakage peak occurs at approximately 1.5 milliseconds, a second peak at 3.5 milliseconds is thought to be due to a larger gap present at the junction of two concrete crash barriers (Figure 4.42). The effect of this larger air gap can be clearly seen in the impulse response measured at a microphone near the junction (Figure 4.43). A defined diffraction peak cannot be identified in the impulse responses measured at these lower microphone positions.

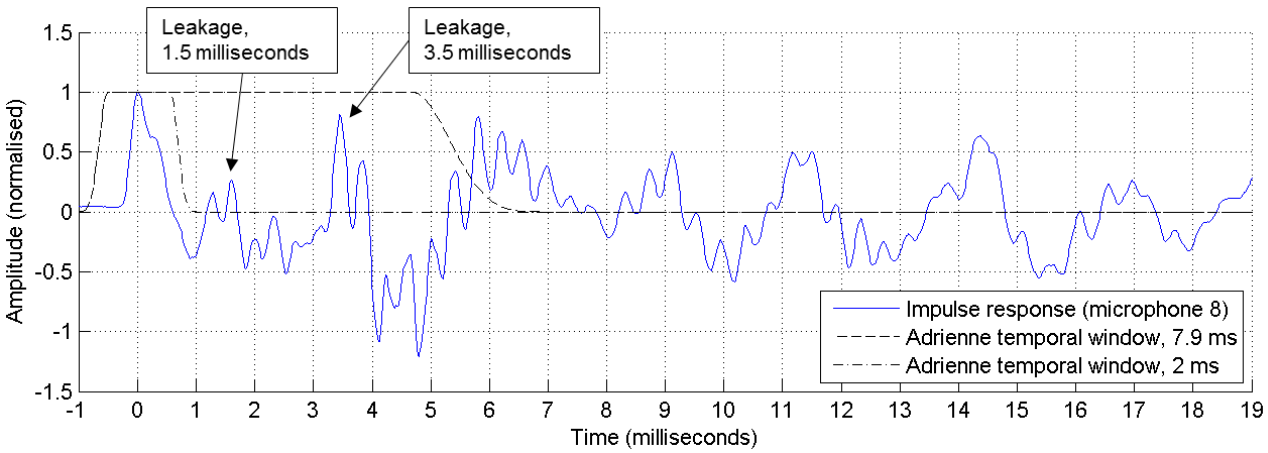

Figure 4.41.: Impulse response for the element measurement at position 3 with two different Adrienne temporal window lengths, centre bottom microphone

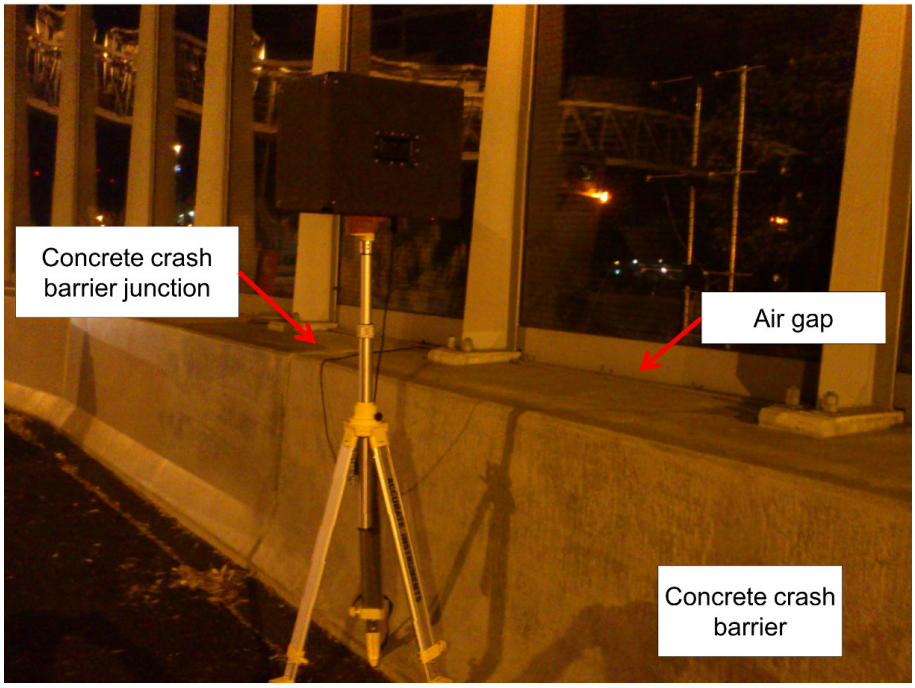

Figure 4.42.: Air gap at junction between two concrete crash barriers

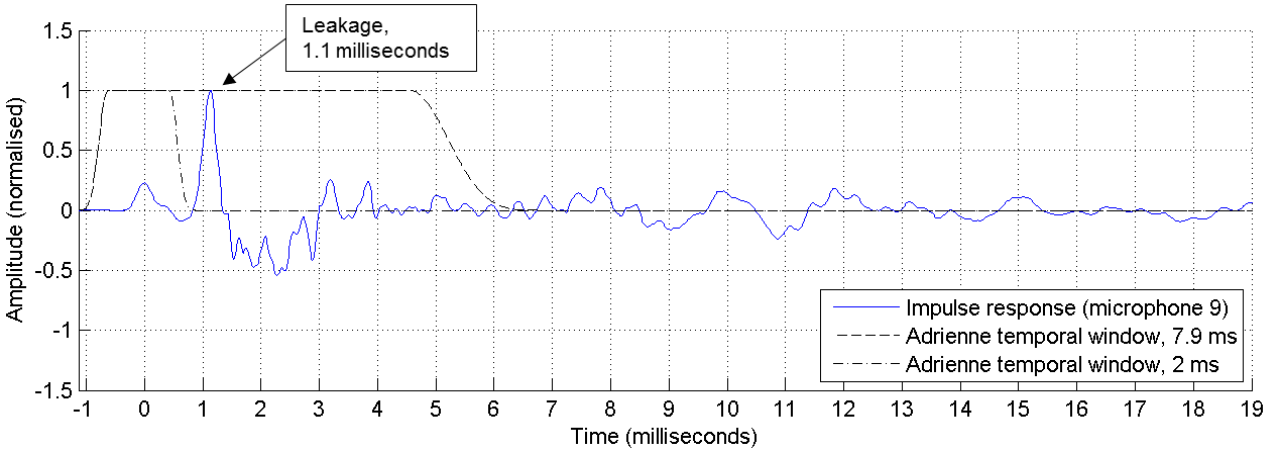

Figure 4.43.: Impulse response for the post measurement at position 2 with two different Adrienne temporal window lengths, bottom right microphone

The sound insulation index of the three St Marys Bay measurements are presented in Figures 4.44 and 4.45 for the elements and posts, respectively. The single number ratings calculated using the valid measurement frequency range are also included in the figures. When the leakage components due to gaps between the acrylic panels and concrete crash barrier are included in the impulse responses (using an Adrienne temporal window length of 7.9 milliseconds) the sound insulation index drops significantly. Results from element measurements (including and excluding leakage) in the 4 kHz and 5 kHz, and from post measurements (excluding leakage) in the 3.15 kHz to 5 kHz one-third octave bands represent a lower limit on the sound insulation index due to the poor signal-to-noise ratios in these bands.

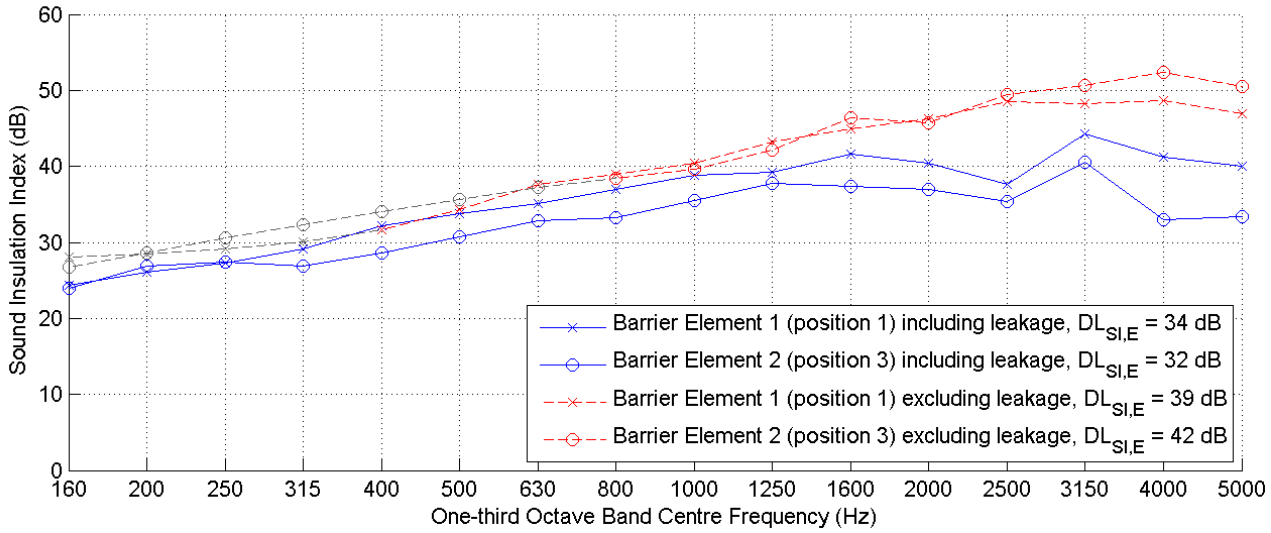

Figure 4.44.: Sound insulation index values at the elements, including and excluding the leakage components. The grey lines represent values below the low frequency limit of the measurement

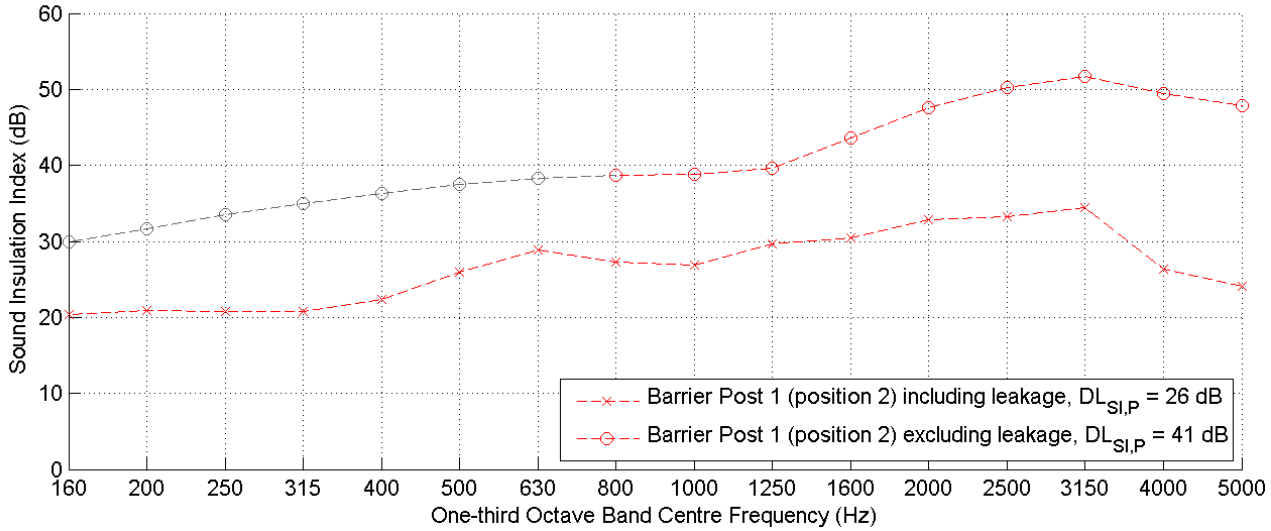

Figure 4.45.: Sound insulation values at the post, including and excluding the leakage components. The grey lines represent values below the low frequency limit of the measurement

For the element measurements, the leakage components result in a drop in performance above the 1250 Hz one-third octave band. The measurement at position 3 is affected to a greater extent by the inclusion on the leakage component, a consequence of the microphones being closer to the air gaps at this position. The differing measurement frequency ranges gives single number ratings that cannot be directly compared to one another; therefore, a reduced measurement frequency range needs to be used to calculate the single number ratings for the measurements using a 7.9 millisecond Adrienne temporal window. The results are presented in Table 4.7.

Table 4.7.: Single number ratings of airborne sound insulation for the 3.6 m acrylic barrier at St Marys Bay, the low frequency limits of the calculation are also included

Measurement	Single Number Rating, DL_{SI}		
	Excluding Leakage	Including Leakage	
		Unmodified	Modified
Barrier Element 1 (position 1)	39 dB (400 Hz)	34 dB (160 Hz)	37 dB (400 Hz)
Barrier Post 1 (position 2)	41 dB (800 Hz)	26 dB (160 Hz)	29 dB (800 Hz)
Barrier Element 2 (position 3)	42 dB (800 Hz)	32 dB (160 Hz)	36 dB (800 Hz)

The single number rating for the element measurement at position 1 drops from 39 dB to 37 dB when the leakage component is included. This 2 dB drop is a direct result of the inclusion of the leakage component. The drop in performance is more significant for the post measurement at position 2 and the element measurement at position 3 due to the microphones being closer to the air gaps, which tend to behave as small sound sources [14]. Excluding the leakage components gives the effective improvement in airborne sound insulation that could be expected if the air gaps were adequately sealed.

Air gaps at Kingsland Cycleway

Multiple air gaps are present in the Kingsland Cycleway barrier due to the timber planks warping with age (Figure 4.46).

Figure 4.47 shows an impulse response measured at an element at position 1 (Figure 4.26). A shortened Adrienne temporal window length of 6.5 milliseconds was used; the diffraction peak occurs at approximately 6 milliseconds. The secondary peaks occurring inside the time window are due to leakage through air gaps between the timber planks.

A large air gap between the barrier and ground causes a reflection peak at 9 milliseconds; this air gap does not affect the measured airborne sound insulation of the barrier as it will always lie outside of the time window. An additional measurement with the microphone grid placed close to the ground is required to investigate the effect of this air gap.

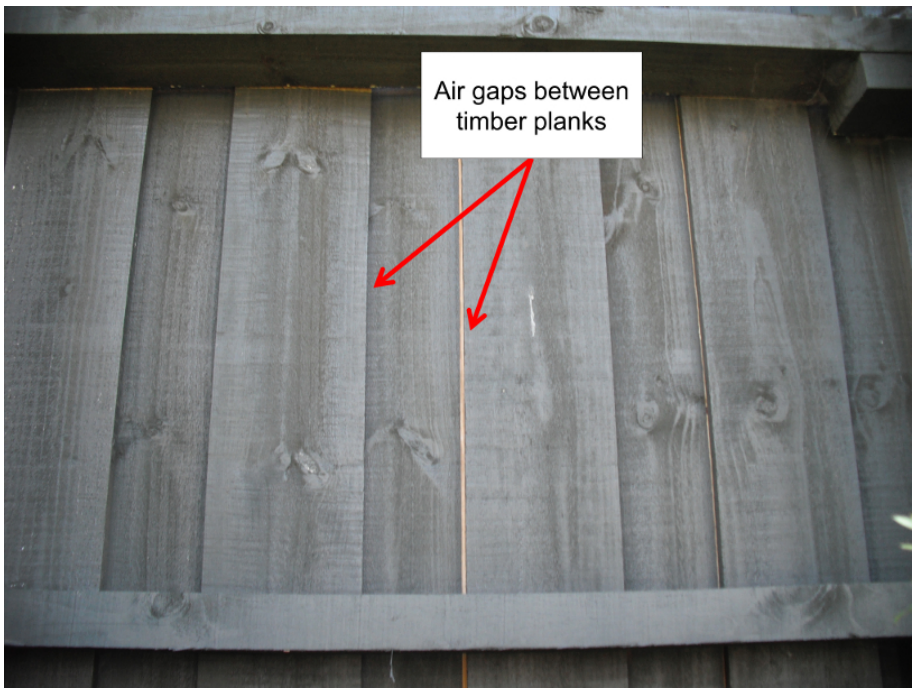

Figure 4.46.: Air gaps between timber planks in the Kingsland Cycleway traffic noise barrier

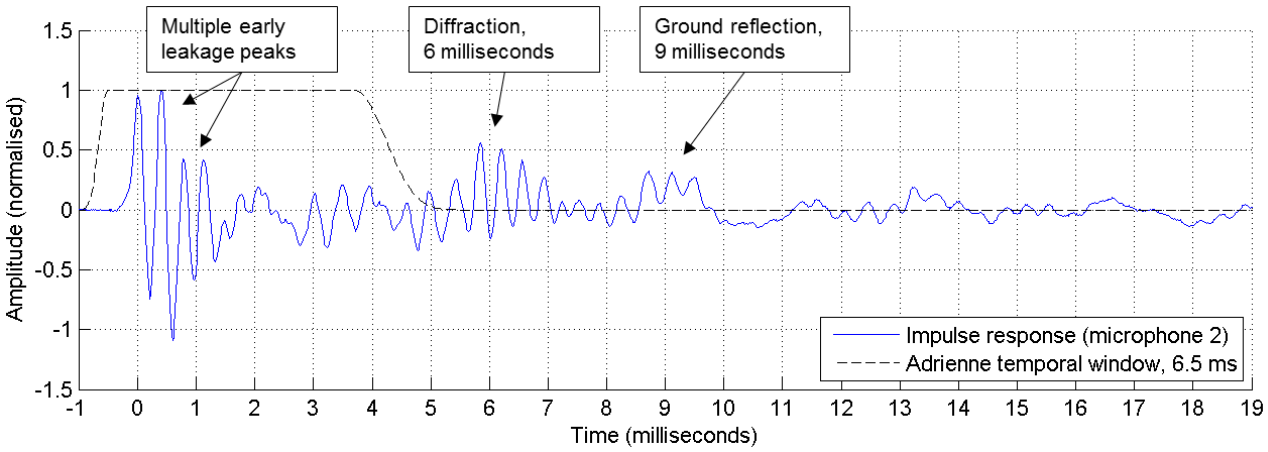

Figure 4.47.: Impulse response for the element measurement at position 1, centre top microphone

The sound insulation index for the two measurements made at the Kingsland Cycleway are presented in Figure 4.27. The single number ratings are included in the figure. The drop in performance at the high frequencies is due to sound leakage through the air gaps between the timber planks; this phenomenon was also observed by Garai and Guidorzi [13].

Air gaps in post at Greenhithe

At the Greenhithe site, the post measurement at position 4 (Figure 4.11) consisted of a corner joint with a visible gap down the centre of the post (Figure 4.48). Poor performance was expected and the impulse responses at the three centre microphones were similar in appearance to the free-field measurements. Figure 4.12 shows the sound insulation index for the four measurements made at the Greenhithe site; the performance at position 4 is significantly poorer than at the other positions.

Figure 4.48.: Air gap in the post at a corner joint in the Greenhithe traffic noise barrier, position 4

Hidden defects at Greenhithe

The impulse response for the element measurement at position 1 (Figure 4.11) is shown in Figure 4.49 for the centre top microphone. The standard Adrienne temporal window length of 7.9 milliseconds was used; the diffraction peak occurs at 8 milliseconds. The secondary peaks occurring inside the time window are due to leakage, most likely in the vicinity of the posts.

Figure 4.50 shows an impulse response measured at a post at position 2. Again the diffraction peak can be seen at a delay of 8 milliseconds. The post leakage alluded to previously can be seen as a small peak at approximately 0.5 milliseconds. This leakage component is more pronounced in the impulse response measured at the top left microphone (Figure 4.51). During the field measurements it was noticed that the element at position 1 was less securely fastened in its posts

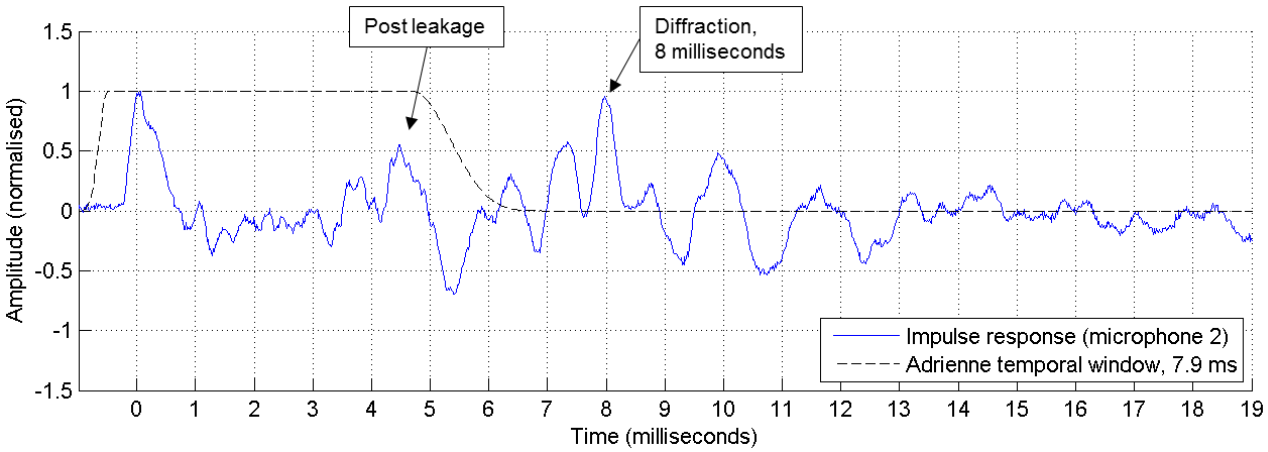

Figure 4.49.: Impulse response for the element measurement at position 1, centre top microphone

than the element at position 3. This explains the larger influence of the leakage component at the top left microphone position, which was located over this loose element.

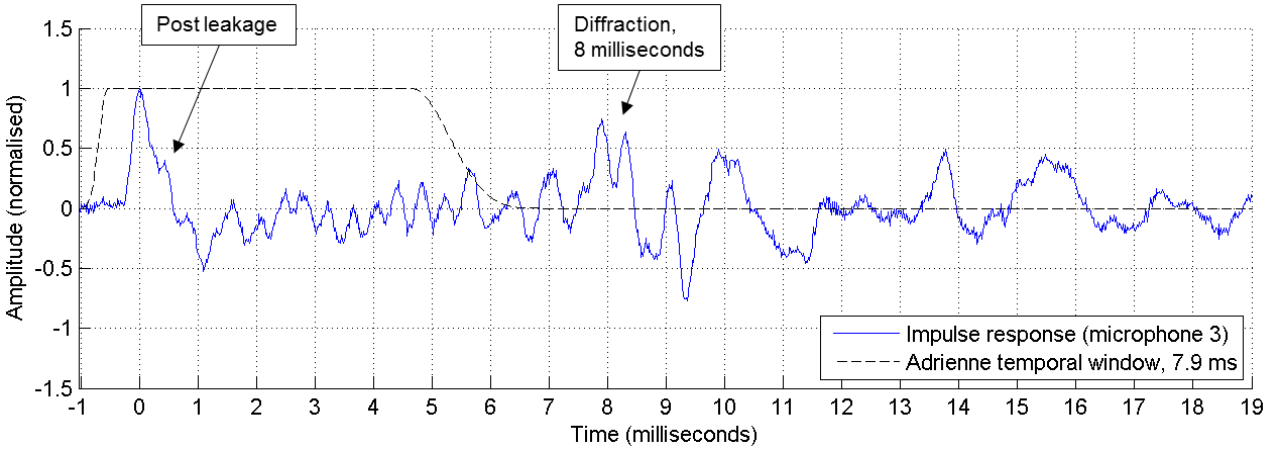

Figure 4.50.: Impulse response for the post measurement at position 2, top right microphone

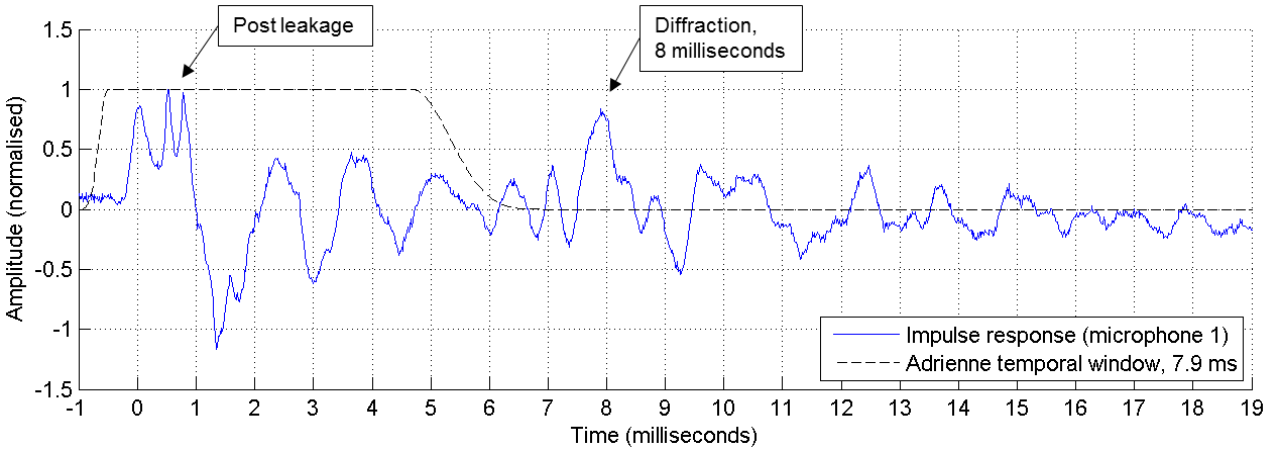

Figure 4.51.: Impulse response for the post measurement at position 2, top left microphone

The sound insulation index for the four measurements made at the Greenhithe site are presented in Figure 4.12. The single number ratings are listed in Table 4.8.

Table 4.8.: Single number ratings of airborne sound insulation for the 4.2 m engineered timber barrier at Greenhithe, the low frequency limits of the calculation are also included

Measurement	Single Number Rating, DL_{SI}
Barrier Element 1 (position 1)	32 dB (160 Hz)
Barrier Post 1 (position 2)	29 dB (160 Hz)
Barrier Element 2 (position 3)	33 dB (160 Hz)
Barrier Post 2 (position 4)	16 dB (160 Hz)

The single number ratings for the two elements (positions 1 and 3) are within 1 dB, with the element at position 3 having the higher value. The small difference in results may be due to the loose element at position 1.

The post at position 2 is influenced by leakage, having a single number rating of 29 dB. Inspection of the sound insulation index values (Figure 4.12) shows a drop in performance between 500 Hz and 1 kHz, and above 2 kHz.

4.4.5. High performance noise barriers

Both concrete traffic noise barriers performed well, with high airborne sound insulation values. Figure 4.52 shows the airborne sound insulation of the two concrete barriers.

There will be an upper limit on the airborne sound insulation values that can be detected by the equipment used in this work. This is possibly being reached when measuring the concrete barriers, where the level of the transmitted signal is comparable to the background noise level and time variances in the system counteract the noise immunity benefits of the impulse response measurement techniques. While the results do not meet the signal-to-noise ratio requirements of EN 1793-6:2012, the true airborne sound insulation of the barriers will not be any lower than the values displayed in Figure 4.52. It is likely that the differences seen in Figure 4.52 are due to the variation in background noise level between the sites.

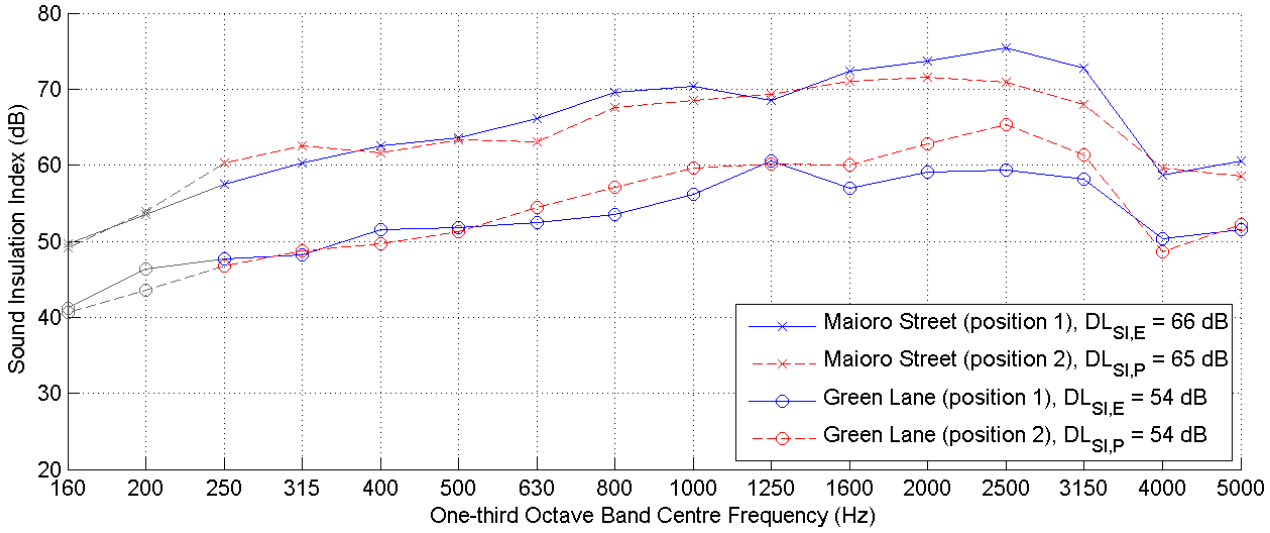

Figure 4.52.: Airborne sound insulation of the concrete barriers at Green Lane and Maioro Street. The grey lines represent values below the low frequency limit of the measurement.

4.4.6. Ageing of the engineered timber barrier

The engineered timber barriers at Greenhithe and Maioro Street are of similar construction, with the Greenhithe traffic noise barrier being approximately four years older than the barrier at Maioro Street. The airborne sound insulation of the elements and posts at each site are shown in Figures 4.53 and 4.54, respectively. A common Adrienne temporal window length of 4 milliseconds was used to allow for a meaningful comparison of the results. The single number ratings are included in the figures.

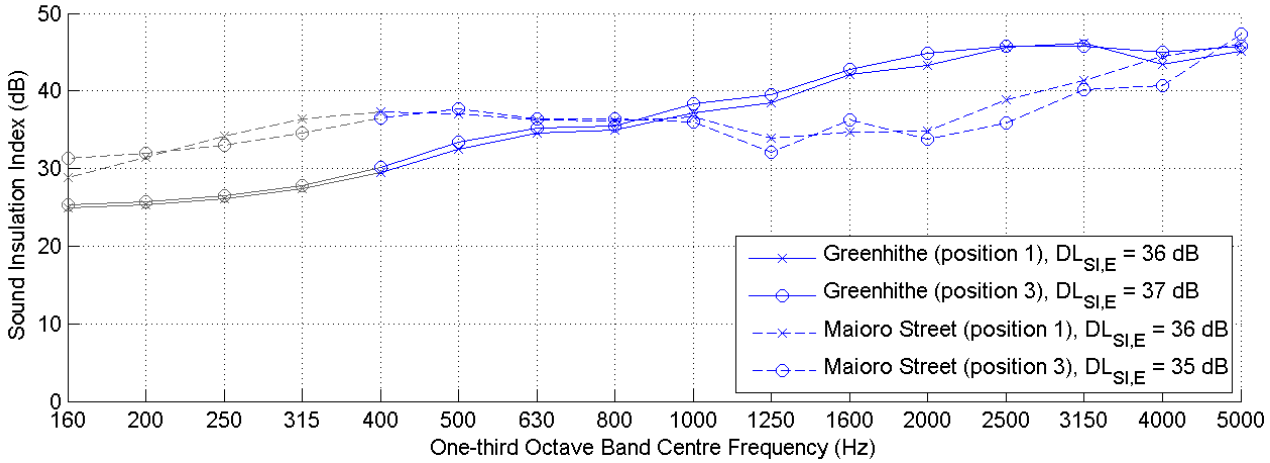

Figure 4.53.: Comparison between the airborne sound insulation values of the elements at Greenhithe and Maioro Street with a common Adrienne temporal window length of 4 milliseconds. The grey lines represent values below the low frequency limit of the measurement

The single number ratings of the elements are similar at both sites, with values between 35 dB and 37 dB. The sound insulation index curves (Figure 4.53) show a drop in performance for the newer Maioro Street barrier in the 1 kHz to 3.15 kHz one-third octave bands. The reason for the differences in performance is unclear, however, there are some slight differences between the barrier constructions that may explain the variation:

- barrier height, 4.2 m at Greenhithe and 2.9 m at Maioro Street
- element width, 2.4 m at Greenhithe and 2.6 m at Maioro Street
- decorative vertical slats on the road-side of the Maioro Street barrier

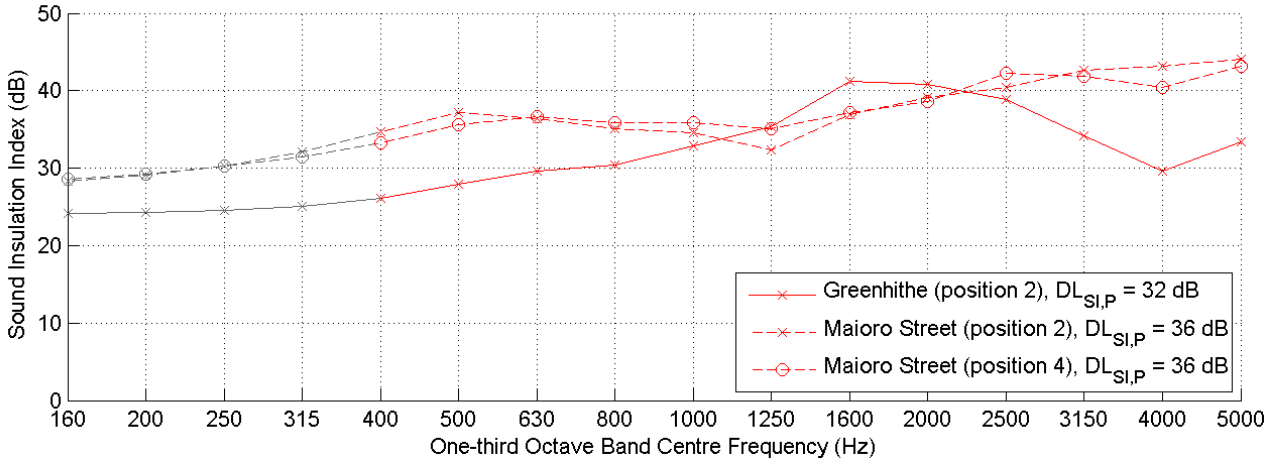

Figure 4.54.: Comparison between the airborne sound insulation values of the posts at Greenhithe and Maioro Street with a common Adrienne temporal window length of 4 milliseconds. The grey lines represent values below the low frequency limit of the measurement

The post at Greenhithe has a single number rating of 32 dB, compared to 36 dB at both Maioro Street posts. The sound insulation index (Figure 4.54) shows a drop in performance at the Greenhithe post in the 2.5 kHz and 3.15 kHz one-third octave bands, compared to the newer Maioro Street posts. The defect at the Greenhithe post has been discussed previously in Section 4.4.4 and may be due to the element-post joints loosening over time.

Conclusions over the differences in performance in the 4 kHz and 5 kHz one-third octave bands cannot be drawn due to the poor signal-to-noise ratios in those bands.

4.4.7. Comparison of different barrier types

The single number ratings of airborne sound insulation are summarised in Table 4.9 for each measurement position, in order of performance and considering the low frequency limits.

Table 4.9.: Single number rating of airborne sound insulation, DL_{SI}, at each measurement position

Name	Material	Low Frequency Limit	Single Number Rating, DL_{SI}			
			1	2	3	4
Maioro Street	concrete	250 Hz	66 dB	65 dB		
Green Lane	concrete	250 Hz	54 dB	54 dB		
St Marys Bay	acrylic	160 Hz	34 dB	26 dB	32 dB	
Greenhithe	engineered timber	160 Hz	32 dB	29 dB	33 dB	16 dB
Maioro Street	engineered timber	400 Hz	36 dB	36 dB	35 dB	36 dB
Hobsonville	plywood	200 Hz	30 dB	30 dB		
Northern Busway	plywood	400 Hz	34 dB			
Kingsland Cycleway	timber	250 Hz	19 dB	19 dB		

The concrete barriers out perform all of the other traffic noise barriers, which is expected due to their mass and lack of air gaps. Considering the low frequency limits of the measurements, the acrylic barrier at St Marys Bay is the next best performing. Air gaps between the acrylic panel and concrete crash barrier reduce the airborne sound insulation at some measurement positions and higher values can be expected if seals were installed.

The engineered timber barriers at Greenhithe and Maioro Street have elements with similar single number ratings, while the frequency dependent sound insulation index shows some variations that could be explained by slight differences in their construction. The corner post at Greenhithe (position 4) contains a large air gap that significantly degrades the barrier performance at that location. A standard post at Greenhithe (position 2) also shows reduced performance compared to the Maioro Street posts; this may be due to the element-post joints loosening with age.

The plywood barriers at Hobsonville and the Northern Busway have similar constructions and the variations in single number ratings can be explained by the different low frequency limits.

The slatted timber barrier at Kingsland Cycleway has the lowest values of airborne sound insulation. The use of overlapping timber planks increases the number of air gaps, consequently

reducing the airborne sound insulation.

These results are in line with previous studies which showed that single number ratings for timber barrier elements ranged from 23 dB to 37 dB depending on construction [16]. Garai and Guidorzi [13] demonstrated the much higher airborne sound insulation values of concrete barriers.

4.4.8. Comparison with laboratory testing data

Previous work has shown good correlation between in situ measurement results made in the Adrienne method and laboratory results using EN 1793-2 [13, 16]. The supplier of the acrylic barrier at St Marys Bay quotes a single number rating of airborne sound insulation (DL_R) of 30 dB measured in accordance with EN 1793-2, for their 15 mm thick acrylic sheets [40]. A similar 20 mm thick acrylic barrier was tested by Garai and Guidorzi and found to have a DL_R of 33 dB and a DL_{SI} of 40 dB (200 Hz low frequency limit) [13].

Equation 1.4 gives an expected in situ single number rating of airborne sound insulation (DL_{SI}) of 34 dB for the acrylic elements at St Marys Bay. This compares well with the measured values of 34 dB and 32 dB, noting that the second value is somewhat affected by sound leakage between the concrete crash barrier and acrylic element. A DL_{SI} value of 26 dB was measured at the post, which is lower than the theoretical value of 32 dB calculated using Equation 1.5 due to the presence of air gaps in the vicinity of the posts.

4.4.9. Comparison with predicted performance

No laboratory testing data is available for the other noise barriers tested, however, comparisons can be made with sound transmission loss prediction results for similar materials. This is done for the plywood and engineered timber barriers using Equation 1.7 and for the acrylic and concrete barriers using Equation 1.4. Table 4.10 shows predicted results using Marshall Day Acoustics Insul 6.4 with the corresponding $DL_{SI,E}$ values. Equation 1.6 is used for the intermediate R_w to DL_R calculation.

Table 4.10.: Predicted R_w and $DL_{SI,E}$ for the noise barrier materials

Material	Sites	Weighted Sound Reduction Index, R_w	Single Number Rating, $DL_{SI,E}$
acrylic sheets (15 mm thick, 18 kg/m^2)	St Marys Bay	32 dB	32 dB
plywood (21 mm thick, 12 kg/m^2)	Hobsonville Northern Busway	25 dB	30 dB
engineered timber (32 mm thick, 18 kg/m^2)	Greenhithe Maioro Street	26 dB	31 dB
concrete (150 mm thick, 350 kg/m^2)	Green Lane Maioro Street	54 dB	58 dB

The predicted DL_{SI} of 32 dB for the acrylic elements agrees well with the measured values of 32 dB and 34 dB. Similarly, the performance at Hobsonville (30 dB, 200 Hz low frequency limit) and at Greenhithe (32 dB and 33 dB, 160 Hz low frequency limit) agree well with the predicted values of 30 dB and 31 dB, respectively. Larger discrepancies between the measured and predicted performance of the elements at Maioro Street and the Northern Busway can be explained by the reduced measurement frequency range that tends to increase the measured values of DL_{SI}. The predicted performance of the concrete barriers (58 dB) suggests that the measured values at Green Lane and Maioro Street are close to the true airborne sound insulation.

4.4.10. Discussion of EN 1793-6:2012

Test signal

EN 1793-6:2012 recommends the use of a maximum length sequence (MLS) test signal, repeated a minimum of 16 times. Impulse response measurements made using MLS signals have been shown to be sensitive to time variances in the system under test [28] and non-linearities caused by the loudspeaker and other components of the measurement system [32]. The use of an exponential swept sine signal (ESS) has been shown to be less sensitive to time variances and non-linearities in the system, allowing higher signal-to-noise ratios (SNR) to be achieved [41]. The use of synchronous averaging to improve the SNR may result in artefacts in the measured impulse response when the system is slightly time variant [30]. It is therefore recommended that

a single period of a longer duration ESS test signal be used to measure the required impulse responses.

Signal-to-noise ratio

There is currently no signal-to-noise ratio calculation method defined in EN 1793-6:2012. Clearly the signal-to-noise ratio depends on the calculation method chosen; as such it is recommended that a standardised calculation procedure be included in a future version of EN 1793-6. Additionally, measurements that do not meet the 10 dB signal-to-noise ratio requirement remain useful in their ability to define a lower limit of the airborne sound insulation of a barrier; this may be particularly useful when assessing the airborne sound insulation of high performance noise barriers. A reliable D3 classification can be quoted if the single number rating of airborne sound insulation is greater than 36 dB, regardless of the signal-to-noise ratio.

Low frequency limit

As discussed in Section 4.4.2, the calculated airborne sound insulation of a noise barrier will vary depending on the low frequency limit used (Table 4.4). Therefore two barriers with identical constructions but differing heights will have different single number ratings of airborne sound insulation. For meaningful comparisons between noise barriers it is important that a common low frequency limit is used or that some adjustment is applied.

An example of an a adjustment technique is to use a shortened Adrienne temporal window to remove the diffraction components, as stated in EN 1793-6:2012, followed by the calculation of the single number rating over the measurement frequency range for a 4 m high barrier (160 Hz to 5 kHz). The effect of this adjustment technique can be seen in Table 4.5.

5. Conclusions and Future Work

5.1. Conclusions

This research thesis involved the measurement of the airborne sound insulation of traffic noise barriers with the goal of gaining a better understanding of the factors that influence the results. During the course of the project a measurement system was developed, based on EN 1793-6:2012, to quantify the airborne sound insulation of traffic noise barriers in situ. Validation testing was performed to ensure that the system components met the requirements of EN 1793-6:2012, and MATLAB code was developed, incorporating all of the required signal processing tasks into a single graphical user interface. Finally, airborne sound insulation measurements were performed on eight existing traffic noise barriers located around Auckland, New Zealand, and an analysis of the results was conducted.

5.1.1. System validation

System validation tests were performed on the microphone array and three loudspeakers. All three loudspeakers were deemed to meet the sound source requirements of EN 1793-6:2012, with the 600 Watt loudspeaker being chosen due to its higher power capacity and consequent enhanced ability to meet the signal-to-noise ratio requirements. The microphone clip was investigated for any reflections; a maximum variation of 1.5 dB was observed in the 5 kHz one-third octave band when compared to the Brüel & Kjær 2260 handheld analyser measurement. Fibreglass wool was attached to various parts of the microphone array to reduce the amplitude of any undesirable reflections; a maximum variation of 1.2 dB was observed in the 3.15 kHz one-third octave band when compared to the Brüel & Kjær 2260 measurement. A measurement of the

Brüel & Kjær type 4189 microphone held in a microphone clip, with and without a windshield, showed a maximum variation of 0.5 dB in the 5 kHz one-third octave band. All measurements revealed that no reflections were introduced that would noticeably modify the measured impulse response of the loudspeaker.

5.1.2. Practical aspects

The measurement method proved to be easy to use in a field testing situation, with a simple setup and short measurement times. The Auckland test sites were separated into three categories; residential, road-inspection and semi-static closure. The semi-static closure sites required the use of truck mounted attenuators to protect the operators while on the road-side of the barrier, with stopping times limited to 30 minutes due to safety concerns. It may be useful to consider scheduling future noise barrier measurements at such sites to coincide with road maintenance activities, thus allowing a larger test sample size. Similarly, a full day should be set aside for testing at the residential and road-inspection sites.

5.1.3. Airborne sound insulation of short barriers

Many traffic noise barriers around New Zealand are shorter than 4 m, thus demanding a reduced Adrienne temporal window length in order to eliminate the diffraction sound component. The single number rating must then be calculated over a modified frequency range, which has the effect of artificially increasing the result and preventing meaningful comparisons between measurements with differing low frequency limits. Therefore, it is necessary to recalculate the single number ratings over a common measurement frequency range before comparing the results.

5.1.4. Variability and the influence of sound leakage

Consistent values of airborne sound insulation were measured at the Greenhithe, Maioro Street engineered timber and the Hobsonville sites. Two element measurements were conducted at each site and the resulting single number ratings were within 1 dB of one another, as expected [20, 21].

Larger variations occur when air gaps or hidden defects are present, as is the case at St Marys Bay, Kingsland Cycleway and the Greenhithe posts. Large air gaps between the element and concrete crash barrier at the St Marys Bay site cause a drop in the sound insulation index above the 1.25 kHz one-third octave band. The single number ratings are calculated over a consistent frequency range to allow meaningful comparisons and show a drop of 2 dB (400 Hz low frequency limit) for an element when the leakage component is included. As the microphones are moved closer to the air gaps the drop in performance becomes more significant, hence it is important that any air gaps present in a sample are documented at the time of testing.

The Kingsland Cycleway traffic noise barrier contains numerous air gaps distributed throughout the elements, caused by the timber planks warping with age. Large secondary peaks occur within the Adrienne temporal window of the measured impulse responses, resulting in low values of airborne sound insulation at the high frequencies and a low overall single number rating of 19 dB.

Hidden defects were detected at a Greenhithe post where one element was not securely fastened to the post. This gave the post a single number rating of 29 dB compared to the elements on either side of it which had values of 32 dB and 33 dB. The sound insulation index at the post showed a drop in performance between 500 Hz and 1 kHz and above 2 kHz.

5.1.5. Comparison with laboratory and predicted performance

Good agreement was obtained between the laboratory results (EN 1793-2, quoted by the supplier) and the in situ results for the acrylic barrier at St Marys Bay, through the use of the relationship derived by Garai and Guidorzi [13]. Predictions of the weighted sound reduction index for each material were also made using Marshall Day Acoustics Insul 6.4. The use of the relationships derived by Garai and Guidorzi [13], and Watts and Morgan [16] gave good agreement between the measured in-situ airborne sound insulation and the predicted performance of the material.

5.1.6. EN 1793-6:2012

Through a review of the literature surrounding impulse response measurements it is recommended that an exponential swept sine test signal be used for future airborne sound insulation measurements. The exponential swept sine signal is more effective in dealing with non-linearities in the system under test, and a single sweep of long duration will eliminate the issues associated with time variances in the system due to changing temperature and wind velocity. Theoretically the signal-to-noise ratio can be increased by 3 dB with each doubling of the test signal length; in practice there will be a maximum value of airborne sound insulation that can be measured by a specific measurement system. Noise barriers with airborne sound insulation values above the limits of the equipment will not meet the signal-to-noise ratio requirements of EN 1793-6:2012; however, a valid D3 classification can still be quoted from the results. It would be beneficial if a future version of EN 1793-6 made an allowance for such cases. Finally, a standardised method for calculating the signal-to-noise ratio should be included in EN 1793-6 and any failures to meet the 10 dB requirement stated in the test reports.

5.2. Recommendation of Future Work

There is scope for further work on the signal processing aspects of the measurement technique to allow reduced constraints on the sound source and a more in depth analysis of the measured impulse responses. This can be accomplished by pre-emphasising the test signal to account for the response of the sound source. A dedicated test barrier will allow the effects of the background noise level, excitation signal, equipment setup and presence of air gaps to be fully quantified, which would help to support the robustness of the measurement technique.

A. References

[1] D Ouis. Annoyance from road traffic noise: A review. *Jounal of Environmental Psychology*, 21(1):101–120, 2001.

[2] E. E. M. M. van Kempen, H. Kruize, H. C. Boshuizen, C. B. Ameling, B. A. Staatsen, and A. E. M. de Hollander. The association between noise exposure and blood pressure and ischemic heart disease: A meta-analysis. *Environmental Health Perspectives*, 110(3):307–317, 2002.

[3] B. M. Shield and J. E. Dockrell. The effects of environmental and classroom noise on the academic attainments of primary school children. *Journal of the Acoustical Society of America*, 123(1):133–144, 2008.

[4] U. Sandberg and J. A. Ejsmont. *Tyre/road noise reference book.* INFROMEX, Harg, SE-59040 Kisa, Sweden, 2002.

[5] R. O. Rasmussen, R. J. Bernhard, U. Sandberg, and E. P. Mun. The Little Book of Quieter Pavements. Technical Report FHWA-IF-08-004, US Department of Transportation, Federal Highway Administration, 2007.

[6] D. Bies and C. Hansen. *Engineering noise control: theory and practice.* Taylor & Francis, 2009.

[7] P. G. Abbott, P. A. Morgan, and B McKell. A review of current research on road surface noise reduction techniques. Technical Report PPR443, Transport Research Laboratory, 2010.

[8] Transit New Zealand. Environmental plan, 2008.

[9] European Committee for Standardization. EN 1793-6:2012 Road traffic noise reducing devices - Test method for determining the acoustic performance - Part 6: Intrinsic characteristics - In situ values of airborne sound insulation under direct sound field conditions, 2012.

[10] G. R. Watts. Effects of sound leakage through noise barriers on screening performance. In *Proc. ICSV 1999*, pages 2501–2508, 1999.

[11] NZ Transport Agency. NZTA State Highway Noise Barrier Design Guide, 2010.

[12] JP. Clairbois, J. Beaumont, M. Garai, and D. Schupp. A new in-situ method for the acoustic performance of road traffic noise reducing devices. *Journal of the Acoustical Society of America*, 103(5):2801, 1998.

[13] M. Garai and P. Guidorzi. European methodology for testing the airborne sound insulation characteristics of noise barriers in situ: Experimental verification and comparison with laboratory data. *Journal of the Acoustical Society of America*, 108(3):1054–1067, 2000.

[14] G. Watts and P. Morgan. The use of MLS based methods for characterising the effectiveness of noise barriers and absorptive road surfaces. In *Proc. Inter-Noise 2003*, pages 1780–1787, 2003.

[15] M. Garai and P. Guidorzi. Using CEN/TS 1793-4 to develop an acoustically effective added device for road traffic noise barriers. In *Proc. ICA 2007*, 2007.

[16] G. Watts and P. Morgan. Measurement of airborne sound insulation of timber noise barriers: Comparison of in situ method CEN/TS 1793-5 with laboratory method EN 1793-2. *Applied Acoustics*, 68:421–436, 2007.

[17] European Committee for Standardization. CEN/TS 1793-5:2003 Road traffic noise reducing devices - Test method for determining the acoustic performance - Part 5: Intrinsic characteristics - In situ values of sound reflection and airborne sound insulation, 2003.

[18] European Committee for Standardization. EN 1793-3:1997 Road traffic noise reducing

devices - Test method for determining the acoustic performance - Part 3: Normalized traffic noise spectrum, 1997.

[19] European Committee for Standardization. EN 1793-2:1997 Road traffic noise reducing devices - Test method for determining the acoustic performance - Part 2: Intrinsic characteristics of airborne sound insulation, 1997.

[20] M. Garai and P. Guidorzi. Case history: In situ verification of the intrinsic characteristics of the acoustic barriers installed along a new high speed railway line. In *Proc. Inter-Noise 2006*, 2006.

[21] M. Garai and P. Guidorzi. In situ measurements of the intrinsic characteristics of the acoustic barriers installed along a new high speed railway line. *Noise Control Engineering Journal*, 56(5):342–355, 2008.

[22] International Organization for Standardization. ISO/IEC Guide 98-3, Uncertainty of measurement - Part 3: Guide to the expression of uncertainty in measurement, 2008.

[23] M. Garai, P. Guidorzi, and E. Schoen. Assessing the repeatability and reproducibility of in situ measurements of sound reflection and airborne sound insulation index of noise barriers. In *Proc. AIA-DAGA 2013*, 2013.

[24] J Borish and J. B. Angell. An efficient algorithm for measuring the impulse response using pseudorandom noise. *Journal of the Audio Engineering Society*, 31(7):478–488, 1983.

[25] GB. Stan, JJ. Embrechts, and D. Archambeau. Comparison of different impulse response measurement techniques. *Journal of the Audio Engineering Society*, 50(4):249–262, 2002.

[26] C. Bleakley and R. Scaife. New formulas for predicting the accuracy of acoustical measurements made in noisy environments using the averaged m-sequence correlation technique. *Journal of the Acoustical Society of America*, 97(2):1329–1332, 1995.

[27] W. T. Chu. Impulse-response and reverberation-decay measurements made by using a periodic pseudorandom sequence. *Applied Acoustics*, 29:193–205, 1990.

[28] U. P. Svensson and J. L. Nielsen. Errors in mls measurements caused by time variance in acoustic systems. *Journal of the Audio Engineering Society*, 47(11):907–927, 1999.

[29] A. Farina. Simultaneous measurement of impulse response and distortion with a swept-sine technique. In *110th AES Convention*, 2000.

[30] A. Farina. Advancements in impulse response measurements by sine sweeps. In *Proc. AES 122nd Convention*, 2007.

[31] S. Muller. Measuring transfer-functions and impulse responses. In *Handbook of Signal Processing in Acoustics*, chapter 5, pages 65–85. Springer New York, 2009.

[32] S. Muller and P. Massarani. Transfer-function measurements with sweeps. *Journal of the Audio Engineering Society*, 49(6):443–371, 2001.

[33] A. Torras-Rosell and F. Jacobsen. Measuring long impulse responses with pseudorandom sequences and sweep signals. In *Proc. Inter-Noise 2010*, 2010.

[34] A. Torger and A. Farina. Real-time partitioned convolution for ambiophonics surround sound. In *IEEE Workshop on the Applications of Signal Processing to Audio and Acoustics*, 2001.

[35] D. D. Rife and J. Vanderkooy. Transfer-function measurement with maximum-length sequences. *Journal of the Audio Engineering Society*, 37(6):419–444, 1989.

[36] D. Ciric, A. Pantic, and D. Radulovic. Transient noise effects in measurement of room impulse response by swept sine technique. In *Telecommunication in Modern Satellite Cable and Broadcasting Services (TELSIKS), 2011 10th International*, pages 269–272, 2011.

[37] M. Garai and P. Guidorzi. In-situ measurements of sound reflection and sound insulation of noise barriers: Validation by means of signal-to-noise ratio calculations. In *Proc. ICA 2013*, 2013.

[38] International Electrotechnical Commission. IEC 61672-1:2002 Electroacoustics - Sound level meters - Part 1: Specifications, 2002.

[39] Brüel & Kjær . *PRODUCT DATA - Modular Precision Sound Analyzer - 2260 Investigator including BZ7206 and BZ7210 Sound Analysis Software*, 2003.

[40] Plastral. Plexiglas Soundstop Brochure, 2011.

[41] P. Cobo, A. Fernandez, and M. Cuesta. Measuring short impulse responses with inverse filtered maximum-length sequences. *Applied Acoustics*, 68:820–830, 2007.

B. File Management and Graphical User Interface

A screenshot of the main GUI is shown in Figure B.1, the tasks required to perform a full measurement are listed below:

1. Choose between *MLS* or *ESS* measurements
2. Generate the excitation signal if necessary using the *Generate Excitation Signal* button and the associated dialogue box
3. Enter a name for the measurement, usually a brief description of the barrier under test
4. Enter the location of the measurement
5. Choose a folder for the measurement data files, the *measurement data folder*
6. Load the excitation file, this must be in the *measurement data folder*
7. Select the type of measurement to be performed (*Free-Field*, *Barrier Element*, *Barrier Post*, *Leak* or *Trial*)
8. Run the measurement using the *Run PULSE* button
9. Refresh the list of measurements and calculate the corresponding impulse responses using the *Refresh/Calculate IR* button
10. Enter the details for a particular impulse response measurement by selecting the desired measurement from the *measurement list* and then editing the *notes table*
11. Display a specific impulse response in the *plot area* by selecting the desired measurement from the *measurement list* and the desired microphone position from the *position list*

12. Adjust the position of the Adrienne temporal window using the *Zoom In*, *Select Point* and *Zoom Out* buttons

13. Calculate the sound insulation index by selecting one free-field measurement and one other measurement from *measurement list* and pressing the *Calculate SI Index* button

14. Display values from a specific sound insulation index calculation in the *SI index table* and the average sound insulation index in the *plot area* by selecting the desired calculation name from the *SI index list*

15. Enter the global measurement details in the *details table*

16. The global single number rating for the selected calculation is displayed in the *DL* box

17. Generate a test report using the *Generate Report* button and the associated dialogue box

18. Reset the measurement and clear the GUI using the *Reset* button

Table B.1.: File management

Filename	Variable Names				Variable Type	Description
	Level 1	Level 2	Level 3	Level 4		
eexc_L1_P17.wav					file	ESS excitation signal (wave file), L1 represents a period length of 1 second, P17 represents 17 periods of the ESS
mexc_O16_P17.wav					file	MLS excitation signal (wave file), O16 represents an MLS order of 16, P17 represents 17 periods of the MLS
ff_1.wav					file	recorded microphone signals (9 channel wav file) for a free-field measurement
be_1.wav					file	recorded microphone signals (9 channel wav file) for a barrier element measurement
bp_1.wav					file	recorded microphone signals (9 channel wav file) for a barrier post measurement
C_permute_O16.mat					file	column permutation matrix for the order 16 MLS
R_permute_O16.mat					file	row permutation matrix for the order 16 MLS
data_file.mat					file	main data file containing processed data and measurement details
	meas_name				string	name of the measurement (generally a short description of the barrier)
	meas_location				string	location of measurement

meas_pathname			string	folder containing the measurement data files
exc_filename			string	filename of the excitation signal used
IR_data			structure	impulse response data
	ff_1		structure	name of the impulse response measurement (*ff_ **, *be_ ** or *bp_ **)
		ir		structure	calculated impulse responses for the 9 microphone positions
			p1,p2,...,p9	vectors	
		adr_w		structure	Adrienne temporal windows for the 9 impulse responses, with the correct delay
			p1,p2,...,p9	vectors	
		ir_adr		structure	windowed impulse responses for the 9 microphone positions
			p1,p2,...,p9	vectors	
		ir_time		vector	time vector
		notes		structure	details of individual impulse response measurements
			temp	string	air temperature (°C)
			RH	string	relative humidity (%)
			pres	string	air pressure (kPa)
			wind	string	windspeed (m/s)
			height	string	microphone height (m)

			date	string	date and time of measurement
			T_w	number	Adrienne temporal window length (sec)
			lowfreqlim	string	low frequency limit of the measurement (Hz)
		fs		number	sampling frequency (Hz)
	be_*	...		structure	names of other impulse response measurements (*ff_ **, *be_ ** or *bp_ **) if they exist
	bp_*	...		structure	names of other impulse response measurements (*ff_ **, *be_ ** or *bp_ **) if they exist
SI_data				structure	sound insulation index data
	ff1_be1			structure	names of the impulse response measurements (*ff*_ be** or *ff*_ bp**) used in the SI index calculation
		p1,p2,...,p9		vectors	SI index at each microphone position (in one-third octave bands)
		mean		vector	average SI index (in one-third octave bands)
		DL		number	global single number rating for airborne sound insulation
		category		string	corresponding category, based on the DL value
		oct3		vector	one-third octave band centre frequencies (Hz)

	ff*_be*	structure	names of other SI index calculations (*ff*_ *be** or *ff*_ *bp**) if they exist
details		structure	details of the traffic noise barrier being tested
	barrier_type	string	type of barrier (eg. plywood)
	manufacture	string	barrier manufacturer
	installdate	string	date of installation
	panelheight	string	panel height
	panelwidth	string	panel width
	panelthickness	string	panel thickness
	barriercondition	string	observed condition (eg. warped, leaks)

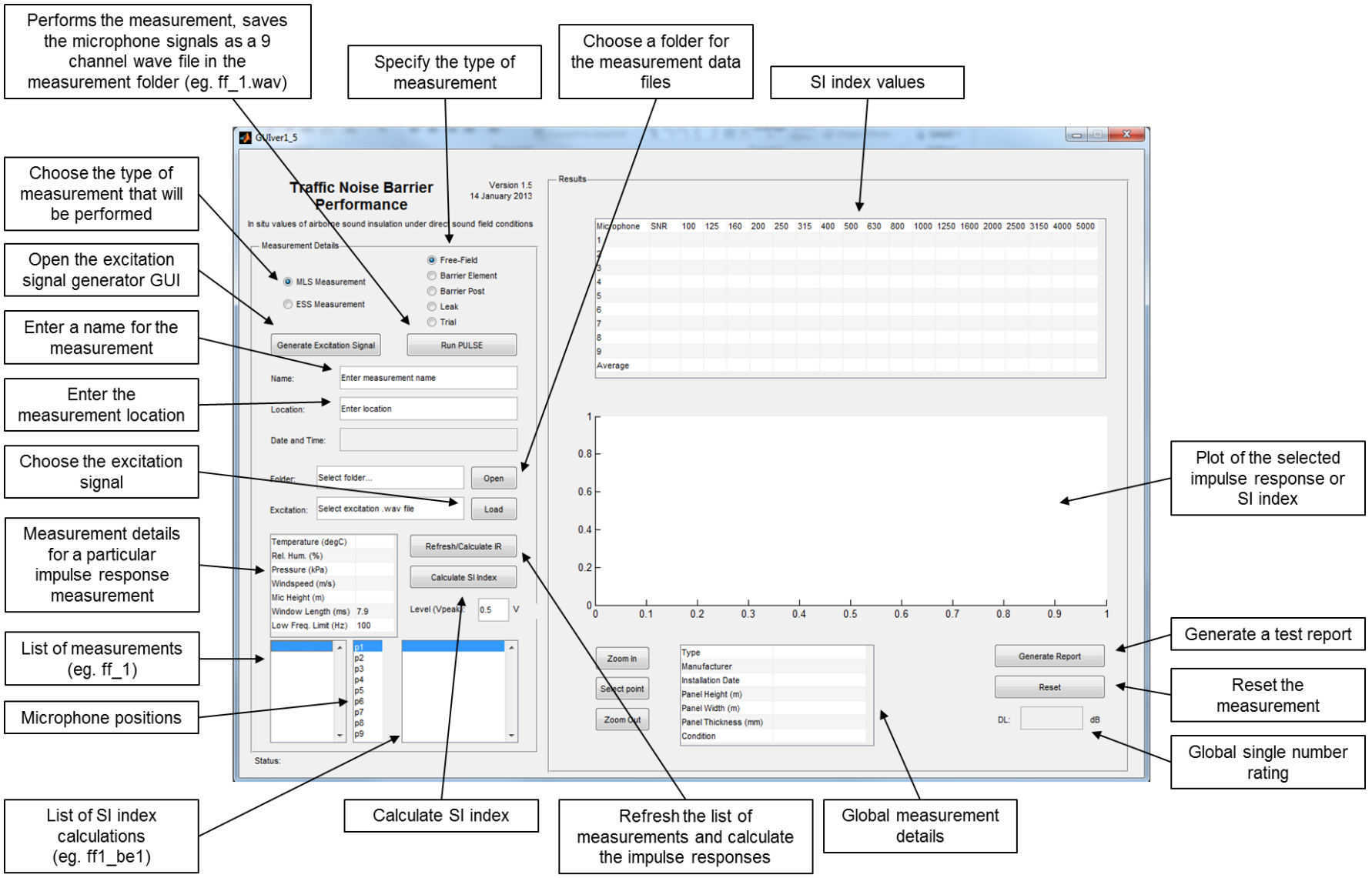

Figure B.1.: Graphical user interface overview

C. Signal-to-Noise Ratios

3.6 m acrylic barrier at St Marys Bay (excluding leakage)

Table C.1.: Signal-to-noise ratios for the nine microphones at position 1 on the St Marys Bay barrier, excluding leakage

	160	200	250	315	400	500	630	800	1k	1.25k	1.6k	2k	2.5k	3.15k	4k	5k
1	**7**	10	13	17	21	23	18	21	21	16	22	15	19	11	**5**	**-3**
2	**6**	**9**	13	18	29	26	20	23	24	19	21	21	21	15	**7**	**4**
3	**4**	**6**	10	15	24	20	14	17	15	20	24	21	15	11	**-4**	**-1**
4	**3**	**6**	**9**	13	18	21	20	26	23	25	24	26	27	16	17	**0**
5	**5**	**8**	12	18	30	19	16	24	19	21	25	28	30	29	18	**5**
6	24	28	33	45	40	34	36	35	32	32	33	33	30	33	31	21
7	17	21	25	32	42	31	30	35	29	30	32	34	33	32	28	25
8	22	25	30	36	38	32	31	41	34	35	33	31	29	29	25	16
9	25	29	34	41	38	32	30	37	47	36	36	37	28	32	24	27

Table C.2.: Signal-to-noise ratios for the nine microphones at position 2 on the St Marys Bay barrier, excluding leakage

	160	200	250	315	400	500	630	800	1k	1.25k	1.6k	2k	2.5k	3.15k	4k	5k
1	27	27	28	29	30	31	32	33	31	28	26	17	13	**5**	10	**8**
2	21	21	22	23	25	29	32	26	23	25	20	23	18	**6**	**-6**	**-7**
3	10	10	11	11	13	15	19	26	29	27	27	20	26	14	**1**	**3**
4	12	12	13	15	17	21	30	32	24	26	25	22	17	17	12	**5**
5	**8**	**9**	**9**	10	11	13	17	29	21	21	19	22	27	14	10	**8**
6	34	34	34	34	34	34	35	36	38	38	37	39	38	32	18	22
7	33	33	33	33	34	35	37	44	49	37	33	33	32	27	36	18
8	45	44	43	42	42	42	43	43	37	35	34	28	31	29	20	**8**
9	37	35	34	33	33	33	34	37	42	34	26	28	39	29	27	18

Table C.3.: Signal-to-noise ratios for the nine microphones at position 3 on the St Marys Bay barrier, excluding leakage

	160	200	250	315	400	500	630	800	1k	1.25k	1.6k	2k	2.5k	3.15k	4k	5k
1	25	25	25	25	25	25	26	28	30	24	16	19	28	15	**-2**	**1**
2	25	26	26	27	28	30	33	35	34	30	25	29	27	20	**3**	**4**
3	27	27	27	28	30	33	36	35	30	27	24	31	28	15	**1**	**2**
4	32	32	32	33	33	33	34	35	37	38	31	30	25	20	10	**6**
5	30	30	31	32	34	36	41	41	36	32	29	36	30	26	18	**9**
6	18	18	19	20	21	24	32	36	26	27	27	30	28	30	23	14
7	16	17	17	18	20	23	31	34	25	24	23	26	24	23	14	17
8	17	17	18	19	21	24	33	34	25	24	25	29	27	30	23	12
9	17	17	18	19	21	24	32	34	25	26	23	29	22	25	12	21

3.6 m acrylic barrier at St Marys Bay (including leakage)

Table C.4.: Signal-to-noise ratios for the nine microphones at position 1 on the St Marys Bay barrier, including leakage

	160	200	250	315	400	500	630	800	1k	1.25k	1.6k	2k	2.5k	3.15k	4k	5k
1	14	24	16	15	30	29	23	30	22	18	18	25	20	13	**8**	**-3**
2	15	24	16	17	23	20	31	36	28	22	24	25	32	17	**8**	**4**
3	14	20	18	13	26	17	23	20	17	17	17	20	22	**7**	**0**	**0**
4	16	19	14	12	26	26	24	27	32	23	30	31	31	15	13	**4**
5	12	20	19	17	21	21	26	24	26	28	20	24	32	24	10	**8**
6	22	26	29	29	25	31	33	36	33	38	33	31	34	37	33	23
7	22	18	23	35	28	35	37	35	32	30	29	30	40	34	27	28
8	20	21	23	30	30	30	37	35	36	37	32	34	37	35	29	25
9	15	20	29	42	28	41	31	34	47	41	37	35	35	34	31	33

Table C.5.: Signal-to-noise ratios for the nine microphones at position 2 on the St Marys Bay barrier, including leakage

	160	200	250	315	400	500	630	800	1k	1.25k	1.6k	2k	2.5k	3.15k	4k	5k
1	20	21	31	33	36	34	37	29	28	20	23	18	28	15	13	12
2	24	25	36	46	43	37	36	36	31	29	30	25	29	19	18	12
3	19	20	26	30	29	24	27	26	34	29	32	23	32	14	13	**2**
4	31	20	18	28	35	40	23	30	34	33	30	25	36	25	19	17
5	27	20	20	28	31	31	33	31	38	35	30	37	41	27	25	16
6	44	42	37	38	48	47	38	45	50	48	42	43	46	40	41	35
7	39	43	41	38	40	39	41	49	48	42	40	40	46	45	41	37
8	51	50	47	47	50	53	46	50	54	49	42	43	45	43	41	43
9	43	42	40	39	44	47	47	53	48	48	39	43	47	44	47	41

Table C.6.: Signal-to-noise ratios for the nine microphones at position 3 on the St Marys Bay barrier, including leakage

	160	200	250	315	400	500	630	800	1k	1.25k	1.6k	2k	2.5k	3.15k	4k	5k
1	12	16	21	21	26	23	31	26	24	28	21	20	28	11	**5**	**5**
2	18	24	27	26	36	35	30	23	25	29	28	24	29	22	**4**	**0**
3	19	25	28	27	23	33	32	32	27	26	25	16	35	15	**8**	**8**
4	19	19	24	28	35	35	30	33	27	31	32	29	26	19	13	11
5	20	21	31	28	33	49	37	38	34	31	30	34	31	22	19	10
6	31	22	16	36	30	29	36	34	36	36	36	35	37	36	34	28
7	30	25	18	19	28	27	36	34	31	32	36	41	40	33	40	35
8	28	15	21	36	28	36	32	31	33	33	33	39	41	39	32	33
9	34	32	29	34	36	37	29	36	38	31	38	40	39	39	40	38

4.2 m engineered timber barrier at Greenhithe

Table C.7.: Signal-to-noise ratios for the nine microphones at position 1 on the Greenhithe barrier

	160	200	250	315	400	500	630	800	1k	1.25k	1.6k	2k	2.5k	3.15k	4k	5k
1	33	35	37	40	45	38	35	31	22	22	18	25	20	12	**9**	**3**
2	23	27	35	42	33	31	37	43	30	23	20	24	20	24	**9**	**8**
3	30	37	44	34	29	27	25	25	29	27	20	19	20	**4**	**8**	**3**
4	19	23	30	41	32	28	34	42	34	32	21	34	31	22	15	**9**
5	22	26	33	44	32	30	32	35	36	31	22	32	38	33	17	12
6	18	22	29	42	32	30	32	24	25	24	21	32	37	35	25	19
7	21	25	30	39	38	32	37	37	38	33	29	30	34	33	21	18
8	19	22	27	32	28	26	31	31	33	33	25	32	29	28	34	26
9	15	19	25	36	28	24	29	23	24	23	24	31	36	27	23	18

Table C.8.: Signal-to-noise ratios for the nine microphones at position 2 on the Greenhithe barrier

	160	200	250	315	400	500	630	800	1k	1.25k	1.6k	2k	2.5k	3.15k	4k	5k
1	16	18	23	33	37	32	39	26	26	38	23	23	25	21	20	11
2	33	24	23	34	28	34	40	41	33	20	18	24	15	15	**7**	**4**
3	19	22	27	22	23	32	26	25	24	22	17	17	25	**6**	**6**	**7**
4	20	24	31	32	36	40	47	42	35	44	28	28	34	31	33	20
5	22	27	28	33	38	33	40	35	31	26	21	21	21	19	14	**9**
6	18	24	26	24	28	25	25	29	30	27	27	29	34	28	33	26
7	26	34	37	37	40	35	37	34	38	38	33	40	50	43	42	32
8	30	41	34	37	36	36	33	40	41	33	34	35	47	36	27	18
9	18	22	33	25	26	25	27	33	31	28	26	31	37	27	25	16

Table C.9.: Signal-to-noise ratios for the nine microphones at position 3 on the Greenhithe barrier

	160	200	250	315	400	500	630	800	1k	1.25k	1.6k	2k	2.5k	3.15k	4k	5k
1	13	15	23	22	29	22	28	23	21	23	20	23	20	13	**6**	**4**
2	14	16	21	28	29	33	29	25	25	31	33	23	21	14	12	**4**
3	21	22	21	30	35	30	39	23	25	39	25	20	29	**5**	**5**	**5**
4	13	14	20	34	38	27	28	23	28	28	25	28	29	17	18	12
5	15	18	24	30	37	35	32	30	31	27	23	27	31	22	13	14
6	35	26	22	32	36	36	37	30	36	30	35	30	45	33	37	29
7	26	21	20	30	29	33	33	27	30	31	30	40	40	28	21	20
8	21	22	26	34	26	32	31	30	33	32	32	33	42	33	27	19
9	26	23	26	44	36	28	39	30	37	31	36	33	43	34	20	22

2.9 m engineered timber barrier at Maioro Street

Table C.10.: Signal-to-noise ratios for the nine microphones at position 1 on the Maioro Street engineered timber barrier

	160	200	250	315	400	500	630	800	1k	1.25k	1.6k	2k	2.5k	3.15k	4k	5k
1	**9**	11	16	25	27	22	29	26	26	35	34	31	24	19	**5**	**-3**
2	15	16	17	17	15	20	33	33	39	38	35	41	30	12	11	**8**
3	11	14	20	30	22	18	28	25	21	37	25	27	30	17	**9**	**4**
4	**4**	**7**	13	23	18	15	22	25	32	25	36	34	39	31	13	**5**
5	**8**	11	15	22	17	20	31	23	30	27	28	41	35	20	**6**	**4**
6	**9**	**8**	**7**	**9**	17	22	25	24	27	29	39	47	51	35	20	**9**
7	20	17	14	12	19	26	27	23	30	32	36	36	34	27	13	15
8	15	14	12	14	26	29	24	32	34	39	38	49	43	31	15	12
9	**8**	**7**	**6**	**9**	16	19	19	21	26	31	40	41	43	32	16	23

Table C.11.: Signal-to-noise ratios for the nine microphones at position 2 on the Maioro Street engineered timber barrier

	160	200	250	315	400	500	630	800	1k	1.25k	1.6k	2k	2.5k	3.15k	4k	5k
1	12	15	19	26	21	17	31	35	26	32	28	23	26	17	**6**	**1**
2	14	16	19	24	32	35	27	27	34	37	24	26	28	18	**7**	**6**
3	15	15	16	17	21	20	13	18	22	32	23	29	32	15	12	**8**
4	**6**	**9**	13	20	25	21	30	21	35	38	26	30	32	18	20	**2**
5	**6**	**9**	13	18	25	21	19	16	25	28	30	27	24	19	11	**5**
6	16	19	23	29	37	22	34	43	46	41	42	44	34	25	14	**9**
7	**7**	10	15	24	21	14	19	23	30	33	30	37	40	34	25	10
8	**8**	11	15	23	23	19	22	12	29	29	29	33	32	**8**	**7**	10
9	**3**	**6**	**9**	17	**8**	13	25	21	20	24	30	29	34	29	18	16

Table C.12.: Signal-to-noise ratios for the nine microphones at position 3 on the Maioro Street engineered timber barrier

	160	200	250	315	400	500	630	800	1k	1.25k	1.6k	2k	2.5k	3.15k	4k	5k
1	13	15	17	18	17	22	31	24	28	27	26	26	26	23	**-1**	**-4**
2	**7**	10	14	17	20	22	27	23	25	31	26	25	31	20	**9**	**0**
3	**7**	10	17	21	12	**7**	22	22	23	33	21	26	30	14	**8**	**-4**
4	14	14	14	16	21	31	28	31	29	35	35	40	32	30	24	**5**
5	**6**	10	14	18	17	18	27	22	26	26	35	30	33	26	15	**7**
6	**8**	11	15	20	22	20	28	24	28	35	33	43	48	37	26	17
7	**8**	11	16	25	26	23	32	23	33	38	36	45	44	30	26	15
8	**7**	11	16	25	29	23	26	25	33	35	32	38	46	21	15	19
9	**8**	11	16	22	25	22	25	23	30	36	29	44	47	27	22	14

Table C.13.: Signal-to-noise ratios for the nine microphones at position 4 on the Maioro Street engineered timber barrier

	160	200	250	315	400	500	630	800	1k	1.25k	1.6k	2k	2.5k	3.15k	4k	5k
1	**9**	11	14	19	23	24	20	11	15	22	23	26	23	16	15	**2**
2	12	12	13	16	20	26	22	26	24	26	13	16	16	17	**6**	**4**
3	10	11	11	12	12	18	24	28	18	22	24	26	28	14	**8**	**0**
4	17	17	19	21	25	30	30	30	32	31	32	32	30	12	11	15
5	11	12	14	18	23	26	24	23	25	30	29	32	28	21	**8**	**5**
6	**7**	10	15	22	19	14	26	24	28	34	27	38	38	29	27	23
7	**5**	**8**	14	22	22	16	22	29	33	37	37	41	38	34	24	20
8	**6**	**9**	14	22	20	16	27	25	24	34	26	33	33	31	13	13
9	**6**	10	14	20	18	16	28	29	32	34	26	27	49	36	20	20

3.9 m plywood barrier at Hobsonville

Table C.14.: Signal-to-noise ratios for the nine microphones at position 1 on the Hobsonville barrier

	160	200	250	315	400	500	630	800	1k	1.25k	1.6k	2k	2.5k	3.15k	4k	5k
1	21	23	20	30	43	39	34	33	23	18	28	23	21	10	11	10
2	25	21	23	27	29	38	30	33	26	22	22	21	24	11	15	**9**
3	32	24	16	29	37	36	21	23	22	27	16	14	26	**5**	**4**	**5**
4	20	18	16	38	41	40	36	32	31	30	31	31	35	19	18	12
5	17	23	30	38	33	37	28	39	28	26	22	30	30	17	12	11
6	20	24	20	26	38	30	34	33	30	31	37	41	43	32	35	26
7	20	20	21	40	42	45	35	35	36	36	34	38	44	25	29	24
8	16	22	29	35	32	40	52	54	35	30	31	36	46	33	23	25
9	20	23	17	28	38	33	28	38	28	33	34	39	46	33	31	25

Table C.15.: Signal-to-noise ratios for the nine microphones at position 2 on the Hobsonville barrier

	160	200	250	315	400	500	630	800	1k	1.25k	1.6k	2k	2.5k	3.15k	4k	5k
1	18	18	18	24	34	22	24	26	18	24	17	17	28	10	**4**	**1**
2	19	20	22	22	28	42	33	35	27	29	17	27	25	11	10	**6**
3	19	16	13	27	35	24	33	25	21	27	15	22	22	10	12	**5**
4	20	24	34	36	33	43	42	31	27	32	20	24	31	20	15	12
5	25	26	28	28	29	32	33	39	33	33	27	34	30	21	18	13
6	20	26	30	32	39	26	38	35	26	35	38	42	41	32	37	27
7	18	20	28	37	32	36	35	31	33	34	33	35	40	32	32	23
8	21	26	28	28	38	40	33	38	35	29	45	46	43	41	35	31
9	22	27	26	35	39	33	43	34	35	30	43	46	39	37	31	30